2014

Development and evaluation of asphalt technologies utilizing renewable resources and innovative pavement systems

Andrew Aaron Cascione
Iowa State University

Development and evaluation of asphalt technologies utilizing renewable resources and innovative pavement systems

by

Andrew Aaron Cascione

A dissertation submitted to the graduate faculty

in partial fulfillment of the requirements for the degree of

DOCTOR OF PHILOSOPHY

Major: Civil Engineering (Civil Engineering Materials)

Program of Study Committee:
R. Christopher Williams, Major Professor
Vernon R. Schaefer
Kejin Wang
Eric Cochran
W. Robert Stephenson

Iowa State University

Ames, Iowa

2014

TABLE OF CONTENTS

LIST OF FIGURES

LIST OF TABLES

ABSTRACT

As the cost of construction materials continues to rise and place financial constraints on transportation agencies, engineers are looking for innovative technologies that minimize construction costs and optimize the selection of materials used in asphalt pavements. This dissertation includes a selection of four papers that advance the development, application, and utilization of innovative asphalt pavement technologies. Among the four papers, three subject areas in asphalt materials are examined to cultivate the use of newly-developed technologies in the asphalt industry. These include: the robust evaluation of hot mix asphalt from multi-state sources that utilize recycled asphalt shingles (RAS), the application and evaluation of a crack-relief interlayer asphalt mix design using new polymer technology, and the development of a bio-based thermoplastic elastomeric block-copolymer as a modifier for asphalt binder. In the case of the bio-based polymer, polymerized triglycerides from soybean oil serve as the "rubbery" block to replace butadiene in butadiene-based styrenic block co-polymers, thereby creating a new thermoplastic elastomeric polymer that is more renewable and biodegradable than its petroleum based counterparts.

For each subject area, laboratory experiments were conducted on experimental asphalt materials to determine the performance characteristics for the development and/or evaluation of new technologies. The results of each study show the advantage of implementing the technologies in pavement applications. Asphalt formulations developed with the bio-based block-copolymer demonstrate the block-copolymer's effectiveness in improving the rheological properties of asphalt binder; crack-relief interlayer mixes utilizing an improved polymer modified binder formulation are effective in delaying reflective cracking in overlay pavement systems; and a variety of asphalt pavements that incorporate

RAS alone or in combination with other cost saving technologies can be successfully produced and meet laboratory performance testing standards.

CHAPTER 1. GENERAL INTRODUCTION

New technologies that utilize renewable resources expand the range of alternative materials that can be used for pavement design and construction. Utilization of renewable materials advances sustainable growth in transportation infrastructure. Sustainable infrastructure is also achieved through design methods that both improve the long term performance of pavement systems and minimize future construction rehabilitation activities. The increased interest in sustainability coupled with the increasing price of asphalt has led many owner/agencies and asphalt paving contractors become more interested in implementing new technologies for apshalt pavements. Three new technologies that can have significant impact toward advancing improved economic, performance, and sustainable pavements in the asphalt industry are recycled asphalt shingles (RAS), crack-relief interlayers, and the use of bio-based polymer modifiers.

Recycled Asphalt Shingles in Hot Mix Asphalt

Transportation agencies in the United States have been increasingly using RAS in hot mix asphalt (HMA) applications over the last 25 years. Each year, an estimated 10 million tons of post-consumer shingles are placed in landfills in the United States. Post-consumer asphalt shingles typically contain 20 to 30 percent asphalt by weight of the shingles, as well as fine angular aggregates, mineral filler, polymers, and cellulosic or fiberglass fibers from the shingle backing material. Utilization of this waste product presents an opportunity to replace virgin asphalt binder with the RAS binder while taking advantage of the additional fibers. Thus a material that has historically been deemed a solid waste and has been placed in landfills can decrease pavement costs and reduce the burden on ever-decreasing landfill space.

With these benefits in mind, more state highway agencies are beginning to see the potential impact RAS could have in lowering the cost of pavements. However, little information

about the performance of pavements with RAS is known because it is a new material that agencies are beginning to use. The challenge agencies have when implementing the use of RAS materials is developing a construction specification for RAS mixtures that ensures a product with similar qualities and performance to non-RAS mixtures. Several nuances about the source and processing of RAS make it important for agencies to understand which factors about RAS affect the material properties essential for good fatigue and low temperature characteristics. These complexities drive the need for a comprehensive study on field produced HMA with RAS materials.

Crack-Relief Interlayer Asphalt Mixes

Reflective cracking in HMA overlays has been a common cause of poor pavement performance in Iowa for many years. Reflective cracks commonly occur in HMA overlays when deteriorated portland cement concrete (PCC) is paved over with HMA. The differential movement of concrete slabs at PCC joints create microcracks at the bottom of the HMA layer that grow and propagate to the surface. Since the rehabilitation strategy for many distressed PCC pavements in Iowa is to overlay them with HMA, the prevalent reflective cracking distresses has resulted in poor ride quality and increased transportation maintenance costs. Different types of mitigation strategies that help delay reflective cracking have been used with varying levels of success. One of the more promising approaches used to delay reflective cracking is incorporating an asphalt-rich, highly flexible, crack-relief HMA interlayer within the asphalt structure that serves as barrier to prevent reflective cracks from either forming or propagating to the surface of the overlay. The crack-relief interlayer is an asphalt-rich, highly flexible HMA that can resist cracking in high strain loading conditions. It is designed to have a high volume of asphalt with a low percentage of air voids and to contain a polymer modified binder with a wide temperature performance grade range.

The Iowa Department of Transportation recently began to implement a crack-relief interlayer mix design specification. However, due to lack of contractor experience, the challenging nature of correctly developing the mix design, and a laboratory performance specification for the interlayer design, additional research is needed to ensure the interlayer is properly designed and to determine the performance benefits of incorporating the interlayer into a pavement system.

Bio-Based Polymer Modifiers

Asphalt binder used for high-performing pavements needs sufficient properties to resist cracking at low temperatures and rutting caused by shear forces from sustained loads at high temperatures. To produce an asphalt binder with these performance characteristics, the binder is commonly modified with elastomeric polymers to improve its rheological properties and lower its temperature susceptibility over a range of in-service pavement temperatures.

The most common elastomeric polymers used for asphalt modification are styrenic block copolymers (SBCs). SBCs are composed of blocks of polybutadiene and polystyrene to produce styrene-butadiene (SB) diblock polymers and styrene-butadiene-styrene (SBS) triblock polymers. The elastic and principal component of SBS polymers is butadiene. For the last decade, butadiene prices have fluctuated and significantly increased, leading state highway agencies to search for economically viable alternatives to butadiene-based materials.

Recent advances in polymerization techniques have led to the development of elastomeric block copolymers produced with polystyrene and polymerized soy-derived triglycerides. While the past two decades of plant-oil based polymer research has yielded

only thermosets, the newly produced polymers are thermoplastic elastomers that are processable at high temperatures. There is excellent potential for the future of these biopolymers to serve as economically and environmentally favorable alternatives to their petrochemically-derived analogs for asphalt modification.

Organization of Dissertation

This dissertation is a compilation of four papers submitted, or to be submitted to scientific journals. It is divided into six chapters. Chapter 1 provides a general introduction. Chapter 2 contains a paper that evaluates the use of RAS in asphalt mixes. The results are a culmination of a comprehensive three year pooled-fund study on the performance of hot mix asphalt containing RAS. Seven states participated in the study. Chapter 3 includes a paper that evaluates an overlay project in Iowa which used a crack-relief interlayer asphalt mix to reduce reflective cracking. Chapter 4 and 5 contain papers that describe the development of a bio-based thermoplastic-elastomeric block-copolymer that is derived from soybean oil. Formulations of asphalt binder and the biopolymer are developed in the laboratory and tested for their rheological properties. General conclusions about each paper are presented in Chapter 6.

CHAPTER 2. COMPREHENSIVE FIELD AND LABORATORY PERFORMANCE INVESTIGATION OF RECYCLED ASPHALT SHINGLE WASTE

Modified from a paper submitted to *Resources, Conservation and Recycling*, published by Elsevier

Andrew A Cascione[1] [2] and R. Christopher Williams[3]

Abstract

In the United States, an estimated nine million metric tons of asphalt shingles are buried in landfills each year. Recycling and reusing this construction waste material in asphalt pavements could yield significant cost savings while reducing the impact on the environment. The components of recycled asphalt shingles (RAS) allow it to be a good candidate as a secondary material in hot mix asphalt (HMA). Transportation agencies have become increasingly interested in modifying asphalt pavements with RAS, yet they share common questions about the effect of RAS on the performance of HMA. In this study, the field and laboratory performance of RAS mixes produced from seven different transportation agencies was investigated as part of Transportation Pooled Fund TPF-5(213). Field

[1] Ph.D. candidate, Department of Civil, Construction, and Environmental Engineering, Iowa State University, Ames, IA 50011. E-mail: aacascio@iastate.edu
[2] Primary researcher and author
[3] Professor of Civil Engineering, Department of Civil, Construction, and Environmental Engineering, Iowa State University, Ames, IA 50011. E-mail: rwilliam@iastate.edu

demonstration projects were conducted that evaluated multiple aspects (factors) of RAS that could impact pavement performance. Field mixes from each demonstration project were sampled and tested for their performance characteristics. Pavement condition surveys were also conducted for each project after completion.

The demonstration projects showed that pavements using RAS alone or in combination with other cost saving technologies (e.g., WMA, RAP, GTR, SMA) can be successfully produced and meet state agency quality assurance requirements. The RAS mixes have very promising prospects since laboratory test results indicate good rutting and fatigue cracking resistance with low temperature cracking resistance similar to the mixes without RAS. The pavement condition of the mixes in the field after two years corroborated the laboratory test results. No signs of rutting, wheel path fatigue cracking, or thermal cracking were exhibited in the pavements. However, transverse reflective cracking from the underlying jointed concrete pavement was measured in the Missouri, Colorado, Iowa, Indiana, and Minnesota projects.

Introduction

Waste asphalt shingles have historically been considered a solid waste and placed in landfills. In the United States, nine million metric tons (Mt) of asphalt shingle waste are generated each year from the renovation and construction of roofs, and another one Mt of waste are produced during the manufacturing process of new shingles (National Association of Home Builders, 1998). In total, asphalt roofing shingle waste represents up to three percent of all construction and demolition debris in the US (Cochran and Townsend, 2010).

A new sustainable construction technology emerging in the United States is the recycling of asphalt roofing shingles for use in asphalt pavements. By diverting waste

shingles from landfills and incorporating them into asphalt pavements, what was previously considered a solid waste can now be upcycled into the transportation network for constructing driving surfaces. This innovative technology reduces the environmental impacts resulting from road construction by reducing the amount of virgin materials used in asphalt mixes (Sengoz and Topal, 2005). Replacing virgin materials with recycled asphalt shingles (RAS) saves resources, reduces the energy burned from using raw materials, eases landfill pressures, and reduces the demand of extraction (Huang et al. 2007, Chiu et al. 2008). Using RAS in asphalt pavements can also reduce greenhouse gas emissions produced during road construction by 9 to 12 percent (US Environmental Protection Agency, 2013).

Increases in crude petroleum prices have considerably raised the cost of asphalt binder in the past several years. This increase, coupled with the advancement of shingle processing technology, has created favorable market conditions for RAS to be used in asphalt pavements (Hughes 1997, Hansen 2009). From 2009 to 2012, the estimated amount of RAS annually used in asphalt pavements in the United States more than doubled, from 0.7 million tons to 1.9 tons (Hansen and Copland, 2013).

The components of RAS allow it to be a good candidate as a secondary (recycled) material in asphalt mixtures. Recycled roofing shingles contain between 19 to 31 percent asphalt (Brock 2007) and include fine angular granules which can improve the resistance to permanent deformation. Shingles also contain fiberglass or cellulose backing, that when crushed during the recycling process, break down into fiber-like particles that may improve the cracking resistance of asphalt (Cascione et al. 2011).

With these benefits in mind, more state highway agencies are beginning to see the potential impact RAS could have in lowering the costs of pavements. However, little

information about the long-term performance of pavements with RAS is known because it is a new material that agencies are beginning to use. The challenge agencies have when implanting the use of RAS materials, is developing a construction specification for RAS mixtures that ensures a product with similar qualities and performance to non-RAS mixtures. Several aspects about the sourcing and processing of RAS make it important for agencies to understand which factors about RAS affect the material properties essential for good pavement performance. This led to the creation of Transportation Pooled Fund TPF-5(213), a partnership of several state agencies in the United States with the goal of researching the effects of RAS on the performance of varied asphalt applications. As part of the pooled fund research program, multiple state demonstration projects were conducted to provide adequate laboratory and field test results to comprehensively answer design, performance, and environmental questions about asphalt pavements containing RAS.

The demonstration projects focused on evaluating different factors of RAS to determine how they influence the performance of pavements. RAS factors addressed in the different demonstration projects included the evaluation of RAS grind size, percentage of RAS in hot mix asphalt (HMA), RAS source (post-consumer versus post-manufacturer), RAS in combination with warm mix asphalt technology, RAS as a fiber replacement for stone matrix asphalt (SMA) pavements, and RAS in combination with ground tire rubber (GTR). Several of the demonstration projects also included control sections to compare traditional mix designs containing either recycled asphalt pavement (RAP) only or no recycled product to mix designs containing RAS.

Literature Review

Asphalt Shingles

Understanding the composition and properties of asphalt shingles is necessary for fully characterizing asphalt mixtures that incorporate their use. The American Society for Testing and Materials (ASTM) has specifications for their production. There are two different types of specifications, ASTM D225 which specifies asphalt shingles made with organic (cellulose or wood fiber) backing, and ASTM D3462 which specifies asphalt shingles made with fiberglass backing. These specifications are fairly broad so the exact composition of shingles will vary among different manufacturers.

Shingles are manufactured by saturating and coating both sides of organic or fiberglass backing felt with liquid asphalt. The shingles are then covered with sand and crushed-stone granules to increase their durability and resistance to weathering. The individual components of asphalt shingles are shown in Figure 1.

Figure 1. Components of Asphalt Shingles (Grzybowski et al. 2010)

The percentages of the individual component materials in asphalt shingles are different in shingles manufactured with organic felt compared to shingles manufactured with fiberglass felt. Brock (2007) summarized the composition of each type of shingles as

presented in Table 1. The shingles manufactured with organic felt have substantially more liquid asphalt then shingles manufactured with fiberglass felt due to the different absorption of the materials. Since asphalt binder is the most valuable product in RAS for paving materials, RAS made from organic felt will have a high economic value. RAS made from post-consumer shingles also has higher asphalt contents than RAS made from post-manufactured shingles due to the loss of a portion of the surface granules from weathering. McGraw et al. (2007) found similar asphalt contents as Brock in post-manufactured shingles and post-consumer shingles after conducting extractions on multiple samples.

Table 1. Asphalt Shingle Composition, % (Brock, 2007)

	Post-Manufacturer (Organic)	Post-Manufacturer (Fiberglass)	Post-Consumer
Asphalt Cement	30	19	31
Mineral Filler	26	40	25
Granules	33	38	32
Fiberglass Mat	0	2	0
Cellulose Felt	10	0	12
Cut-out	1	1	0

The other components used in the manufacturing of shingles are also a valuable commodity in HMA. The crushed-stone granules for example can reduce the amount of manufactured sand needed for an asphalt mixture. Additionally, the fiberglass or cellulose backing in shingles breaks up into fiber-like particles when crushed during the recycling process. These fibers are of particular interest to researchers and HMA producers since fibers are used as an additive in asphalt with a gap-graded or open-graded aggregate structure to prevent drain-down of the asphalt binder.

The asphalt used to coat the felt material is different than asphalt used in paving materials. The asphalt used in roofing shingles is much harder and stiffer because the manufacturers use an “air-blown” process to increase the viscosity of the asphalt. The

process infuses oxygen into the asphalt which changes the chemical composition of the asphalt making it stiffer. Furthermore, post-consumer shingles have been in service for a number of years and have undergone additional oxidative aging. As a result, the performance grade (PG) of the asphalt binder in RAS is higher than the performance grade of asphalt binder used for pavements. This may impact fatigue and low temperature cracking potential of asphalt pavements. Asphalt mixtures containing stiffer asphalt binder can exhibit higher resistance to rutting but decreased resistance to low temperature cracking and fatigue cracking (SHRP-A-367 1994).

To counter the effect of adding a stiffer binder, a softer virgin asphalt is often used. Historically, blending charts have been used in designing HMA with two different grades of asphalt binder (The Asphalt Institute 2007). With the advent of performance graded binders, "grade bumping" is practiced by agencies as an easy method to account for the introduction of the stiffer binder in the mixture matrix. When the percentage of recycled asphalt binder exceeds a certain amount, the specified virgin binder performance is reduced one or two grades on the low temperature and/or high temperature side.

To help regulate the amount of recycled asphalt being added to HMA when RAS is used so the final blend meets the design criteria, state highway agencies have implemented either maximum "percent binder replacement" specifications or maximum RAS percentage specifications. Typical percent binder replacement specifications require a maximum of 30 percent replaced binder as recommended by AASHTO PP53 *Design Considerations When Using Reclaimed Asphalt Shingles in New Hot Mix Asphalt.* Today there are more than 20 states that have either current specifications, developmental specifications, or are considering

the use of RAS in asphalt applications. Table 2 below summarizes the status of state agencies that have RAS specifications for asphalt pavements.

Table 2. State DOT Specifications for RAS

State	State specifications for using RAS[1]
Post-Manufacturer RAS (M); Post-Consumer RAS (C)	
AL	State Specification allowing 5% M or 3% C
GA	State Specification allowing 5% M or C
IA	State Specification allowing 5% M or C
IL	State Specification allowing 5% M or C
IN	State Specification allowing binder replacement of 15% M or C for surface coarse mixes (Maximum 25% binder replacement for mixes less than 9 million ESALs)
KS	State Specification allowing 5% M or C
KY	24% Binder Replacement
MA	State Specification allowing 5% M
MD	State Specification allowing 5% M
MN	State Specification allowing 5% M or C
MO	State Specification allowing 7% M or C
NC	State Specification allowing 5% M or C
NJ	State Specification allowing 5% M
NH	State Specification allowing 0.6% binder replaced with M or C from % of total mix
NY	State Specification allowing 5% M
OH	State Specification allowing 5% M or C
PA	State Specification allowing 5% M or C
SC	State Specification allowing 5% M or C
TX	State Specification allowing 5% M or C
VA	State Specification allowing 5% M or C
WI	State Specification allowing binder replacement of 20% M or C (5% max when used in combination with RAP)

1 Reflects specifications for RAS utilization without RAP. Each state has additional requirements for RAS used in combination with RAP and different virgin binder requirements. See state DOT construction specifications for details.

While asphalt binder with a higher modulus is desirable for highway pavement surface courses at high service temperatures to avoid permanent deformation, stiffer binders are susceptible to premature cracking in pavements (Roberts et al. 1996). However, the fibers in RAS are desirable for improving the tensile strength and cracking resistance of mixes.

The different backings on the shingle will ultimately provide different fiber particles in the RAS. Various fiber modifiers, such as cellulose, polyester, and mineral fibers, have been widely used in asphalt mixtures (Wu et al. 2007). Incorporating fibers into HMA has shown promising fatigue results. Fibers appear to increase the stiffness of the asphalt binder resulting in stiffer mixtures. This improves the resistance to permanent deformation. The tensile strength and toughness of the mixtures with fibers are also improved (Cleven 2000). An investigation by Lee et al. (2005) showed that fiber reinforcement extended the fatigue life of asphalt mixtures by 20 to 25 percent due to the increase in fracture energy. However, fibers with greater tensile strength (polyester, carbon fiber) have improved these properties to a greater extent than cellulose fibers (Putman 2004).

Processing Roofing Waste

Challenges in utilizing RAS are found to be in the quality control and quality assurance of the final product. When RAS is crushed and screened during processing, recyclers can change its end-product gradation (grind size). Obtaining a consistent RAS gradation that blends well with the other mix components can be the most challenging aspect of processing RAS. Test results that demonstrate differences between grind size underscore the necessity for proper field quality control specifications.

Sourcing

Asphalt roofing manufacturers have waste shingles that are accepted by recycling asphalt shingle facilities. The shingles are delivered on pallets wrapped in plastic or in roll-offs with and without the wrapping. Asphalt contents can vary among different manufacturers, and therefore it can be advantageous to stockpile materials from each source separately to control the asphalt contents of the final product. Documentation of the source

and tonnages should be required to be kept on file and available for review by environmental and transportation agencies.

For post-consumer shingles, asphalt shingle recycling facilities should be required to document the source of the post-consumer shingles accepted at their facilities. Recycling facilities should screen in-coming loads to ensure no hazardous materials are accepted and loads do not exceed ten percent by weight of non-shingle material.

Over 60 percent of post-consumer asphalt shingles come from storm damage. Many times these storms can damage newer roofs with recently installed shingles. When loads of post-consumer shingles are delivered to a recycling facility due to storm damage, asphalt contents and granular material percentages can vary. Newer post-consumer shingles may contain lower asphalt contents and lower binder viscosities compared to older post-consumer shingles, which may have binder that is stiffer due to more aging and higher asphalt contents. Therefore, asphalt shingle recyclers that closely monitor their intake can have better control over stockpiling.

Asbestos Testing and Analysis

Asphalt shingles manufactured in the United States prior to the mid 1980's may have contained asbestos. As a result, asphalt shingle recycling facilities are required to meet Asbestos National Emission Standards for Hazardous Air Pollutants (NESHAP) and Occupational Safety and Health Act (OSHA) requirements. NESHAP requirements state that asbestos-containing roofing materials may not be ground up for recycling. NESHAP defines asbestos-containing material (ACM) as any material containing more than one percent asbestos as determined using polarized light microscopy. To ensure that delivered loads of post-consumer shingle scrap do not contain asbestos, many state agencies require the owner

of the recycling facility to follow a specified sampling and testing plan. Samples are required to be obtained and tested for ACM using the polarized light method by an accredited laboratory. Typical sampling and testing frequencies require a sample to be obtained every 50 to 100 tons. In the event that a sample is found to contain greater than one percent ACM, the pile is required to be stockpiled separately and disposed of in accordance with state environmental regulations.

The incidence of ACM being found in shingles today is extremely low. Based upon available data from Florida, Iowa, Maine, Massachusetts, Minnesota, and Missouri, 1.5 percent of samples of more than 27,000 loads contained asbestos above the one percent limit (Townsend et al 2007).

Sorting

Post-manufacturer shingles usually do not have specific sorting protocols since they are delivered on pallets and are easily identified as clean of construction debris. However, post-manufacturer shingles delivered in roll-offs can include shingle globs, metal, or other objects that could damage the industrial grinders used in the processing and are many times screened to limit costly repairs.

Post-consumer shingles are often first sorted by trained personnel to remove all non-shingle material (i.e. paper, metal, plastic, felt paper). Sorting is done by hand over a conveyor belt or on the ground at the time of load dumping and again at the time of grinding (Figure 2). Removing all non-shingle materials is important to the shingle recyclers as hammers or other large metal objects incur costly repairs to the industrial grinders and loss of time for machines down for repair. Recyclable material such as paper, metals, and plastics

can be separated and recovered at a recycling facility. All non-recyclable material can be disposed of at a landfill.

When processing post-consumer shingles, it is especially important that construction debris must be removed from the shingle. This includes wood, nails, and other contaminates. Usually manual labor is utilized to separate the shingle from the wood. Removal of nails and other material removal is accomplished by using magnets at different locations on plant conveyer belts before and after the crushing process.

Figure 2. Post-consumer shingle manual sorting

Processing

For shingles to be successfully used in asphalt paving mixtures they need to be shredded or ground down to relatively small particle sizes. Different types of industrial grinders, including rotary shredders and hammer mills, are used to process shingles. The

industrial grinders utilize water nozzles to control dust and reduce heat build-up during the grinding process. Post-manufactured RAS can be more challenging to grind due to the softer asphalt which can clump together. This may contribute to further heat build-up which requires more water and additional screening (Figure 3). In the case of nails present in the shingles during the grinding process, grinders can be fitted with pulley magnets and cross-bar magnets which can effectively remove them.

In order to maximize the benefits of RAS, past research has helped identify how HMA performance is affected by the grind size of the RAS. Research completed by Button et al. (1996) and Abdulshafi et al. (1997) found that a finer grind produced a more consistent and better performing mix. Button et al. (1996) also found that the mixes containing a finer grind post-consumer RAS increased the tensile strength more than a coarser grind.

The size of the RAS particle can also be expected to affect the fraction of shingle asphalt binder that contributes to the final blended binder. A smaller RAS particle will have a larger surface area and more exposed binder. With more binder exposed on the surface of the RAS particle, more binder may be activated and blended with the virgin asphalt.

AASHTO MP 15-09 *Use of Reclaimed Asphalt Shingles as an Additive in Hot Mix Asphalt*, requires that 100 percent of the RAS pass a 12.5 mm (0.5 inch) sieve. In order to realize the benefits of a smaller RAS grind size, some state agencies have adopted a construction specification for RAS by specifying 100 percent of the RAS pass either the 9.5 mm (0.375 inch) sieve or the 4.75 mm (No. 4) size.

Figure 3: RAS screening

Storage

Asphalt shingles can hold up to 20 percent moisture, and so it is important to keep the use of water during processing to a minimum. A moisture content of seven percent or less is optimum. RAS stockpiles can also absorb moisture from the bottom of the pile so it is important to place piles on a non-permeable surface and/or a surface with proper drainage to deter standing water. Higher moisture contents can result in clumping, bridging in the bins, or slower production rates.

Moisture contents and clumping can be better controlled when stockpiles are covered. Covering the RAS at the asphalt plant can protect it from rain and direct sunlight (Figure 4). To help prevent RAS clumping in a stockpile, some agencies allow HMA producers to blend in a percentage of sand with RAS stockpile.

RAS also has a very limited time in the heating drum in a HMA plant. If the heat from the plant burner is working at removing the moisture, there is little time for the heat to reduce the viscosity of the RAS binder allowing it to separate from the RAS granules. RAS with high moisture contents then ultimately increase the potential for a poor bond between the RAS and virgin components.

Figure 4. Covered RAS stockpile

Quality Control for Asphalt Facilities

It is important to know the properties of RAS prior to use in HMA. Having consistent asphalt contents and gradations throughout both post-consumer and post-manufacturer stockpiles helps ensure the final HMA end product contains the targeted mix volumetric properties and field density. As a result, state agencies require asphalt producers to verify the asphalt content, gradation, deleterious materials content, and moisture content of RAS used in mix designs. Some agencies such as the Illinois DOT require continual testing of RAS

properties (i.e., asphalt content, gradation, Gmm) at specified frequencies as it is being stockpiled. If more than 20 percent of the stockpile contains RAS with properties that deviate outside the targeted production range, than the stockpile may not be used for DOT projects.

RAS is typically introduced in the HMA plant through a separate recycling bin and can vary depending on plant configurations (e.g., drum plant or batch plant). Many drum plant facilities introduce RAS into the drum recycle collar where RAP is normally introduced. Load cells or weigh belts measure the amount of RAS as it is metered into the collar. Some facilities load RAP over the RAS on the same conveyor belt to eliminate the blowing of RAS fines.

Load cells can give the highest accuracy in weighing the RAS, however, inconsistencies can still be found in the ability to keep the flow of RAS even and consistent on the belt. This includes bridging and clumping in the bins, which creates uneven distribution on the belt and leads to variability in asphalt contents in plant production mixes. One strategy to reduce variability on the belt is to use an auger system that distributes the RAS onto the belt.

Higher temperatures at drum plants can help remove moisture from RAS more quickly and facilitate the blending of RAS binder with virgin binder. However, agencies are becoming increasingly concerned that higher temperatures accelerate RAS aging during construction. Additionally, the cost to the asphalt producer to increase temperatures during mixing can reduce the savings benefits of RAS both environmentally and economically.

Experimental Plan

To evaluate how different factors of RAS materials effect pavement performance, an experimental plan was developed where each state highway agency in the pooled fund study

proposed a unique field demonstration project that investigated a different aspect of RAS mixes. Field demonstration projects were sponsored by the Department of Transportation agencies in Missouri, Iowa, Minnesota, Indiana, Wisconsin, Colorado, and Illinois. The asphalt mixes evaluated from each field demonstration project (Table 3) demonstrate the experimental plan of agency.

The Missouri demonstration project investigates how RAS grind size affects pavement performance and how replacing five percent RAP with RAS affects the properties of the asphalt pavement. The Iowa demonstration project investigates asphalt mixes with an increasing percentage of RAS. The Minnesota demonstration project investigates the difference between using post-consumer (PC) RAS and post-manufacturer (PM) RAS. The Indiana demonstration project investigates replacing RAS with RAP in asphalt mixes and the effect of producing RAS at reduced plant temperatures by using warm mix asphalt (WMA) foaming technology during production. The Wisconsin demonstration project investigates the effect of using Evotherm® 3G chemical WMA additive as a compaction aid at hot mix temperatures in mixes that contain RAS. The Colorado demonstration project investigates using three percent RAS as a replacement for five percent RAP. The Illinois demonstration project investigates using five percent RAS in stone asphalt matrix (SMA) in place of added fibers. While SMA mixes are always designed with fibers to prevent drain-down of the asphalt binder due to its gap-graded aggregate structure, the Illinois mixes did not contain any fibers since RAS has fibers in it. The Illinois project also contained different types of mixes to evaluate mixes produced with zero percent RAP versus 11 percent RAP, mixes produced in the field versus mixes produced in the laboratory, and mixes produced with ground tire rubber (GTR) modified binder versus polymer modified binder.

Table 3. Mix design properties

State Agency	Mix ID	% RAS	% RAP	% Total Binder	% Binder Replaced	RAS Source	Mix Source	PG[3]	% GTR[4]	NMAS[5] (mm)	Design Gyrations
Missouri	15 RAP	0	15	4.3	14.9	-	Plant	64-22	10	12.5	80
Missouri	5 FRAS[1]/10 RAP	5	10	4.8	30.2	PC[2]	Plant	64-22	10	12.5	80
Missouri	5 CRAS[2]/10 RAP	5	10	4.8	30.2	PC	Plant	64-22	10	12.5	80
Iowa	0 RAS	0	0	5.3	0	-	Plant	58-28	-	12.5	76
Iowa	4 RAS	4	0	5.5	16.3	PC	Plant	58-28	-	12.5	76
Iowa	5 RAS	5	0	5.8	19.4	PC	Plant	58-28	-	12.5	76
Iowa	6 RAS	6	0	5.3	22.8	PC	Plant	58-28	-	12.5	76
Minnesota	30 RAP	0	30	5.5	33.3	-	Plant	58-28	-	12.5	90
Minnesota	5 PC RAS	5	0	3.9	26.0	PC	Plant	58-28	-	12.5	90
Minnesota	5 PM RAS	5	0	4.8	18.8	PM[2]	Plant	58-28	-	12.5	90
Indiana	15 RAP HMA	0	15	5.6	19.3	-	Plant	70-22	-	9.5	100
Indiana	3 RAS HMA	3	0	6.0	12.9	PC	Plant	70-22	-	9.5	100
Indiana	3 RAS WMA	3	0	6.0	12.9	PC	Plant	70-22	-	9.5	100
Wisconsin	Evotherm® 3G	3	13	4.7	30.4	PC	Plant	58-28	-	19.0	75
Wisconsin	No Evotherm®	3	13	4.8	30.4	PC	Plant	58-28	-	19.0	75
Colorado	20 RAP	0	20	4.5	17.6	-	Plant	64-28	-	12.5	100
Colorado	3 RAS/15 RAP	3	15	4.9	23.1	PM	Plant	64-28	-	12.5	100
Illinois	5 RAS/0 RAP Field	5	0	6.0	21.0	PC	Plant	70-28	-	12.5	80
Illinois	5 RAS/0 RAP Lab	5	0	6.2	21.0	PC	Lab	70-28	-	12.5	80
Illinois	5 RAS/0 RAP Lab-GTR	5	0	5.6	21.0	PC	Lab	58-28	12	12.5	80
Illinois	5 RAS/11 RAP Field	5	11	5.6	35.0	PC	Plant	70-28	-	12.5	80
Illinois	5 RAS/11 RAP Lab	5	11	6.3	35.0	PC	Lab	70-28	-	12.5	80
Illinois	5 RAS/11 RAP Lab-GTR	5	11	5.7	35.0	PC	Lab	58-28	12	12.5	80

[1]FRAS – finely ground RAS; CRAS – coarsely ground RAS [2]PC – post consumer; PM – post manufactured
[3]PG – performance grade of asphalt binder prior to GTR modification [4]GTR – terminally blended ground tire rubber modifier
[5]NMAS – nominal maximum aggregate size

During each field demonstration project, representative samples of each RAS source and asphalt mixture were collected for binder characterization and mixture laboratory performance testing. The asphalt was recovered from the RAS and asphalt mixtures following AASHTO T164 Method A (Centrifuge Method) by using a blend of toluene and ethanol as the extraction solvent. The fines were removed from the binder extract by using a centrifuge at high speeds. Solvent was removed from the extract by following the rotovaper recovery process in ASTM D5404. The Performance Grade (PG) of the extracted asphalt binders was determined by following AASHTO R29 "Standard Practice for Grading or Verifying the Performance Grade of an Asphalt Binder".

Washed gradations of the aggregates after extractions were also conducted by following AASHTO T27. For the RAS samples, a dry gradation was conducted prior to extraction to evaluate the grind size distribution of the RAS product.

Laboratory performance testing was conducted on laboratory compacted samples of loose mix collected in the field during the demonstration projects. In the case of the Illinois demonstration project, performance testing was conducted on both field and laboratory produced mixes. Dynamic modulus tests were conducted to characterize the stiffness of the asphalt mixtures over a wide range of temperatures and frequencies. The flow number test was conducted to evaluate the permanent deformation resistance of the asphalt mixtures. Asphalt mixture durability and resistance to fatigue cracking was evaluated using the four-point bending beam apparatus. The semi-circular bending (SCB) test was conducted to evaluate the low-temperature cracking susceptibility of the asphalt mixtures.

Dynamic Modulus

The dynamic modulus |E*| test was conducted to determine the stress-strain relationship of the asphalt mixtures under continuous sinusoidal loading for a wide range of temperature and frequency conditions. A higher dynamic modulus indicates that lower strains will result in a pavement structure when the asphalt mixture is stressed from repeated traffic loading. The mechanistic-empirical pavement design guide (MEPDG) uses |E*| as the stiffness parameter to calculate an asphalt pavement's strains and displacements.

The test was conducted by following AASHTO T342. Replicate test specimens of each asphalt mixture were compacted to 100 mm in diameter and 150 mm in height at 7 ± 0.5 percent air voids. The specimens were directly compacted to their geometry using a Pine gyratory compactor with a compaction mold modified to a 100 mm inner diameter. Specimens were tested by applying a continuous sinusoidal load at nine different frequencies (0.1, 0.3, 0.5, 1, 3, 5, 10, 20, and 25 Hz) and three different temperatures (4, 21, and 37°C). Sample loading was adjusted to produce strains between 50 and 150 μstrain in the sample.

A UTM-25 servo-hydraulic testing machine from IPC Global, which is capable of applying a load up to 25 kN, was used to test asphalt mixture specimens. The UTM-25 was housed in an environmental chamber capable of controlling the temperature of the test specimens. Three linear variable differential transformers (LVDTs) were mounted between gauge points glued to the test specimens to measure the deformations in the sample. The LVDTs were spaced 120 degrees apart. Dynamic modulus computer software from IPC Global was used to control the load settings and calculation of the dynamic modulus for each test run. This is the same software designed to control the Asphalt Mixture Performance Tester.

The dynamic modulus test data was analyzed to determine which RAS materials and other mix treatments affect the mean dynamic modulus values at 37°C and 5 Hz. The test data was also used to construct master curves, where dynamic modulus data from frequency sweeps were shifted to obtain one smooth curve that plots the dynamic modulus over a wide frequency range at a designated reference temperature.

The following sigmoidal function was used to model the mater curves.

$$\text{Log}|E^*| = \delta + \frac{\alpha}{1 + e^{\beta+\gamma(log f_r)}}$$

where:

fr = reduced frequency at the reference temperature;
δ = minimum value of *E**;
δ + α = maximum value of *E**; and
β, γ = parameters describing the shape of the sigmoidal function.

The following second-order polynomial equation was used to calculate the shift factors for each frequency sweep at a fixed temperature.

$$\log f_r = log f + a_1(T_R - T) + a_2(T_R - T)^2$$

where:

fr = reduced frequency at the reference temperature;
f = loading frequency at the test temperature;
a_1, a_2 = the fitting coefficients;
T_R = the reference temperature, °C; and
T = the test temperature, °C.

The reference temperature was selected as 21°C. Fitting parameters were determined using numerical optimization with the "Solver" function in Microsoft Excel.

Flow Number

The flow number test was conducted to measure the permanent deformation resistance of the asphalt mixtures. A repeated dynamic load was applied to the specimen for up to several thousand load cycles. The flow number was defined as the number of load cycles an asphalt mixture can tolerate until it flows. Cumulative permanent deformation in the sample was plotted versus load cycles. The flow number was reached at the onset of tertiary flow, which was determined at the cycle corresponding to the lowest cumulative percent strain rate.

Tests were conducted following procedures used in NCHRP Report 465 (Witczak et al. 2002). The same specimens used for dynamic modulus test were used for the flow number test since the dynamic modulus test is nondestructive. The specimens were placed in the UTM-25, unconfined, with a testing temperature of 37°C to simulate the climactic conditions that cause pavement to be susceptible to rutting. An actuator applied a vertical haversine pulse load of 600 kPa for 0.1 sec followed by 0.9 sec of dwell time. The loading cycles were repeated for a total of 10,000 load cycles or until the specimen reached five percent cumulative strain. Three LVDT's were attached to each sample during the test to measure the cumulative strains.

Four-Point Bending Beam

Four-point bending beam testing was conducted according to AASHTO T321, "Determining the Fatigue Life of Compacted Hot-Mix Asphalt (HMA) Subjected to Repeated Flexural Bending". Samples of field produced asphalt were compacted to 7 ± 0.5 air voids in a linear kneading compactor to obtain a compacted slab with dimensions 380 mm in length, 210 mm in width, and 50 mm in height. Each slab was saw-cut into three beams

with dimensions 380 mm in length, 63 mm in width, and 50 mm in height. Two slabs were compacted for each asphalt mixture to produce six beams for testing.

The equipment used to conduct the four-point bending beam test included a digitally controlled, servo-pneumatic closed loop bending beam apparatus from IPC Global. A control data and acquisition system (CDAS) was connected to the bending beam apparatus which connected to a computer that controlled the load during the test. The bending beam apparatus was housed in an environmental chamber maintained at the testing temperature of 20 ± 0.5 °C. Beams were placed in the environmental chamber at least two hours prior to testing to allow them to equilibrate to the testing temperature. The mode of loading used for the test was strain controlled. Haversine wave pulses were applied to the specimen during the test at 10 Hz.

Testing was conducted at varying strain levels to generate a fatigue curve for each asphalt mixture. For each of the six beam specimens prepared for each asphalt mixture, strain levels of 375, 450, 525, 650, 800, and 1000 micro-strains were applied. Testing at these strain levels were repeated for all the mixtures tested except for the two Indiana mixtures containing 3% RAS. Due to a limited amount of material, only 3 three beams of these mixtures were tested at 400, 700, and 1000 micro-strain levels.

During testing of a beam specimen, properties of flexural stiffness, modulus of elasticity, dissipated energy, and phase angle were recorded by the software every 10 cycles. On the 50^{th} cycle, the stiffness of the beam specimen was recorded as the initial stiffness. The beam specimens were tested until failure, which was defined as the cycle corresponding to a 50 percent reduction of the initial beam flexural stiffness.

A phenomenological approach for fatigue analysis was selected as the chosen methodology to evaluate the fatigue life properties of the mixtures. The phenomenological approach relates the tensile strain at the bottom of an asphalt pavement layer to the number of load repetitions to failure (Ghuzlan et al. 2006). In this approach, fatigue life is plotted versus stress or strain on a log-log scale.

Since strain-controlled was used as the mode of loading, a log-log regression was performed between strain and the number of cycles to failure (N_f), (Figure 5). The relationship between strain and N_f can be modeled using the power law relationship as presented in the following equation.

$$N_f = K1\left(\frac{1}{\varepsilon_o}\right)^{K2}$$

where:

N_f = cycles to failure;
εo = flexural strain;
K1 = regression constant; and
K2 = regression constant.

The fatigue model can be calibrated to relate laboratory to field conditions by applying a shift factor, the hypothesis being that laboratory fatigue tests can simulate field conditions. Because of the challenging nature of duplicating field conditions in a laboratory, no universal shift factor has been measured. Rather, shift factors have ranged between 4 and 100 (NCHRP 2010).

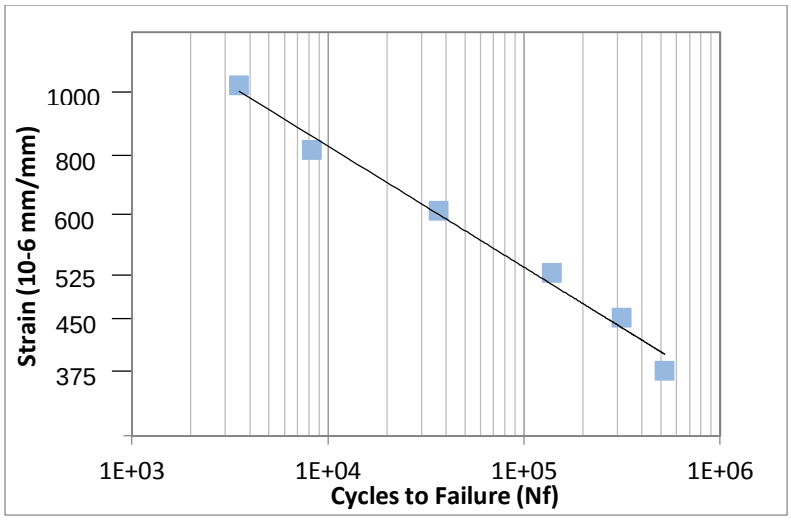

Figure 5. Sample fatigue curve

Pavements that have a higher resistance to tensile strains that develop at the bottom of an asphalt layer due to repeated traffic will have a greater resistance to fatigue cracking. Therefore, fatigue curves of several asphalt mixtures can be used to rank the mixtures resistance to fatigue cracking. However, the results must take into consideration the mode of loading. Research from the Strategic Highway Research Program (SHRP) A003-A project (Tangella et al. 1990) showed that materials that are more flexible (lower stiffness) perform better in constant strain. The constant strain mode of loading best represents the performance of thin pavements (less than 4 inches) while the constant stress mode of loading best represents the performance of thick pavements (greater than 6 inches). Materials that are stiffer may not perform as well under constant strain in the laboratory, but when used in thick pavements, lower tensile strains will develop under field loading. Therefore, when fatigue testing is done in a constant strain mode of loading, fatigue evaluations should be made in the context of the pavement structure.

If tensile strains are low enough in a pavement structure, the pavement has the ability to heal and therefore no damage cumulates over an indefinite number of load cycles. The level of this strain is referred to as the fatigue endurance limit (FEL). Identifying the fatigue endurance limit in a laboratory is somewhat elusive because it is impossible to test a sample to an infinite number of cycles. The researchers under NCHRP Report 646 (2010) developed a practical definition of FEL as the strain level at which a sample could withstand 50 million load cycles. If a shift factor of 10 was applied to the test results, it would be estimated that the pavement could withstand 500 million loading cycles which represents 40 years of traffic. Because it can take up to 50 days of testing to see if a sample reaches 50 million cycles, the NCHRP Report 646 researchers developed a procedure to estimate the FEL of asphalt mixture from a fatigue curve. They found that the lower 95% prediction limit at 50 million load cycles from a regression analysis of fatigue data corresponded reasonably close to the FEL. This technique uses the following equation to estimate the fatigue life.

$$\text{Lower Prediction Limit} = \hat{y}_o - t_\alpha s\sqrt{1+\frac{1}{n}+\frac{(x_o-\bar{x})^2}{S_{xx}}}$$

where:

yo = the one-sided lower 95% prediction interval at the micro-strain level corresponding to 50,000,000 cycles;
tα = value of t distribution for n-2 degrees of freedom for a significance level of 0.05;
s = standard error of the regression analysis;
n = number of samples;
Sxx = sum of squares of the x values;
xo = log 50,000,000; and
$\bar{x}$ = average of the fatigue life results.

Semi-Circular Bending

To evaluate the low temperature fracture properties of the mixes, 150 mm diameter specimens containing 7 ± 0.5 percent air voids were compacted in Iowa State University's laboratory and delivered to the University of Minnesota for semi-circular bend (SCB) testing. SCB tests were conducted by following the procedure in "Investigation of Low Temperature Cracking in Asphalt" (Marasteanu et al., 2007). Testing was conducted at four different low temperatures: PG low temperature, PG low temperature +4°C, PG low temperature +10°C, and PG low temperature +16°C. Replicate specimens were tested at each temperature.

All tests were performed inside an environmental chamber, and liquid nitrogen was used to obtain the required low temperature. The temperature was controlled by the environmental chamber temperature controller and verified using an independent platinum resistive-thermal-device (RTD) thermometer. The load line displacement (LLD) was measured on both faces of the test specimens using a vertically mounted Epsilon extensometer with 38 mm gage length and ±1 mm range. One end was mounted on a button that was permanently fixed on a specially made frame, and the other end was attached to a metal button glued to the sample. The average LLD measurement was used for each specimen. The crack mouth opening displacement (CMOD) was recorded by an Epsilon clip gage with 10 mm gage length and a +2.5 and -1.0 mm range. The clip gage was attached at the bottom of the specimen. A constant CMOD rate of 0.0005mm/s was used and the load and load line displacement (P-u), as well as the load versus LLD curves were plotted. A contact load with a maximum load of 0.3 kN was applied before the actual loading to ensure uniform contact between the loading plate and the specimen. The testing was stopped when the load dropped to 0.5 kN in the post peak region. The load and load line displacement data

were used to calculate the fracture toughness and fracture energy (G_f). A typical load line displacement versus load plot is shown in Figure 6.

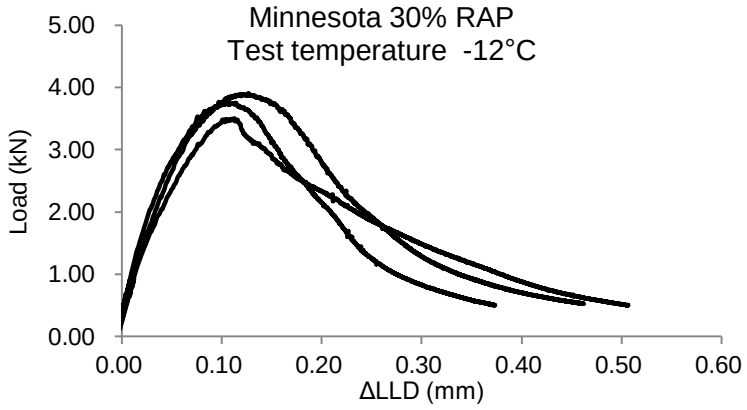

Figure 6. Typical LLD versus load plot of three test replicates

Pavement Condition Surveys

Pavement condition surveys were conducted following the construction of each demonstration project and after every winter season to assess the field performance of the pavement concerning cracking, rutting, and raveling. The surveys were conducted in accordance with the *Distress Identification Manual for Long-Term Pavement Performance Program* by Federal Highway Administration. For each demonstration project, three 500-foot sections were randomly selected for each mix type paved. The surveys were conducted in these locations.

Results and Discussion

RAS Characterization

The results of the RAS gradation analysis are presented in Table 4. All the state agencies for the demonstration projects specified at least a 12.5 mm minus RAS grind size. Both Missouri and Illinois RAS suppliers successfully produced a minus 9.5 mm RAS grind size. In the case of the Missouri demonstration project, a minus 9.5 mm grind was compared to a minus12.5 mm grind.

Table 4: RAS grind sizes

Sieve Size (mm)	Percent Passing Sieve Size								
	MO	MO	IA	MN	MN	IN	WI	CO	IL
	PC-CRAS	PC-FRAS	PC	PM	PC	PC	PC	PM	PC
19	100	100	100	100	100	100	100	100	100
12.5	98	100	97	100	100	100	100	99	100
9.5	94	99	95	95	99	97	99	95	100
4.75	75	82	84	70	85	74	83	70	91
2.36	62	67	67	56	73	62	70	55	74
1.18	42	43	44	32	49	38	47	31	48
0.6	22	21	22	12	24	18	24	13	24
0.3	12	12	10	4	10	9	11	6	11
0.15	5	5	3	1	3	4	3	2	3
0.075	1.2	0.9	0.6	0.4	0.5	0.7	0.6	0.3	0.5

PC – post consumer; PM – post manufactured
CRAS – coarsely ground RAS; FRAS – finely ground RAS

The asphalt contents of the post-manufacturer RAS sources (Minnesota and Colorado) range from 14.6 to 18.1 percent asphalt (Figure 7). This is lower than the asphalt content measured in the post-consumer RAS sources which range in asphalt content from 20.5 to 36.7 percent asphalt. RAS from post-consumer shingles will contain a larger percentage of asphalt because older shingles were made with a cellulose-fiber paper-backing which absorbs more asphalt than currently used fiberglass-mat backing shingles. Also, as shingles age on a roof, the loss of aggregate granules increases the percentage of asphalt in the shingle. The

larger range in asphalt contents of post-consumer shingles highlights the variability of different post-consumer shingle sources and the importance of keeping shingles from different sources separate during recycling operations.

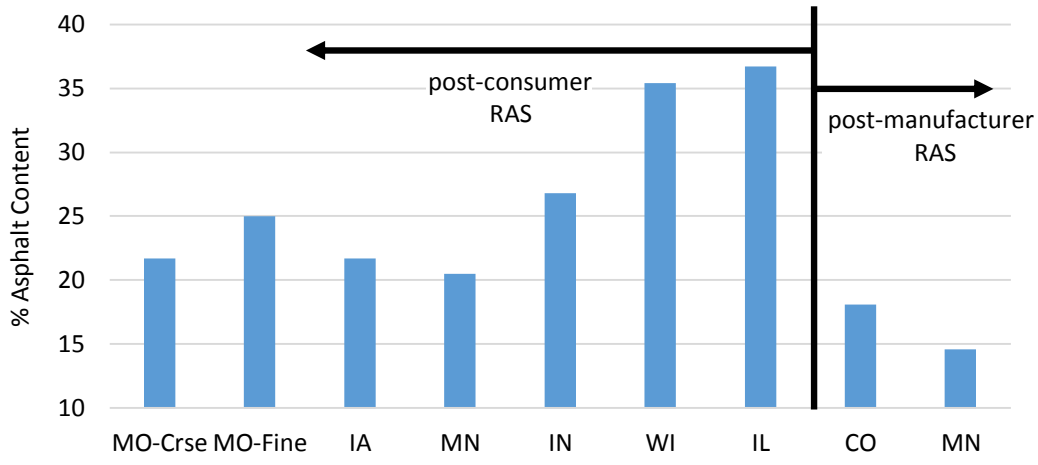

Figure 7. RAS percent asphalt content

All the RAS sources were tested for their high temperature PG using the dynamic shear rheometer (DSR) (Figure 8). The high temperature PG of the RAS binders is higher than traditional paving grade binders. This is expected since the binder in roofing shingles is produced with an air-blowing process which oxidizes the asphalt.

The high temperature PG of the post-consumer RAS binder ranges from 122.2°C to 146.1°C. These temperatures are noticeably higher than the post-manufacturer RAS binder which ranges from 109.1°C to 111.2°C. The post-consumer RAS binders are stiffer because they come from in-service roofing shingles that have experienced at least several years of aging. Post-manufacturer RAS comes from waste produced during shingle manufacturing.

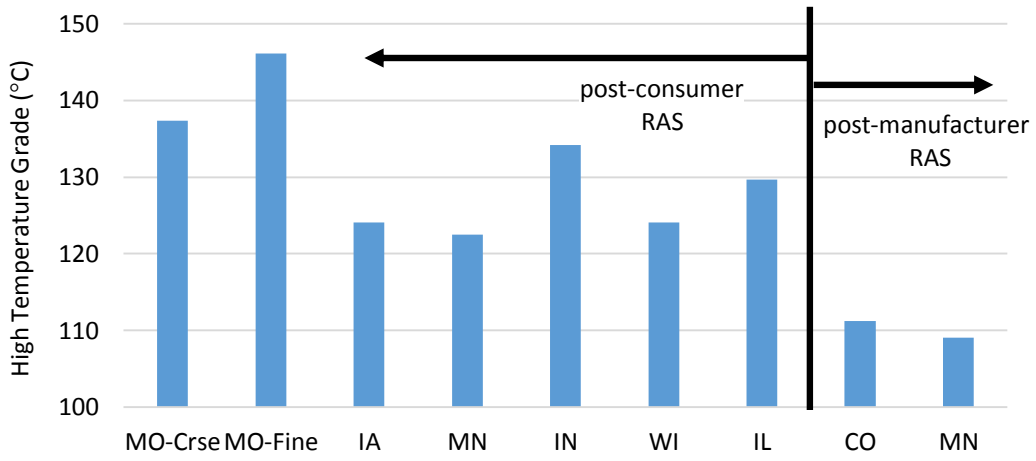

Figure 8. RAS high temperature performance grade

Recovered Asphalt Binder

The performance grade of the binder extracted from the field samples and the asphalt binder used during production is presented in Table 5. When RAS and/or RAP is added to the mix designs of each state demonstration project, the binder performance grade increases on the high and low side as expected. While the increase on the high PG side will stiffen the asphalt mixture to help reduce permanent deformation, the increase on the low PG side could increase the low temperature cracking potential of the mixture.

To compensate for the increased low temperature stiffness due to the addition of RAS and/or RAP materials, it is common practice to use a softer virgin binder with a lower PG. However, RAS and RAP have different performance grades and asphalt contents. Knowing which virgin binder to use or the amount of recycled product to add to the virgin binder is necessary to achieve a desired final PG.

The average results of all the mixes show that for every one percent increase in RAS, the low temperature grade will increase 1.9°C; and for every one percent increase in RAP, the low temperature grade will increase 0.3°C. Therefore, based on these mixes, three percent

RAS or 20 percent RAP would be the amount of recycled material needed for no more than one low temperature grade bump (6°C).

The wide range of asphalt contents in the RAS materials used in this study (from 14.6 percent to 36.7 percent) demonstrates the importance of evaluating the effects of RAS binder based on the percent binder replaced in the mix, rather than the percentage of RAS. The average RAS asphalt content was 24.5 percent and the average optimum asphalt content of the mixtures was 5.5 percent. Using these values and the binder grading results, for every 1 percent increase in binder replacement with RAS, the low temperature grade will increase 0.43 percent. For every 1 percent increase in binder replacement with RAP, the low temperature grade will increase 0.3 percent. Therefore, to cap the increase in the low temperature performance grade by one grade bump (6°C), either a maximum of 14 percent binder replacement with RAS binder could be used or a maximum of 20 percent binder replacement with RAP binder could be used.

This above analysis is only based on the average results when using all the data from the demonstration projects. It is important to also consider the large differences in material properties, sources, and factors in the experimental design for each state's demonstration project. Some demonstration projects used post-consumer RAS while others used post-manufactured RAS. Also, some demonstration projects used polymers and/or recycled tire rubber to modify the virgin binder which may have confounding effects when blended with recycled binders. Therefore, the variety of demonstration projects shows the necessity for state highway agencies to consider multiple factors when developing a RAS construction specification for asphalt pavements.

Table 5. Asphalt binder performance grades

State Agency	Mix ID	PG of Base Binder Sampled from HMA Plant		PG of Extracted Binder from Field HMA Sample	
		High Temp °C	Low Temp °C	High Temp °C	Low Temp °C
Missouri	15 RAP	70.3	-22.8	75.0	-16.8
Missouri	5 FRAS/10 RAP	70.3	-22.8	90.1	-8.7
Missouri	5 CRAS/10 RAP	70.3	-22.8	88.3	-4.9
Iowa	0 RAS	61.1	-17.9	73.0	-19.7
Iowa	4 RAS	61.1	-17.9	75.8	-19.1
Iowa	5 RAS	61.1	-17.9	81.3	-16.8
Iowa	6 RAS	61.1	-17.9	86.1	-14.7
Minnesota	30 RAP	58[1]	-28[1]	68.8	-22.7
Minnesota	5 PC RAS	58[1]	-28[1]	71.1	-21.2
Minnesota	5 PM RAS	58[1]	-28[1]	71.3	-21.7
Indiana	15 RAP HMA	72.2	-24.2	75.6	-20.1
Indiana	3 RAS HMA	72.2	-24.2	77.6	-14.2
Indiana	3 RAS WMA	72.2	-24.2	78.8	-15.1
Wisconsin	Evotherm® 3G	60.7	-29.1	68.5	-24.0
Wisconsin	No Evotherm®	60.7	-29.1	69.5	-22.5
Colorado	20 RAP	66.4	-34.8	67.6	-27.5
Colorado	3 RAS/15 RAP	66.4	-34.8	71.9	-21.1
Illinois	5 RAS/0 RAP Field	73.2	-29.9	72.8	-24.3
Illinois	5 RAS/0 RAP Lab	73.2	-29.9	72.7	-23.7
Illinois	5 RAS/0 RAP Lab-GTR	73.2	-29.9	77.2	-21.3
Illinois	5 RAS/11 RAP Field	73.2	-29.9	82.8	-18.1
Illinois	5 RAS/11 RAP Lab	73.2	-29.9	84.4	-14.5
Illinois	5 RAS/11 RAP Lab-GTR	73.2	-29.9	81.8	-17.7

[1] Asphalt binder sample was not available. PG58-28 was the specified base binder.

Aggregate Gradations

The aggregate gradations presented in Figure 9 demonstrate the wide range of aggregate structures for asphalt mixes utilized in different states. Iowa, Indiana, Minnesota, Wisconsin, and Colorado utilize mixes with fine aggregate gradations that extend above the restricted zone on a 0.45 power chart, while Missouri mixes and one mix from Minnesota utilize course gradations that plot below the restricted zone. The SMA mixes from Illinois plot well below the maximum density line to achieve the gap graded aggregate structure for SMA mixes.

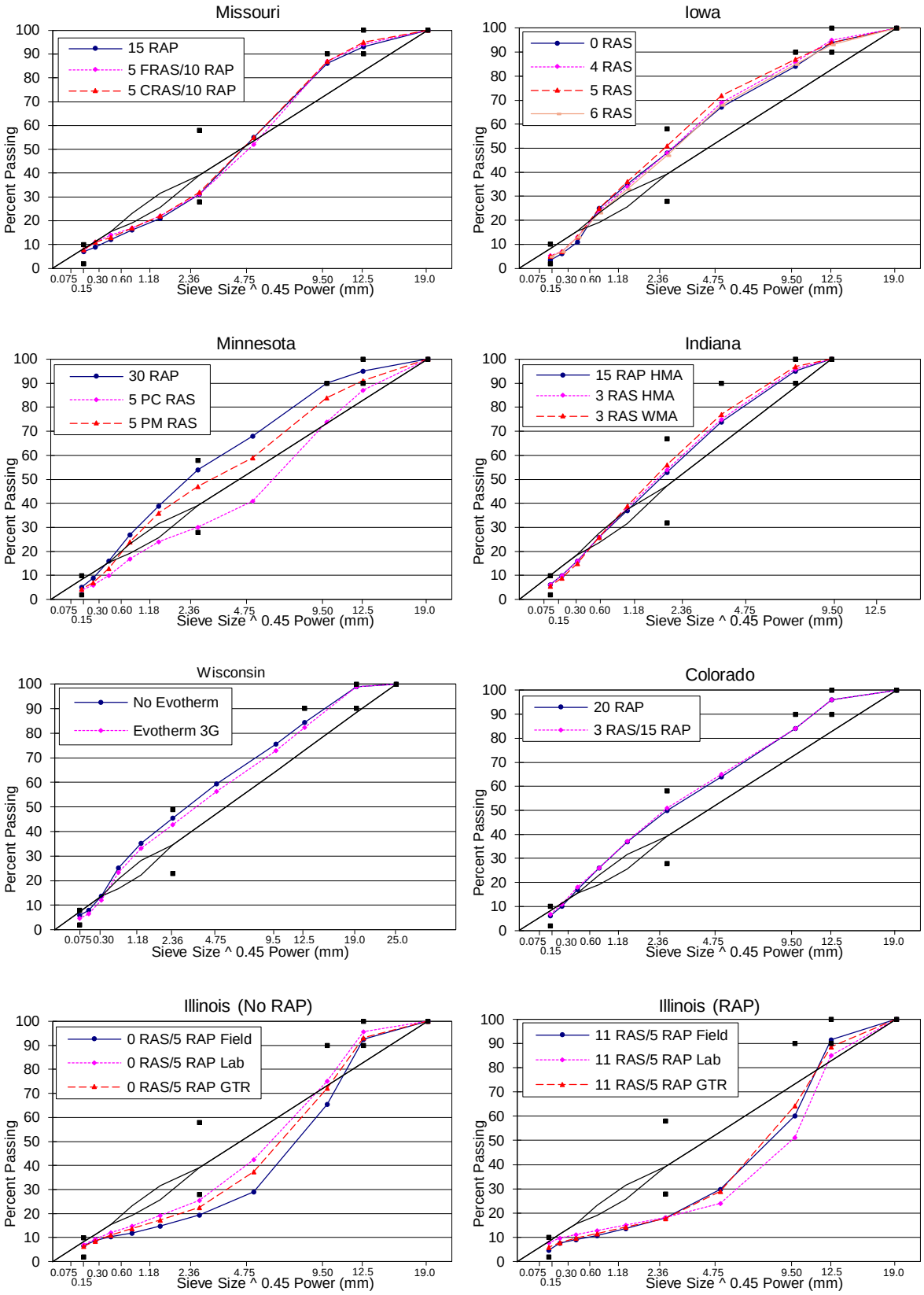

Figure 9. Aggregate gradations

Dynamic Modulus

The dynamic modulus master curves presented in Figure 10 show the how the modulus of the asphalt mixes decrease with temperature and increase with frequency. The dynamic modulus was selected for analysis as a simple performance test to evaluate the mixes resistance to permanent deformation. The temperature-frequency combination used for the analysis was 37°C and 5 Hz, since dynamic modulus values close to this temperature at 5 Hz have been correlated to the permanent deformation performance of asphalt mixes (NCHRP 2002). Figure 11 shows the mean dynamic modulus values and with error bars one standard deviation from the mean. The Missouri mixes have the highest dynamic modulus values which correlates to their high asphalt binder performance grade and coarse aggregate structure. Their high modulus values seem reasonable since they were designed for hotter climates and heavier traffic compared to mixes with lower modulus values such as Wisconsin or Iowa.

To statistical analyze the tests results from each demonstration project, a statistical analysis was conducted using a one-way analysis of variance (ANOVA) to determine if any differences among the mean dynamic modulus values were significant or to due random error. The statistical software program JMP (2014) was used to conduct the analysis. A 95 percent significance level was used in the analysis for an alpha value of 0.05. A pair-wise comparison was then performed to compare and rank the mix treatment levels within each state with regard to dynamic modulus. The outcome is reported in Table 6, in which statistically similar treatments are grouped together. Letter A indicates the best performing group of mixtures; letter B the second best, and so on. Groups with the same letter are not statistically different, whereas mixtures with different letters are statistically different.

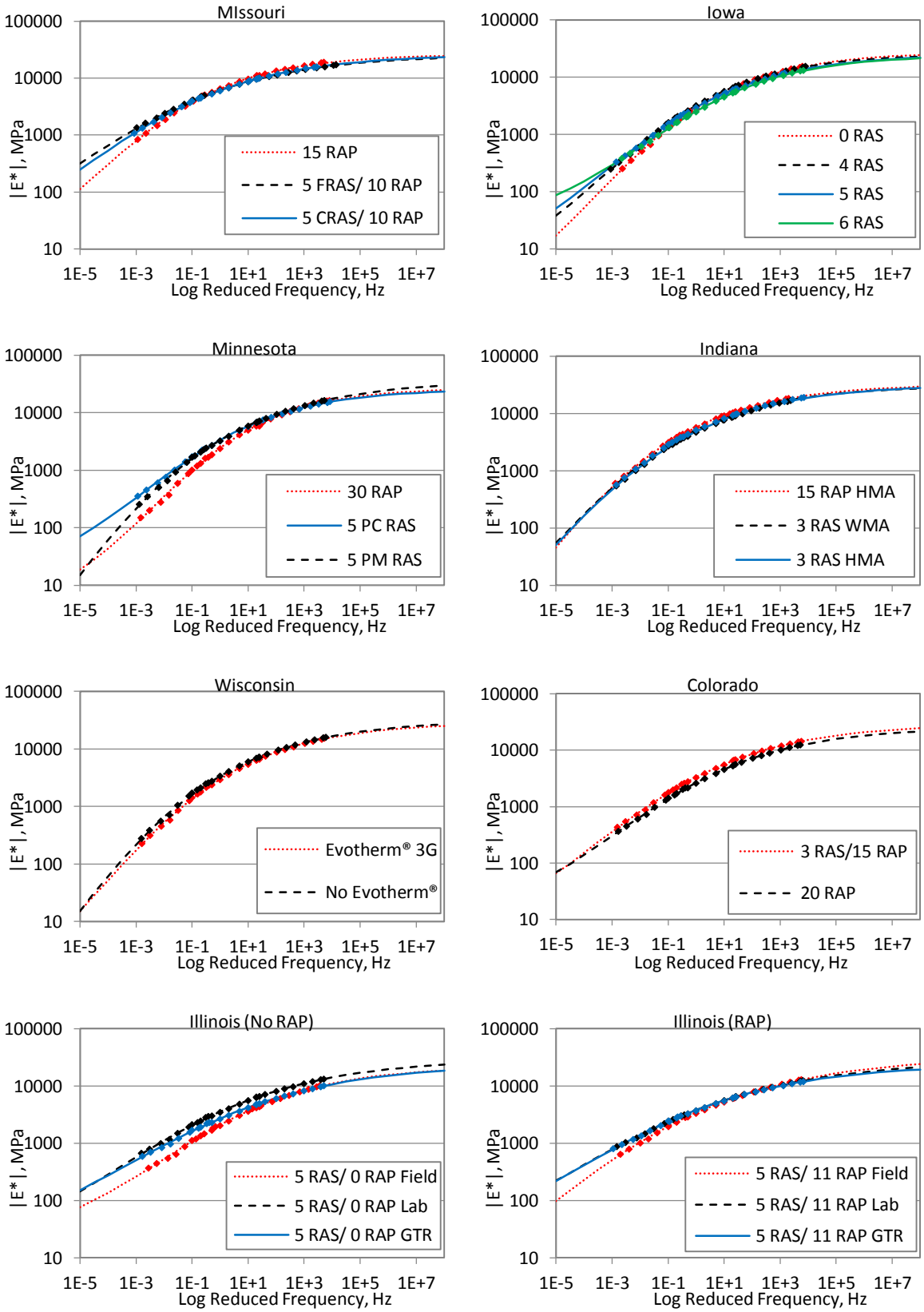

Figure 10. Dynamic modulus master curves

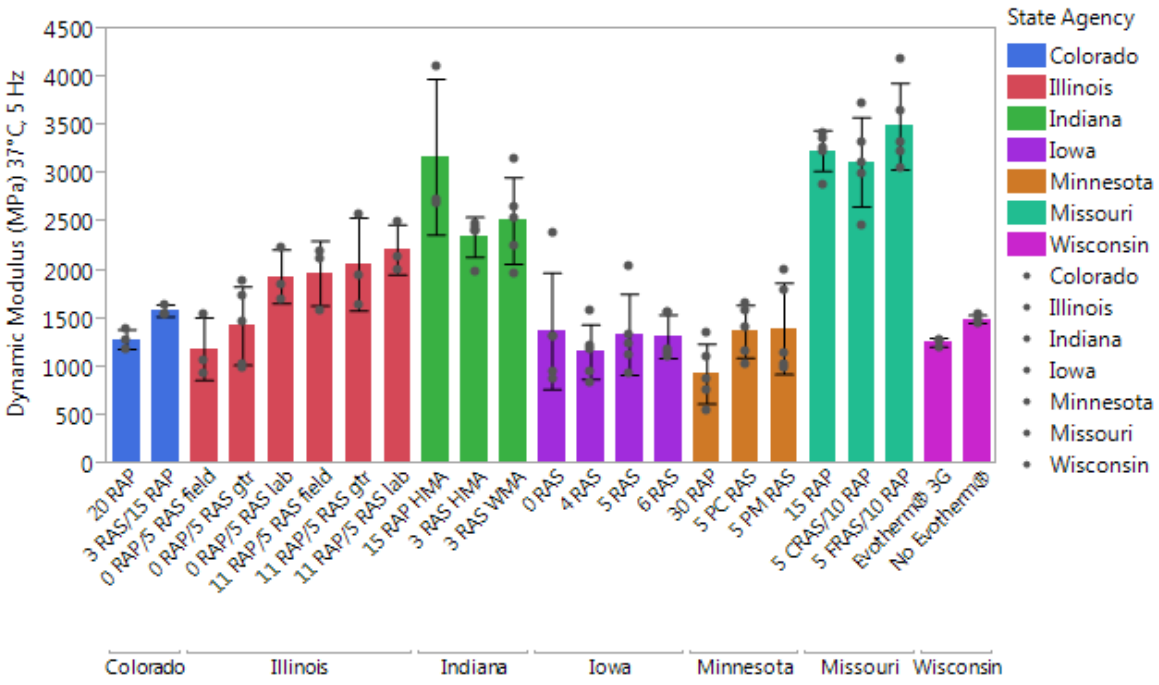

Figure 11. Dynamic modulus at 37°C, 5 Hz

The analysis demonstrates that for the Colorado mixes, replacing five percent RAP with three percent RAS will significantly increase the dynamic modulus of the HMA, and thus may increase the mix's resistance to permanent deformation. For the Wisconsin mixes, using Evotherm® 3G statistically decreased the dynamic modulus of the HMA. Since the two Wisconsin mixes were both produced at regular plant temperatures, the only construction variable between the mixes was the use of Evotherm® 3G as a compaction aid. For the Missouri, Iowa, Indiana, and Minnesota mixes, no statistical differences were measured among the treatment groups.

Table 6. Statistical grouping of mean E* values

State Agency	Mix ID	ANOVA *p*-value	Tukey Statistical Rank	Group mean E*(MPa)	Sample Size
Missouri	15 RAP	0.3441	A	3243.2	5
Missouri	5 FRAS/10 RAP		A	3495.6	5
Missouri	5 CRAS/10 RAP		A	3126.6	5
Iowa	0 RAS	0.8440	A	1376.6	5
Iowa	4 RAS		A	1160.1	5
Iowa	5 RAS		A	1339.9	5
Iowa	6 RAS		A	1319.8	5
Minnesota	30 RAP	0.1146	A	933.9	5
Minnesota	5 PC RAS		A	1371.4	5
Minnesota	5 PM RAS		A	1401.6	5
Indiana	15 RAP HMA	0.0996	A	3112.3	3
Indiana	3 RAS HMA		A	2349.8	5
Indiana	3 RAS WMA		A	2519.0	5
Wisconsin	No Evotherm®	0.0026	A	1500.0	3
Wisconsin	Evotherm® 3G		B	1258.3	3
Colorado	3 RAS/15 RAP	0.0121	A	1587.0	3
Colorado	20 RAP		B	1290.7	3
Illinois	5 RAS/0 RAP Field	*	*	3069.3	3
Illinois	5 RAS/0 RAP Lab		*	4862.0	3
Illinois	5 RAS/0 RAP Lab-GTR		*	3656.8	3
Illinois	5 RAS/11 RAP Field		*	4645.0	3
Illinois	5 RAS/11 RAP Lab		*	4942.0	3
Illinois	5 RAS/11 RAP Lab-GTR		*	4911.7	3

For the Illinois mixes, several statistical models were used to test the additional treatment groups of RAP versus no RAP (mix type), laboratory versus field samples (sample type), and polymer modified mixes versus GTR modified mixes (binder modification). A one-way ANOVA analysis was conducted for the RAP treatment group, while a two-way factorial ANOVA analysis was conducted to test the main effects of sample type and mix type and their interaction. Likewise, a two-way factorial ANOVA analysis was conducted on laboratory prepared samples to test for the main effects of binder modification and mix type and their interaction. The results demonstration a significant increase in the dynamic modulus when 11 percent RAP is added to the mixes (Table 7 and 8). There is also a significant difference

between lab and field dynamic modulus values indicating that the curing time for laboratory prepared samples does not match the amount of curing in field produced samples. The use of GTR does not change modulus properties of the mix, and no interaction effects were significant.

Table 7. Main and interaction effects of Illinois E* values

Test statistic	Main effects		Interaction effect
p-value	RAP Level 0.0082		
p-value	Sample Type 0.0209	RAP Level 0.0154	Sample Type X RAP Level 0.1829
p-value	Binder Type 0.1842	RAP Level 0.0640	Binder Type X RAP Level 0.5487

Table 8. Illinois statistical grouping of E* values

Illinois Mix Comparisons	Tukey Statistical Rank	Group mean E*(MPa)
11 RAP	A	2087.0
0 RAP	B	1562.9
Lab Samples	A	2079.5
Field Samples	B	1582.3
Polymer Modified	A	2079.5
GTR Modified	A	1813.0

Flow Number

The mean flow numbers are presented in Figure 12, and the multiple comparisons of the mix treatment groups for each state are reported in Table 9. The results demonstrate that higher amounts of RAS and/or RAP will increase the flow number, and thus the permanent deformation resistance, of the asphalt mixture. For example, as RAS is increased in the mix design for the Iowa project, the flow number increases. There is a statistical increase in flow number when comparing the means of the zero percent RAS mixes to the six percent RAS mixes. Likewise, when 30 percent RAP was replaced with five percent RAS in the Minnesota mixes, the flow number also increased. The Minnesota mixes also demonstrate that using post-consumer RAS can improve the flow number of an asphalt mix to a greater extent than using post-manufacturer RAS. For the Indiana mixes, replacing RAP with RAS also improved the flow number of the asphalt mixes. In the case of the Missouri and Illinois mixes, the flow numbers of the mixes reached the end of the test at 10,000 load cycles without reaching tertiary flow. The strains accumulated in the mixes after 10,000 load cycles was very small at less than one percent strain. Hence, the Missouri and Illinois mixes exhibited the highest flow numbers.

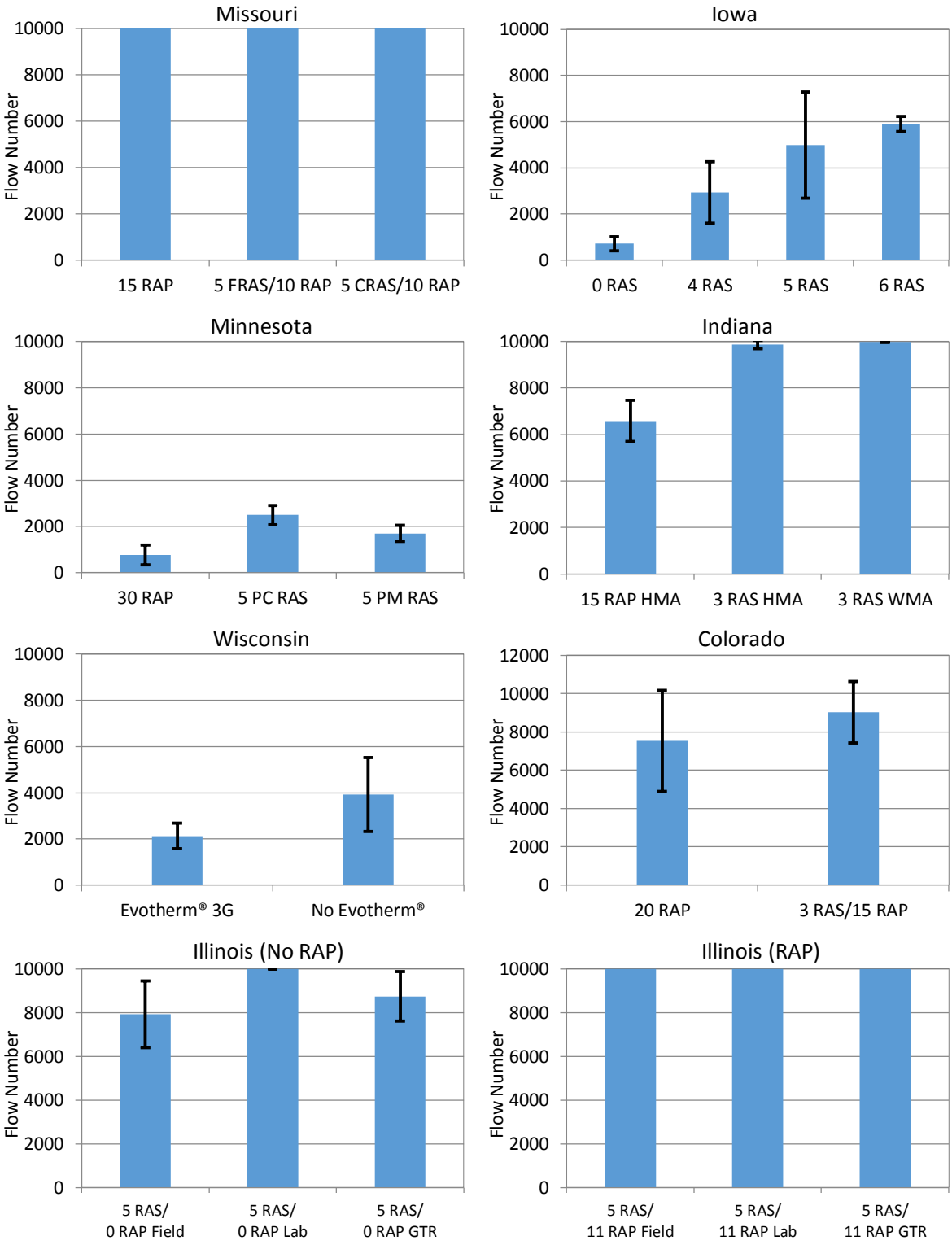

Figure 12. Flow number

Table 9. Flow number statistical grouping

State Agency	Mix ID	Flow Number			
		ANOVA *p*-value	Tukey Statistical Rank	Group mean Flow Number	Sample Size
Missouri	15 RAP	*	*	>10000	5
Missouri	5 FRAS/10 RAP		*	>10000	5
Missouri	5 CRAS/10 RAP		*	>10000	5
Iowa	6 RAS	0.0007	A	5899	4
Iowa	5 RAS		A/B	4988	4
Iowa	4 RAS		B/C	2938	4
Iowa	0 RAS		C	711	4
Minnesota	5 PC RAS	<0.0001	A	2497	5
Minnesota	5 PM RAS		B	1700	5
Minnesota	30 RAP		C	767	5
Indiana	3 RAS WMA	<0.0001	A	9986	5
Indiana	3 RAS HMA		A	9865	5
Indiana	15 RAP		B	6578	3
Wisconsin	Evotherm® 3G	0.1425	A	2128	3
Wisconsin	No Evotherm®		A	3912	3
Colorado	20 RAP	0.4521	A	7533	3
Colorado	3 RAS/15 RAP		A	9020	3
Illinois	5 RAS/0 RAP Field	*	*	7923	3
Illinois	5 RAS/0 RAP Lab		*	>10000	3
Illinois	5 RAS/0 RAP Lab-GTR		*	8737	3
Illinois	5 RAS/11 RAP Field		*	>10000	3
Illinois	5 RAS/11 RAP Lab		*	>10000	3
Illinois	5 RAS/11 RAP Lab-GTR		*	>10000	3

Four-Point Bending Beam

The four-point bending beam results, as presented by the strain versus "loading cycles to failure" curves, are reported in Figure 13. The K1 and K2 coefficients, R^2 value, and predicted endurance limit for all the mixes are presented in Table 10. With exception of the Illinois SMA mixes with GTR, all fatigue curves have an R^2 value above 0.9. The SMA mixes with GTR tended to segregate more than other mixes in the compaction mold resulting in higher amounts of variability in the air voids of the performance testing samples.

The K1 coefficient of the fatigue model characterizes the flexural modulus, and the K2 coefficient indicates the rate of damage accumulation in a sample. When using this relationship as failure criterion for a pavement design, a lower K2 value is more conservative as it assumes faster accumulation of fatigue damage. Suggested values for K2 are 4.477 by The Asphalt Institute, 4.0 by Shell, and 3.571 by the University of Nottingham (Huang 2004). Carpenter (2006) recommended the Illinois Department of Transportation use a K2 value in the range of 3.5 to 4.5. All the mixes, with or without RAS, performed well with respect to fatigue cracking since all the K2 coefficients are above 4.

With respect to the predicted fatigue endurance limit of the mixes, the SMA mixes from Illinois, in particular, have the greatest endurance limits and thus possess the highest fatigue cracking resistance in a strain-controlled environment. In the case of the Iowa, Missouri, Minnesota, and Colorado demonstration projects, the RAS mixes exhibited better fatigue lives and higher predicted endurance limits than the non-RAS mixes. These results demonstrate that mixes containing RAS can possess similar or better fatigue properties to mixes without RAS.

For the Iowa mixes, fatigue life increases with the addition of RAS. Since the fatigue tests were conducted in a controlled-strain mode of loading, the results indicate that RAS will improve the fatigue life of a thin lift pavement. The four Iowa mixes contain vary similar gradations and volumetric properties. They all have approximately the same asphalt content. The only difference between the mixes is percentage of RAS. Because RAS contains stiffer binder than virgin binder, it is expected that an increase in RAS percentage would increase the stiffness of the mixture. Yet, the average initial beam stiffness of the 0% RAS mixture was 3497 MPa while the average initial beam stiffness of the 4%, 5%, and 6% RAS mixtures

was 3090 MPa, 3106 MPa, and 3156 MPa respectively. Past beam fatigue studies in controlled strain mode of loading showed that when stiffness decreases from a change in binder type or grade, beam fatigue life is typically increased (SHRP-A-404). These results appear to follow the same trend as well, since the mixes with lower initial stiffness demonstrated longer fatigue lives. However, as the percentage of RAS increases from 0 to 4 to 5 percent in the mixture, which stiffens the binder grade, the fatigue life uncharacteristically increases.

A possible explanation of this phenomenon, could be from the complex RAS-aggregate-binder interactions and the contribution of fibers from the RAS. As the percent RAS content increases from 5% to 6%, the fatigue life no longer increases but decreases. While still significantly higher than the fatigue life of the 0% RAS mixes, the decrease could result from the effect of the stiffer binder (now at 22.8 percent replacement) having a more influential effect on the fatigue properties.

It is also of interest that the 11 percent RAP mixes for Illinois have higher endurance limits than the 0 percent RAP mixes. These results are counter intuitive since a higher percentage of recycled binder can increase the stiffness of an asphalt mixture and reduce its fatigue life in a strain-controlled mode of loading. The RAP mixes may possess higher endurance limits because they have a higher total binder content than the non-RAP mixes.

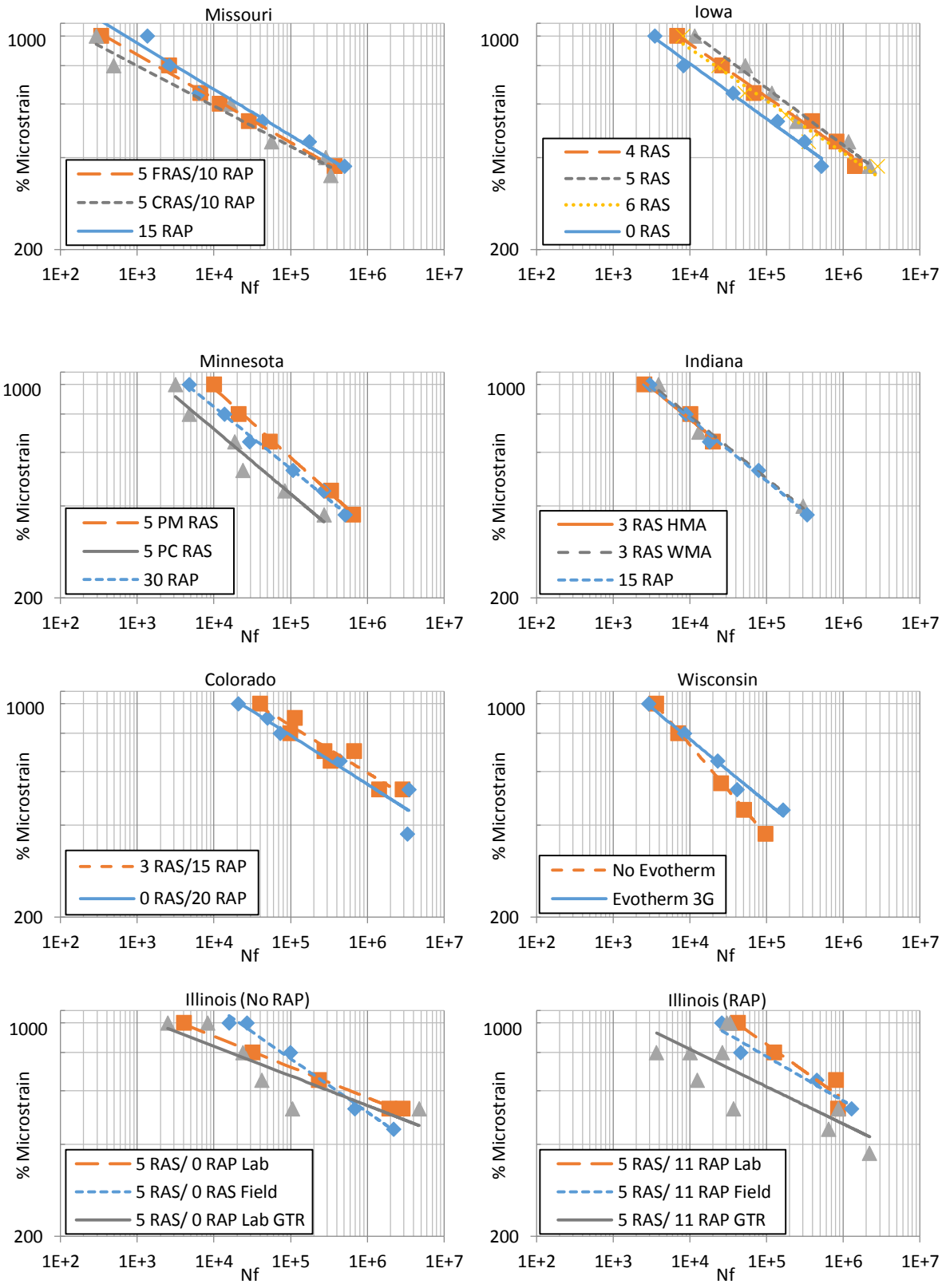

Figure 13. Four-point bending beam fatigue curves

Table 10. Fatigue model coefficients and predicted endurance limit

State Agency	Mix ID	K1	K2	R^2	Endurance Limit (microstrain)
Missouri	15 RAP	5.15E-17	6.40	0.968	139
Missouri	5 FRAS/10 RAP	7.25E-19	6.91	0.992	145
Missouri	5 CRAS/10 RAP	2.07E-20	7.37	0.968	159
Iowa	4 RAS	1.43E-13	5.45	0.987	144
Iowa	6 RAS	6.75E-14	5.68	0.987	182
Iowa	5 RAS	1.97E-12	5.27	0.982	175
Iowa	0 RAS	7.07E-14	5.65	0.967	162
Minnesota	30 RAP	6.66E-11	4.51	0.982	89
Minnesota	5 PC RAS	2.22E-09	4.19	0.996	123
Minnesota	5 PM RAS	9.19E-12	4.90	0.994	131
Indiana	15 RAP HMA	7.04E-12	4.87	0.993	114
Indiana	3 RAS HMA	1.41E-11	4.77	0.970	118
Indiana	3 RAS WMA	1.17E-11	4.81	0.985	110
Wisconsin	Evotherm® 3G	1.70E-11	4.74	0.976	74
Wisconsin	No Evotherm®	3.75E-10	4.32	0.984	53
Colorado	20 RAP	2.34E-13	5.69	0.907	195
Colorado	3 RAS/15 RAP	9.22E-14	5.89	0.907	244
Illinois	5 RAS/0 RAP Field	5.97E-16	6.51	0.946	195
Illinois	5 RAS/0 RAP Lab	2.92E-11	5.07	0.907	138
Illinois	5 RAS/0 RAP GTR	2.15E-11	4.86	0.593	152
Illinois	5 RAS/11 RAP Field	2.61E-13	5.64	0.985	208
Illinois	5 RAS/11 RAP Lab	5.26E-27	9.95	0.996	359
Illinois	5 RAS/11 RAP GTR	8.29E-20	7.56	0.735	204

Semi-Circular Bending

The fracture energy results from the semi-circular bend (SCB) tests for each state's mixes are shown in Figure 14. The SCB samples from each state were used to conduct a completely randomized two-way factorial statistical experiment with mix type and temperature as the treatment groups. In the case of the mixes from Illinois, two additional three-way factorial experiments were conducted to test for the effects of sample type (lab vs field), temperature, and RAP level and to also test for the effects of binder modification (GTR vs polymer), temperature, and RAP level in laboratory prepared samples. The significant main effects for each state's experiment are reported in Table 11. The temperature of the SCB test had a significant impact of the facture energy of the mixes from all the states.

This indicates that the mixes have a reduced fracture energy, and thus reduced cracking resistance, as their temperature decreases.

Using a pair-wise comparison of the mix type group mean from each state, the mixes are ranked according to their fracture energy in Table 12. Mixes from Minnesota have the highest fracture energy whereas mixes from Missouri and neighboring states have much lower fracture energies. Interestingly, this trend is associated with the geographic location where the mixes were designed and placed. For the northern climate states, softer asphalt binders were used in the mixes. As demonstrated by the results, the use of a softer asphalt binder resulted in mixes with a greater resistance to cracking.

With respect to the Missouri mixes, when five percent RAP is replaced with RAS, the fracture energy does not change. While the mixture with a coarse grind RAS decreases the fracture energy from 427 to 378 J/m^2, the difference is not statistically significant. The Missouri mixes also contain a significant mix type to temperature interaction. As the temperature treatment decreases from -6°C to -12°C, the 15 percent RAP mix significantly decreases in fracture energy while the post-manufacturer and post-consumer RAS mixes do not. However, from -18°C to -22°C there are no significant interaction effects among the mix types.

For the Iowa mixes, the 4% RAS mix has the highest fracture energy and the 0% RAS mix has the lowest fracture energy. The differences are statistically significant. The ranking of the mixtures by fracture energy is almost identical to the ranking of the mixtures by fatigue endurance limit, where RAS also has an effect on reducing the cracking susceptibility of the mix. These results indicate that small percentages of RAS will either decrease or have no detrimental effect on the cracking performance of asphalt pavements.

The results of the Minnesota mixes indicate similar low temperature cracking resistance between the RAS and RAP mixes. The 30 percent RAP mix has an average fracture energy of 741 J/m^2. When five percent RAS is used in the mix design in place of 30 percent RAP, the fracture energy increased to 768 J/m^2 for the post-manufacturer RAS mix and 777 J/m^2 for the post-consumer RAS mix. Since all the mixes are statistically ranked with the letter A, no statistical differences exist between the results of the three mixes.

For the Indiana mixes, when 15 percent RAP is replaced with three percent RAS, the fracture energy decreases from 551 to 502 J/m^2, although the difference are not statistically significant. The SCB test does not detect any difference in low temperature cracking performance when either RAS or WMA technology are used in the mixes.

For the Wisconsin mixes, when Evotherm® 3G is added to the HMA as a compaction aid, the fracture energy does not change. While the Evotherm® 3G mix does have a lower fracture energy (329 J/m2) than the non-Evotherm® 3G mix (364 J/m2), the difference is not statistically significant. Although not statistically significant at the 95% confidence level, these results do correlate well with the PG of the extracted binders. The low temperature performance grade of the extracted HMA binder containing Evotherm® 3G is higher than the extracted HMA binder not containing Evotherm® 3G, thus also indicating slightly lower resistance to cracking at low temperatures.

For the Colorado mixes, when 5 percent RAS with is replaced with 3 percent RAS in the HMA, the fracture energy does not statistically change. While the RAS/RAP mixture does have a lower fracture energy (318 J/m2) than the RAP only mixture (350 J/m2), the difference is not statistically significant. Although not statistically significant at the 95 percent confidence level, these results also correlate well with the PG of the extracted

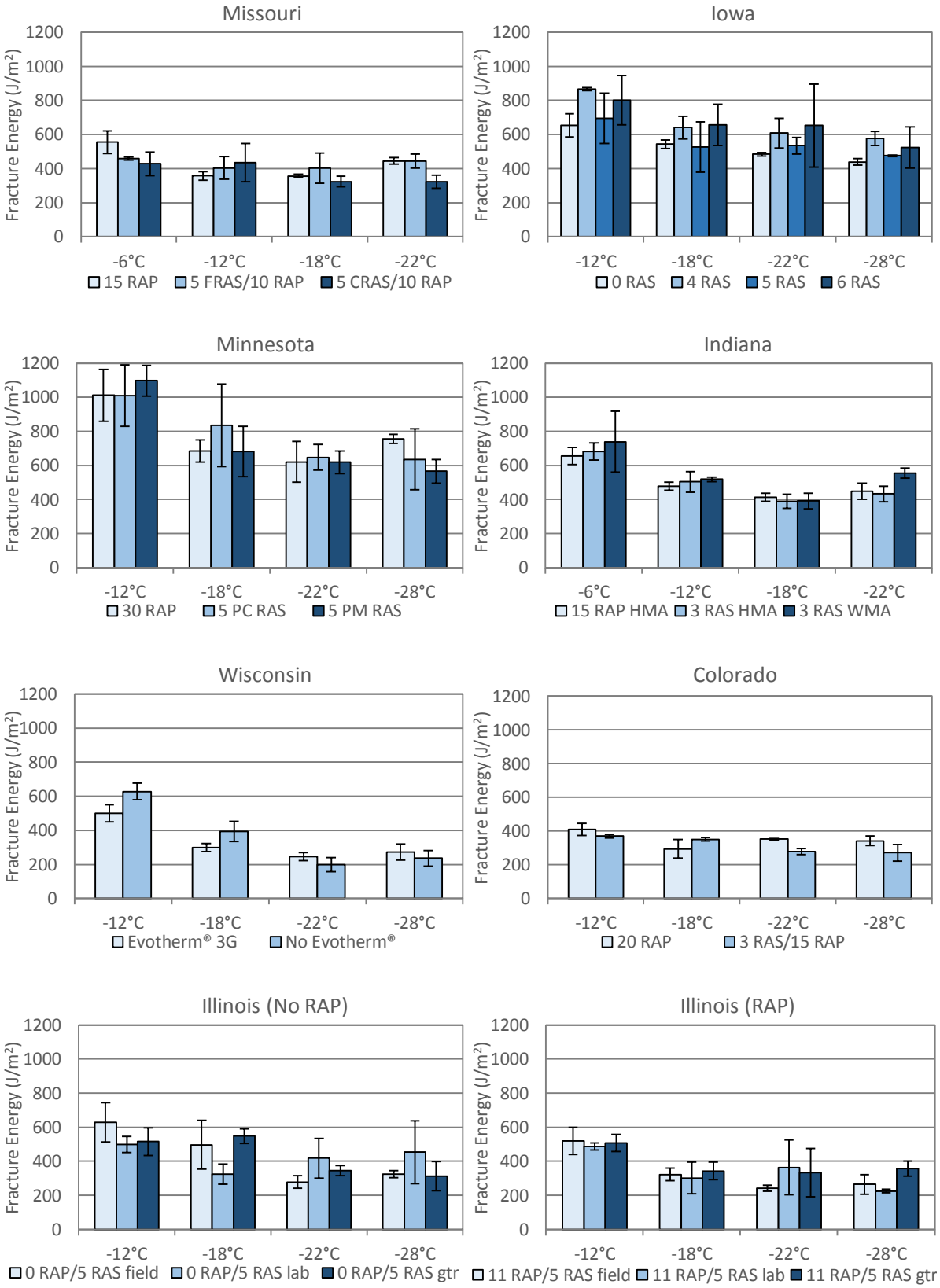

Figure 14. Fracture energy (Gf) of mixes from each state

Table 11. Effects tests from ANOVA analysis of fracture energy

Main and interaction effects	Test statistic p-value
Missouri Mix Type	0.0669
Temperature (°C)	0.0017*
Missouri Mix Type*Temperature (°C)	0.0363*
Iowa Mix Type	0.0098*
Temperature (°C)	0.0001*
Iowa Mix Type*Temperature (°C)	0.9935
Minnesota Mix Type	0.7652
Temperature (°C)	<.0001*
Minnesota Mix Type*Temperature (°C)	0.5085
Indiana Mix Type	0.1136
Temperature (°C)	<.0001*
Indiana Mix Type*Temperature (°C)	0.5715
Wisconsin Mix Type	0.2962
Temperature (°C)	0.0002*
Wisconsin Mix Type*Temperature (°C)	0.1946
Colorado Mix Type	0.0787
Temperature (°C)	0.0209*
Colorado Mix Type*Temperature (°C)	0.0619
Illinois RAP Level	0.0362*
Temperature (°C)	0.0020*
Illinois RAP Level *Temperature (°C)	0.2848
Illinois RAP Level	0.0781
Temperature (°C)	0.0518
Illinois RAP Level *Temperature (°C)	0.5596
Sample Type	0.8072
Illinois RAP Level*Sample Type	0.4028
Temperature (°C)*Sample Type	0.1134
Illinois RAP Level *Temperature (°C)*Sample Type	0.4217
Illinois RAP Level	0.2254
Temperature (°C)	0.0517
Illinois RAP Level *Temperature (°C)	0.5950
Binder Modification	0.7757
Illinois RAP Level *Binder Modification	0.9027
Temperature (°C)*Binder Modification	0.2547
Illinois RAP Level *Temperature (°C)*Binder Modification	0.2531

binders. The low temperature performance grade of the extracted HMA binder containing RAP and RAS is higher than the extracted HMA binder containing RAP only, thus also indicating slightly lower resistance to cracking at low temperatures.

For the Illinois mixes, when 11 percent RAP is added to the mixes, the fracture energy significantly decreases, resulting in a mix with a greater susceptibility to cracking (Figure 15). The main effects of binder modification type (GTR vs polymer) and sample type (laboratory vs field) were not significant.

Table 12. Ranking of mixes by Gf mean for each demonstration project

State Agency	Mix ID	Tukey Statistical Rank	Group mean G_f (J/m^2)	Sample size at each temp.	Test temperatures °C
Missouri	15 RAP	A	428	3	-6, -12,-18,-22
Missouri	5 FRAS/10 RAP	A	427	3	
Missouri	5 CRAS/10 RAP	A	378	3	
Iowa	0 RAS	A	674	3	-12, -18, -24, -28
Iowa	4 RAS	A/B	659	3	
Iowa	5 RAS	A/B	558	3	
Iowa	6 RAS	B	531	3	
Minnesota	30 RAP	A	741	3	-12, -18, -24, -28
Minnesota	5 PC RAS	A	777	3	
Minnesota	5 PM RAS	A	768	3	
Indiana	15 RAP HMA	A	551	3	-6, -12,-18,-22
Indiana	3 RAS HMA	A	502	3	
Indiana	3 RAS WMA	A	500	3	
Wisconsin	Evotherm® 3G	A	329	2	-12, -18, -24, -28
Wisconsin	No Evotherm®	A	364	2	
Colorado	20 RAP	A	350	2	-12, -18, -24, -28
Colorado	3 RAS/15 RAP	A	318	2	
Illinois	5 RAS/0 RAP Field	*	482	2	-12, -18, -24, -28
Illinois	5 RAS/0 RAP Lab	*	432	2	
Illinois	5 RAS/0 RAP Lab-GTR	*	430	2	
Illinois	5 RAS/11 RAP Field	*	337	2	
Illinois	5 RAS/11 RAP Lab	*	369	2	
Illinois	5 RAS/11 RAP Lab-GTR	*	385	2	

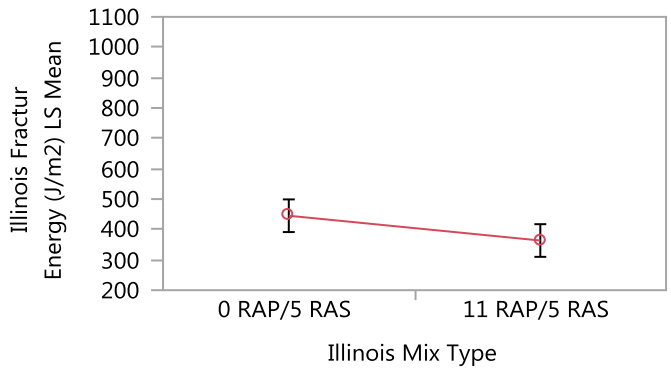

Figure 15. Fracture energy group means for Illinois mixes by RAP level

Pavement Condition Surveys

The results of the pavement condition surveys for each demonstration project are reported in Table 13. The number of pavement surveys conducted for each project was dependent on the timing and location of the project. Three post-winter surveys were completed for Minnesota and Indiana; two post-winter surveys were completed for Missouri and Iowa; and one post-winter survey was completed for Colorado, Illinois and Wisconsin.

During each survey, there was no measureable amount of permanent deformation. The clearest and most telling distress regarding pavement performance for all the projects was transverse cracking. This cracking was most likely reflective cracking since all the pavements with transverse cracks were asphalt overlays placed over jointed concrete pavement. The severity level and linear length of the transverse cracks was measured in each section. It is reported in linear feet per 500 feet of one traffic lane width.

For the Missouri and Minnesota projects, the RAS pavements exhibited more cracking than the non-RAS pavements. However, for the Iowa and Indiana projects RAS pavements exhibited the same amount of cracking or less than the non-RAS pavements. The Indiana WMA pavement with RAS exhibited more cracking than the HMA pavement with

Table 13. Pavement transverse cracking

State Agency	Mix ID	Transverse cracking (feet per 500 feet of 1 traffic lane)				
		After construction	1 winter after construction	2 winter after construction	3 winter after construction	4 winter after construction
Missouri	15 RAP	0	30	46		
Missouri	5 FRAS/10 RAP	0	52	97	-	-
Missouri	5 CRAS/10 RAP	0	41	139	-	-
Iowa	0 RAS	0	144	156	-	-
Iowa	4 RAS	0	137	142	-	-
Iowa	5 RAS	0	148	153	-	-
Iowa	6 RAS	0	146	147	-	-
Minnesota	30 RAP	-	-	-	0	0
Minnesota	5 PC RAS	-	-	-	143	173
Minnesota	5 PM RAS	-	-	-	150	199
Indiana	15 RAP HMA	-	4	158	191	-
Indiana	3 RAS HMA	-	35	162	172	-
Indiana	3 RAS WMA	-	47	264	277	-
Wisconsin	Evotherm® 3G	0	0	-	-	-
Wisconsin	No Evotherm®	0	0	-	-	-
Colorado	20 RAP	0	0	-	-	-
Colorado	3 RAS/15 RAP	0	25	-	-	-
Illinois	0 RAS/5 RAP Field	0	0	-	-	-
Illinois	0 RAS/5 RAP Lab	0	0	-	-	-
Illinois	0 RAS/5 RAP GTR	0	0	-	-	-
Illinois	11 RAS/5 RAP Field	0	0	-	-	-
Illinois	11 RAS/5 RAP Lab	0	0	-	-	-
Illinois	11 RAS/5 RAP GTR	0	0	-	-	-

RAS. In the case of the Wisconsin project, using Evotherm® with RAS did not decrease the pavement performance after one winter season. In the Minnesota project, slightly more cracking was observed in the mix using post-manufacturer RAS compared to the mix using post-consumer RAS. When taking into consideration the variability of the existing pavement condition beneath the asphalt overlays and the small difference in crack length among the different mix types for some projects, definitive conclusions about RAS pavements solely based on the surveys should be reserved.

Summary and Conclusions

This paper presents the results of Transportation Pooled Fund (TPF)-5(213), a collaboration of state transportation agencies in the United States with the goal of researching the effects of RAS on the performance of asphalt applications. As part of TPF-5(213), each state highway agency proposed a unique field demonstration project that investigated different aspects of asphalt mixes containing RAS specific to their state needs. The objective of these projects was to provide adequate laboratory and field test results to answer design, performance, and environmental questions about asphalt pavements with RAS. The demonstration projects focused on evaluating different aspects (factors) of RAS that were deemed important for each state to move forward with a RAS specification. RAS factors addressed in the different demonstration projects included the evaluation of the RAS grind size, RAS percentage, RAS source (post-consumer versus post-manufactured), RAS in combination with warm mix asphalt technology, RAS as a fiber replacement for stone matrix asphalt (SMA) pavements, and RAS in combination with ground tire rubber. Several of the demonstrations projects also included control sections to compare traditionally used mix designs containing either RAP only or no recycled product to mix designs containing RAS.

Field mixes from each demonstration project were sampled for conducting the following tests: dynamic modulus, flow number, four-point beam fatigue, semi-circular bending, and binder extraction and recovery with subsequent binder characterization. Pavement condition surveys were then conducted for each project after completion. The results of the study are summarized below:

- Observations from the demonstration projects show that RAS pavements can be successfully produced and meet state agency quality assurance requirements for mix asphalt content, gradation, and volumetrics. This includes the SMA mixes produced in Illinois which used five percent RAS in place of fibers; the RAS mixes produced in Indiana and Wisconsin that used foaming and Evotherm® WMA technologies, respectively; and the RAS mixes produced in Missouri which used RAS, RAP, and GTR.
- When RAS is used in HMA, the shingle binder blends with the base binder which increases the performance grade of the base binder on the high and low side. The average results of all the mixes in the study show that for every 1 percent increase in RAS, the low temperature grade of the base binder will increase 1.9°C; and for every 1 percent increase in RAP, the low temperature grade of the base binder will increase 0.3°C. Therefore, on average, 3 percent RAS or 20 percent RAP would be the maximum amount of recycled material allowed without requiring a low temperature grade bump (6°C) in the base binder. This corresponds to a 14 percent binder replacement when using RAS and a 20 percent binder replacement when using RAP, when considering the average asphalt content values for all the mix designs. However, this should only be used as a starting point of estimating how RAS will

affect HMA binder since the PG of the asphalt blends did vary among the different projects. When estimating how RAS will affect an HMA binder, agencies should consider the RAS source (post-manufacturer versus post-consumer) and whether a modifier is used in the base asphalt.

- The flow number and dynamic modulus results from the demonstration project mixes show that using RAS or a combination of RAS/RAP in HMA improves its rutting resistance. The pavement condition surveys confirmed the high rutting resistance of the mixes as there was no measurable amount of wheel path deformation in the pavements.
- All the mixes, with or without RAS, performed well with respect to fatigue cracking in the four-point bending beam test. The K2 coefficients ranged from 4.19 to 9.95 and the estimated fatigue endurance limits ranged from 53 to 359 micro-strain. The SMA mixes from Illinois which used five percent RAS exhibited the most desirable fatigue characteristics. In the case of the Indiana demonstration project, the RAS mixes performed the same as the RAP mix; and in the case of the Iowa, Missouri, Minnesota, and Colorado demonstration projects, the RAS mixes exhibited slightly better fatigue lives than the non-RAS mixes. Fibers in the RAS could be contributing to the improved mix performance. Based on the four-point bending beam results, HMA with RAS should perform as well as HMA without RAS with respect to fatigue performance.
- The SCB test results were evaluated by comparing the low temperature fracture energy group means of the mixtures for each demonstration project. There were no statistical differences at the 95 percent confidence level among the mix fracture

energies for every project except Iowa. For the Iowa mixes, the 0% RAS mix had a statistically lower fracture energy than the 4% RAS mix which suggests that RAS can improve the fracture resistance of HMA. With regards to the Missouri, Minnesota, Indiana, Wisconsin, Illinois, and Colorado demonstration projects, the lack of statistical differences in fracture energy indicates that the mixes with RAS have the same fracture resistance as the mixes without RAS. Based on the SCB results, the addition of RAS materials to HMA is not detrimental to its fracture resistance.

- The pavement condition surveys in Missouri revealed the pavement containing coarsely ground RAS exhibited more transverse cracking than the pavement containing finely ground RAS. In both the Missouri and Colorado demonstrations projects, the RAS pavements exhibited slightly more cracking than the non-RAS pavements. In contrast, the RAS pavements exhibited the same amount of cracking or less than the non-RAS pavements for the Iowa, and Indiana demonstration projects. In the Indiana project, more cracking was observed for the RAS mix produced with foaming WMA technology than the RAS mix produced without foaming. In the Minnesota project, slightly more cracking was also observed in the mix using post-manufacturer RAS compared to the mix using post-consumer RAS. However, when taking into consideration the variability of the existing pavement condition beneath the asphalt overlays and the small difference in crack length among the different mix types for some projects, definitive conclusions about RAS pavements solely based on the surveys should be reserved.

Acknowledgements

The authors would like to thank Dr. Mihai Marasteanu at University of Minnesota for conducting SCB testing, Jim McGraw at the Minnesota DOT for conducting the asphalt binder extractions, and Debra Haugen for her support on the project. The authors would like to also thank Joe Schroer (formally at the Missouri DOT) and Bill Stone at the Missouri DOT, Scott Schram at the Iowa DOT, Greg Johnson at the Minnesota DOT, Mike Prather at the Indiana DOT, Judith Ryan at the Wisconsin DOT, Roberto DeDios at the Colorado DOT, Abdul Dahhan at the Illinois DOT (IDOT), Hamid Moussavi at the California DOT, Audrey Copeland formerly at the Federal Highway Administration and now at the National Asphalt Pavement Association, and Victor Lee Gallivan at the FHWA. The research work was sponsored by the Federal Highway Administration and the Transportation Pooled Fund state agency partners: Missouri (lead agency), California, Colorado, Illinois, Indiana, Iowa, Minnesota, and Wisconsin.

References

AASHTO MP15 "Standard Specification for Use of Reclaimed Asphalt Shingles as an Additive in Hot-Mix Asphalt," Standard Specifications for Transportation Materials and Methods of Sampling and Testing, Washington D.C., 2009

AASHTO PP53 "Standard Practice for Design Considerations When Using Reclaimed Asphalt Shingles in New Hot-Mix Asphalt," Standard Specifications for Transportation Materials and Methods of Sampling and Testing, Washington D.C., 2009

AASHTO R29 "Standard Practice for Grading or Verifying the Performance Grade of an Asphalt Binder," Standard Specifications for Transportation Materials and Methods of Sampling and Testing, Washington D.C., 2012

AASHTO T27 "Standard Method of Test for Sieve Analysis of Fine and Coarse Aggregates," Standard Specifications for Transportation Materials and Methods of Sampling and Testing, Washington D.C., 2011

AASHTO T321 "Standard Method of Test for Determining the Fatigue Life of Compacted Hot-Mix Asphalt (HMA) Subjected to Repeated Flexural Bending," Standard Specifications for Transportation Materials and Methods of Sampling and Testing, Washington D.C., 2007

AASHTO T342 "Standard Test Method for Determining Dynamic Modulus of Hot-Mix Asphalt Concrete Structures," Standard Specifications for Transportation Materials and Methods of Sampling and Testing, Washington D.C., 2011

AASHTO T164 "Standard Method of Test for Quantitative Extraction of Asphalt Binder from Hot-Mix Asphalt," Standard Specifications for Transportation Materials and Methods of Sampling and Testing, Washington D.C., 2008

Abdulshafi, O.; Kedzierski, B.; Fitch, M.; and Muhktar, H. "Evaluation of the Benefits of Adding Waste Fiberglass Roofing Shingle to Hot-Mix Asphalt", Report Number FHWA/OH-97/006m, Ohio Department of Transportation, July 1997.

Asphalt Institute "Asphalt Handbook" Manual Series No. 4, Asphalt Institute, Lexington, KY, 2007

ASTM D225 "Standard Specification for Asphalt Shingles (Organic Felt) Surfaced With Mineral Granules," Annual Book of ASTM Standards. West Conshohocken, PA: ASTM International, 2001

ASTM D3462 "Specification for Asphalt Shingles Made from Glass Felt and Surfaced with Mineral Granules," Annual Book of ASTM Standards. West Conshohocken, PA: ASTM International, 2009

ASTM D5404 "Standard Practice for Recovery of Asphalt from Solution Using the Rotary Evaporator," Annual Book of ASTM Standards. West Conshohocken, PA: ASTM International, 2012

Brock, Ben, "Economics of RAS in HMA", Presentation at the 3rd Asphalt Shingle Recycling Forum, Chicago, Illinois, November 1-2, 2007.

Button, J.; Williams, D.; and Scherocman, J. "Roofing Shingles and Toner in Asphalt Pavements", Texas Transportation Institute, Research Report 1344-2F, July 1996.

Cascione, A., R.C. Williams, W.G. Buttlar, S. Ahmed, B. Hill, D.S. Haugen, and S. Gillen, "Laboratory Evaluation of Field Produced Hot Mix asphalt Containing Post-consuemr Recycled Asphalt Shingles and Fractionated Recycled Asphalt Pavement," Journal of the Association of Asphalt Paving Technologists, volume 80, p. 377, 2007.

Hansen, K. Guidelines for the use of Reclaimed asphalt shingles in asphalt pavements. IS-136. National Asphalt Pavement Association. Lanham, Maryland. 2006.

Hansen, KR and Copland, A. Annual Asphalt Pavement Industry Survey on Recycled Materials and Warm-Mix Asphalt Usage 2009-2012. National Asphalt Pavement Association's 3rd Annual Asphalt Pavement Industry Survey. IS-138. December 2013.

Hughes, CS. Uses of waste asphalt shingles in HMA – state of the practice. Special Report 179. National Pavement Association. Lanham, Maryland. 1997.

Huang Y, Bird RN, Heidrich O. "A review of the use of recycled solid waste materials in asphalt pavements." Resources, Conservation and Recycling. 52:58-73, 2007

Carpenter, S.H. "Fatigue Performance of IDOT Mixtures," Research Report FHWA-ICT-07-007, Illinois Center for Transportation, July 2006

Cleven, M.A., "Investigation of the Properties of Carbon Fiber Modified Asphalt Mixtures" (2000) MS Thesis, Michigan Technological University, Houghton, Michigan.

Cochran KM, Townsend TG. "Estimating construction and demolition debris generation using a materials flow analysis approach." Waste Management. 30:2247-2254, 2010.

Ghuzlan, K.A., Carpenter, S.H. 2006. "Fatigue damage analysis in asphalt concrete mixtures using the dissipated energy approach", Canadian Journal of Civil Engineering, Volume 33, pp890-901

Chiu C-T, Hsu T-H, Wang W-F. Life cycle assessment on using recycled materials for rehabilitating asphalt pavements. Resources, Conservation and Recycling. 2008;52:545-556

Grzybowski, K., Lewandowski, L. "Multi-Disciplinary Characterization of Recycled Roofing Materials for Asphalt Pavement Applications," *Presentation by PRI Asphalt Technologies Inc. presented at the Pavement Performance Prediction Symposium*, Laramie, Wyoming, July 2010

Huang, Yang H. "Pavement Analysis and Design," Second Edition, Prentice Hall, New Jersey, 2004

JMP, Version 8.02. SAS Institute Inc., Cary, NC, 1989-2014

Johnson, E., Johnson, G., Dai, S., Linell, D., McGraw, J., Watson, M. "Incorporation of Recycled Asphalt Shingles in Hot Mixed Asphalt Pavement Mixtures," Minnesota Department of Transportation, St. Paul, MN, 2010

Lee, J., Rust, J.P, Hamouda, H., Kim, Y.R., Borden, R.H., "Fatigue Cracking Resistance of Fiber-Reinforced Asphalt Concrete" (2005) Textile Research Journal, 75: 123.

Marasteanu, M.; Zofka, A.; McGraw, J.; Krivit, D.; Schroer, J.; and Olson, R. "Recycled Asphalt Shingles in Hot Mix Asphalt", Journal of the Association of Asphalt Paving Technologists, Volume 76, pp 235-274, 2007.

McGraw, J., Zofka, A., Krivit, D., Schroer, J., Olson, R., and Marasteanu, M. "Recycled asphalt shingles in hot mix asphalt," *Journal of the Association of Asphalt Paving Technologists*, Vol. 76, 235-274, 2007

National Association of Home Builders. From roofs to roads: Recycling asphalt roofing shingles into paving materials. NAHB Research Center, Upper Marlboro, MD. 1998.

NCHRP Report 646. 2010. "Validating the Fatigue Endurance Limit for Hot Mix Asphalt", Transportation Research Board, National Highway Research Council, Washington D.C.

Putman, B.J., Amirkhanian, S.N., 2004, "Utilization of Waste Fibers in Stone Matrix Asphalt Mixtures" (2004) Resources, Conservation and Recycling, Vol. 42, 265-274.

Roberts, F. L., Kandhal, P. S., Brown, E. R., Lee, D., and Kennedy, T. W. "Hot Mix Asphalt Materials, Mixture Design, and Construction," 2nd Ed. National Asphalt Pavement Association Research and Education Foundation, Lanham, Maryland, 1996

Sengoz B, Topal A. Use of asphalt roofing shingle waste in HMA. Construction and Building Materials. 2005;19:337-3463

Strategic Highway Research Program, "Binder Characterization and Evaluation, Volume 1: Physical Characterization," SHRP-A-367, National Research Council, Washington D.C. 1994

Tangella, S.C.S.R., Craus, J., Deacon, J.A., Monismith, C.L., 1990. "Summary Report on Fatigue Response of Asphalt Mixtures", Prepared for Strategic Highway Research Program Project A-003-A

Townsend, T.; Powell, J.; and Xu, C. "Environmental Issues Associated with Asphalt Shingle Recycling." Prepared for the Construction Materials Recycling Association and the US EPA Innovations Workgroup, October 19, 2007, Gainesville, Florida.

U.S. Environmental Protection Agency, Region 8. Analysis of Recycling of Asphalt Shingles in Pavement Mixes from a Life Cycle Perspective. July 2013. Contract No. EPW07020

Witczak, M.W., K. Kaloush, T. Pellinen, M. El-Basyouny, "Simple Performance Test for Superpave Mix Design," *National Cooperative Highway Research Program (NCHRP)*, Report 465, Washington D.C., 2002

Wu, S., Ye, Q., Li, N., "Investigation of Rheological and Fatigue Properties of Mixtures Containing Polyester Fibers" (2008) Construction and Building Mat., 22:2111-2115.

CHAPTER 3. PERFORMANCE-BASED DESIGN OF AN ASPHALT INTERLAYER FOR JOINTED CONCRETE OVERLAYS

Modified from a paper submitted to the *Journal of Materials in Civil Engineering*, published by the American Society of Civil Engineers (ASCE)

Andrew A Cascione[1] [2] and R. Christopher Williams[3]

Abstract

Reflective cracking in hot mix asphalt (HMA) overlays has been a common cause of poor pavement performance in Iowa for many years. Reflective cracks commonly occur in HMA overlays when deteriorated portland cement concrete is paved over with HMA. This results in HMA pavement surfaces with poor ride quality and increased transportation maintenance costs. To delay the formation of cracks in HMA overlays, the Iowa Department of Transportation (Iowa DOT) has begun to implement a crack-relief interlayer mix design specification. The crack-relief interlayer is an asphalt-rich, highly flexible HMA that can resist cracking in high strain loading conditions. In this project, the field performance of an

[1] Ph.D. candidate, Department of Civil, Construction, and Environmental Engineering, Iowa State University, Ames, IA 50011. E-mail: aacascio@iastate.edu

[2] Primary researcher and author

[3] Professor of Civil Engineering, Department of Civil, Construction, and Environmental Engineering, Iowa State University, Ames, IA 50011. E-mail: rwilliam@iastate.edu

HMA overlay using a one inch interlayer was compared to a conventional HMA overlay without an interlayer. Both test sections were constructed on US 169 in Adel, IA as part of an Iowa DOT overlay project. The laboratory performance of the interlayer mix design was assessed for resistance to cracking from repeated strains by using the four-point bending beam apparatus. An HMA using a highly polymer modified binder was designed and shown to meet the laboratory performance test criteria. The field performance of the overlay with the interlayer exceeded the performance of the conventional overlay that did not have the interlayer. After one winter season, 29 percent less reflective cracking was measured in the pavement section with the interlayer than the pavement section without the interlayer. The level of cracking severity was also reduced by using the interlayer in the overlay.

Introduction

Distressed portland cement concrete (PCC) pavements in Iowa are commonly rehabilitated with hot mix asphalt (HMA) overlays. HMA overlays are a cost effective measure that extend the life of the existing pavement structure and provide a smooth driving surface. This method of pavement rehabilitation is accomplished by paving one or more lifts of HMA over an existing PCC pavement.

The service life of an HMA overlay is often reduced from reflective cracking occurring at PCC transverse and longitudinal joints. As PCC deteriorates, cracks typically form at the joints which create discrete sections of concrete slabs that contract and expand due to thermal or moisture changes (Mukhtar et al. 1996). This mechanism of differential movement below an HMA overlay induces stress concentrations at the bottom of the HMA overlay that are large enough to initiate microcracks in the HMA at the PCC interface. Over time, the cracks grow and propagate to the surface of the HMA layer. Reflective cracking is

generally not load initiated; however, traffic loading can cause a breakdown of the HMA at the initial crack (Huang 2004).

Reflective cracks are initially low-severity cracks (less than 0.25 in thick) and do not influence pavement performance significantly. However, if left unsealed, moisture will infiltrate the pavement and increase the crack width. With the application of traffic loads and heavier axle loads, the cracks will eventually become moderate to severe (greater than 0.75 in thick) and significantly contribute to pavement deterioration (O-Antwi et al. 2007). Different types of mitigation strategies that help delay reflective cracking have been used with varying levels of success. These include: cracking and seating of the PCC pavement, concrete rubbilization (Chen et al. 2014), placement of a geosynthetic fabric (Button et al. 2006), and sawcutting and sealing of the HMA overlay at the PCC joint locations.

One of the more promising approaches used to delay reflective cracking is incorporating an asphalt-rich, highly flexible, crack-relief HMA interlayer within the asphalt structure that serves as barrier to prevent reflective cracks from either forming or propagating to the surface of the overlay. A crack-relief interlayer usually contains a nominal maximum aggregate size of 4.75mm and is placed either at the bottom of the HMA overlay or between the leveling and surface course mixes. Its asphalt-rich properties result in a lower modulus material that does not add structural value to the pavement system. Therefore, it is not typically placed in a lift thickness greater than one inch.

Literature Review

Interlayer HMA mixes should be designed with soft materials that have the ability to dissipate excessive stresses induced by cracks or joints (Baek et al. 2011). This has been

successfully accomplished by designing an HMA with a low air void content and high asphalt content that uses a highly polymer modified asphalt binder (Blankenship et al. 200). In 1998 the Missouri Department of Transportation compared an HMA overlay containing a crack-relief interlayer with a traditional overlay containing no interlayer on Route I-29 (MDOT 2000). After three years of service, the interlayer section contained 36 percent less reflective cracks than the control section (Blankenship et al. 2005). Wisconsin Department of Transportation also documented their use of crack relief interlayers for several overlay projects from 1996 to 2002 (Makowski et al. 2005). In three out of four projects, there was a clear delay of cracking (42 percent average crack reduction) when using a pavement overlay with an interlayer.

In 2003 the Illinois Department of Transportation constructed an HMA overlay with a sand mix interlayer on Illinois Route 130. The sand mix interlayer contained an asphalt content of 8.6 percent using a polymer modified PG76-28. After three years, the pavement section with the sand mix interlayer contained 21 percent less reflective cracks than the control section without the interlayer (Baek et al. 2011).

Similar crack relief interlayer mixes have also been previously used by the Iowa Department of Transportation (Iowa DOT). An overlay containing the STRATA® interlayer system was paved in 2001 on Iowa Highway 9 in Decorah, Iowa. A control section containing no interlayer was also paved for comparison. After four years, the interlayer section contained approximately 54 percent less reflective cracks than the control section (Buttlar 2007).

Some state transportation agencies, such as the Utah DOT, have implanted the use of interlayers by creating construction specifications for designing reflective cracking relief

bituminous mixtures (Hajj 2008). The specifications for these mix designs meet general HMA mix design criteria except the mix is designed to a target air void of 0.5 to 2.5 percent at 50 design gyrations along with criteria for VMA, Hveem stability, and flexural beam fatigue testing.

Not all HMA overlays with crack relief interlayers perform comparability or better than HMA overlays without interlayers. Blankenship et al. (2005) demonstrated that well designed overlays containing highly flexible, asphalt-rich interlayers only substantially reduce reflective cracking if the interlayers meet laboratory performance testing criteria on the four-point bending beam following AASHTO T-321. Interlayer mixes tested in the four-point bending beam at 2000 μstrain that experienced a greater than 50 percent reduction in flexural stiffness before reaching 100,000 load cycles did not reduce the crack rate growth in the HMA overlays in two Wisconsin DOT test sections. However, based on the results of Iowa, New Jersey, Illinois, Virginia, and Missouri test sections, interlayer mixes that passed 100,000 load cycles in the four-point bending beam before experiencing a greater than 50 percent reduction in flexural stiffness had reduced the average crack rate growth per year in the test sections by an average of 52 percent.

Project Objectives

In 2012, the Iowa DOT developed a performance-based specification for crack-relief interlayer mix designs. To assess the effectiveness of an interlayer, the Iowa DOT selected an overlay project on US 169 in Adel, IA in 2013 for conducting a field performance evaluation project. The project included two test sections: one section was paved with a traditional overlay and a second section was paved with an overlay containing the interlayer. The objectives of this project were to assess the interlayer mix design by conducting laboratory

performance testing on the four-point bending beam. Following construction of the overlays, analysis of pavement cracking in both test sections was conducted by surveying the pavement after one winter season and obtaining cores at cracked locations in each test section.

Asphalt Interlayer Description

Mix Design Specifications

The interlayer mix design was engineered to follow the Iowa DOT's Special Provision titled "Special Provisions for Reflective Crack Delay System". The goal of the specification is to create a highly flexible, asphalt-rich HMA that meets laboratory performance criteria in the four-point bending beam. The material requirements and volumetric specifications for the interlayer mix design are listed in Table 14 and 15. The PG+ 64-34 binder specification is designed to ensure the asphalt binder is polymer modified to enhance its elastic properties. The wide performance grade temperature range and polymer modification maximizes the asphalt binder's ability to recover from high levels of stress induced from concrete slab movements at pavement joints. By possessing a maximum low critical failure temperature of -34°C, the binder contains elastic properties at low temperatures to recover from deformations caused by thermal and repeated loading stresses. By possessing a minimum high failure temperature of 64°C, the binder has a high viscosity to resist deformation and plastic flow. The 3/8 inch maximum aggregate size allows for paving thin lifts that are one inches or less.

Table 14. Interlayer mix design specifications

Asphalt Binder	PG+ 64-34
Gradation	Minus 3/8”
Ndesign	50 gyrations
Design Target Air Voids	0.5% to 2.0%
Minimum Voids in the Mineral Aggregate (VMA)	16%
Minimum Voids Filled with Aggregate (VFA)	70% to 95%

Table 15. Interlayer gradation specification

Sieve	**Percent Passing**
3/8 inch	100%
No. 4	80-100%
No. 8	60-85%
No. 16	40-70%
No. 30	25-55%
No. 50	15-35%
No. 100	8-20%
No. 200	6-14%

In addition to volumetric and gradation requirements, the Iowa DOT interlayer mix design specification also contains a performance testing requirement using the four-point bending beam apparatus (Figure 16) in accordance with AASHTO T-321: *Determining the fatigue life of compacted HMA subjected to repeated flexural bending*. The four-point bending beam test was conducted at Iowa State University’s (Iowa State) Advanced Asphalt Laboratory on two replicate hot mix asphalt specimens for fatigue resistance. Specimens were fabricated using aggregates and asphalt binder supplied by Des Moines Asphalt, Inc. An aggregate batch representative of the mix design was mixed with the asphalt binder at 135°C. After two hours of oven aging at 135°C, the mix was compacted in a linear kneading slab compactor to fabricate an asphalt slab within +/-1.0 percent of the design air voids of 2.0 percent. The slab was subsequently saw cut into beam specimens. Specimens were

conditioned and tested in a 20°C environmental test chamber. Two replicate beam specimens were tested in the four-point bending beam in a cyclic loading condition at 2000μstrain with a 10Hz rate of loading. Cyclic loading of the specimens was complete until the specimens either obtained 50 percent of their initial flexural stiffness or passed the Iowa DOT specification of 100,000 load cycles without obtaining 50 percent of their initial stiffness. The initial flexural stiffness was determined as the average flexural stiffness of the first 200 cycles.

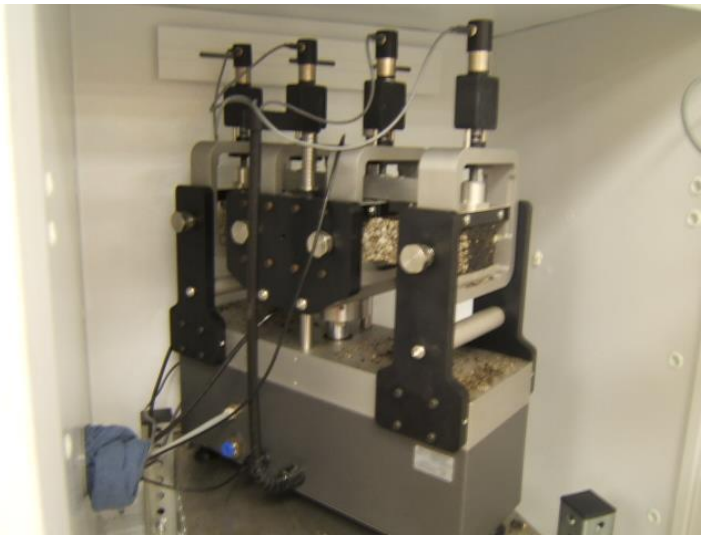

Figure 16. Four-point bending beam apparatus

Mix Design Assessment

Des Moines Asphalt, Inc. designed the interlayer mix for the project which contained an asphalt content of 7.38 percent and an air void content of 1.5 percent (Table 16). The initial binder supplied during the mix design phase, supplied by Bituminous Materials in Tama, IA, contained two percent SBS polymer. Initial performance testing of the mix design at Iowa State (discussed in the next section) indicated the mix did not meet the four-point bending beam testing requirements of passing 100,000 load cycles (Figure 17). The research team at Iowa State proposed that either the gradation of the mix design should be adjusted to

achieve a higher binder content at a 1.5 percent air void level or the polymer content should be increased to five percent. Due to time constraints, the second option was pursued.

Table 16. Interlayer mix design properties

Asphalt Content	7.38%
Air Voids	1.5%

A second mix design sample was then batched in the laboratory using a binder modified with five percent SBS polymer. The binder was prepared at Iowa State's laboratory using a PG 52-34 for the base asphalt and Kraton D1101 SBS for the polymer. Using a laboratory shear mill, the D1101 polymer was blended with the base asphalt for three hours at 180°C. No crosslinking agent was added during the process. The performance of the new mix design in the four-point bending beam improved, but it still not meet the minimum 100,000 load cycle requirement (Figure 17).

At this point in the project, the Iowa State research team proposed the asphalt binder be modified with Kraton D0243 polymer, a new SBS polymer manufactured by Kraton, Inc. that can be formulated with asphalt binder as high as seven to eight percent. High-polymer modified mixes using this polymer have demonstrated superior fatigue resistance (Willis et al. 2012). Improved mix performance results from the polymer forming a continuous elastomeric network within the binder. A third mix design was then batched in the laboratory using the same PG 52-34 base binder modified with 7.5 percent D0243. Procedures recommended by Kraton were followed for preparing the polymer modified binder in the laboratory. No crosslinking agent was added during the process.

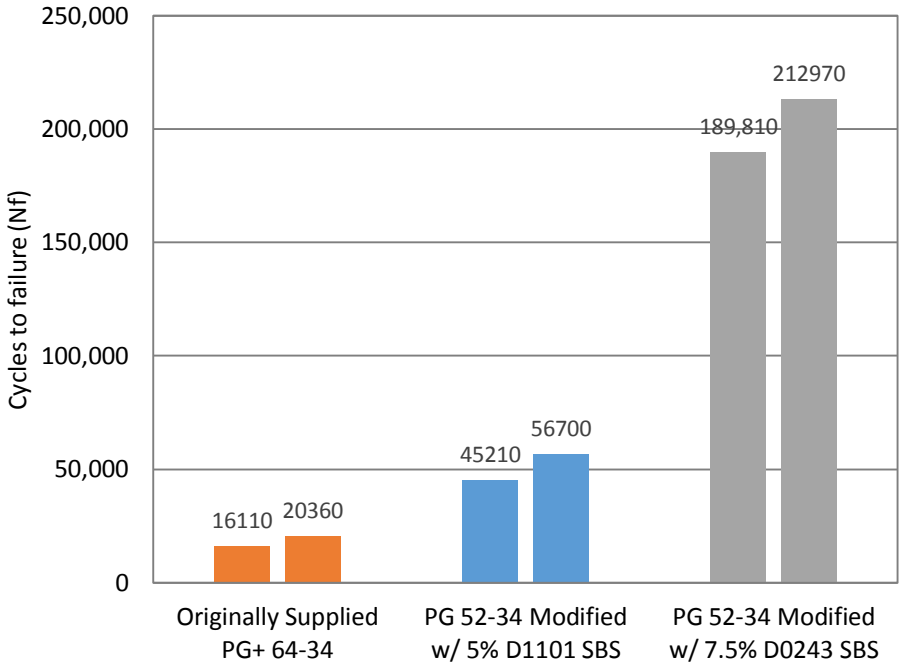

Figure 17. Four-point bending beam results on different interlayer mixes

The asphalt mix design using the high-polymer modified binder passed the 100,000 load cycle requirement in the four-point bending beam (Figure 17). A regression analysis of the flexural stiffness data was performed in accordance with AASHTO T-321 on each of the two beams that were tested (Figures 18 and 19). The regression analysis results are presented in Table 17. For the two beam samples tested, both the number of load cycles and the regressed failure number of load cycles exceeded the minimum fatigue life of 100,000 load cycles. The average regressed failure load cycles for the two beams was 244,623. Once the mix design with the 7.5 percent polymer modified binder passed the four-point bending beam results, the interlayer was approved by the Iowa DOT for paving.

Table 17. Four-point bending beam results on interlayer using 7.5% polymer

	Beam-1	Beam-2	Average
Air Voids	1.9	1.7	1.8
µStrain	2000	2000	
Initial Stiffness (@ 200 Load Cycles) (MPa)	790	828	
Failure Flexural Stiffness (50% of Initial) (MPa)	395	414	
Load Cycles at end of test	212,970	189,810	
Flexural Stiffness at end of test (MPa)	505	513	
Regressed Failure Load Cycles	156,795	220,512	244,623

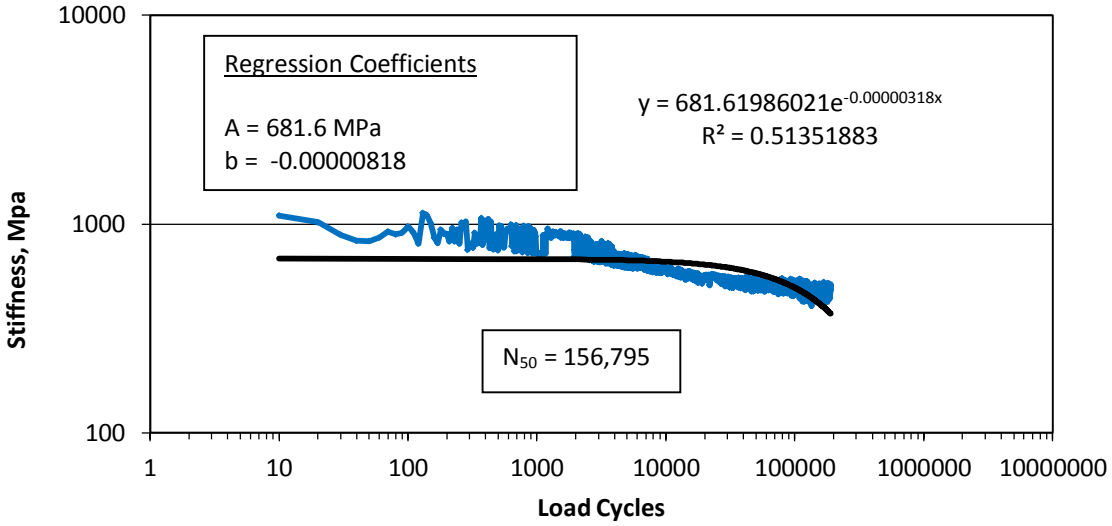

Figure 18. Stiffness versus load cycles (repetitions), beam-1

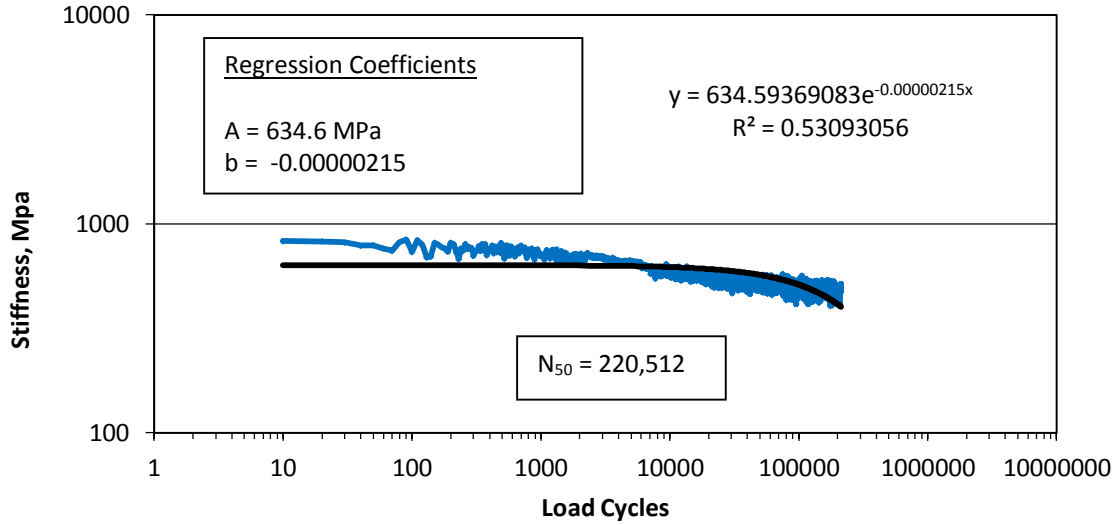

Figure 19. Stiffness versus load cycles (repetitions), beam-2

Pavement Construction

Construction of the interlayer was completed by Des Moines asphalt on August, 23 2013 (Figure 20). The project was located on US 169 in Adel, Iowa from the North Raccoon River to the South Raccoon River for a total length of 0.75 miles. The interlayer was part of Iowa DOT project MP-169-4(706)—76-25, an HMA resurfacing project which consisted of overlaying eight inches of a jointed concrete pavement with four inches of HMA. The project was divided into two sections: the northbound and southbound lane from station 101+63.5 to 121+39.5 was paved with a two inch surface course over a two inch intermediate course; the northbound and southbound lane from station 121+39.5 to 141+15 was paved with a two inch surface course over the one inch interlayer over a one inch intermediate course (Figures 21 and 22).

Figure 20. Interlayer paving on US 169

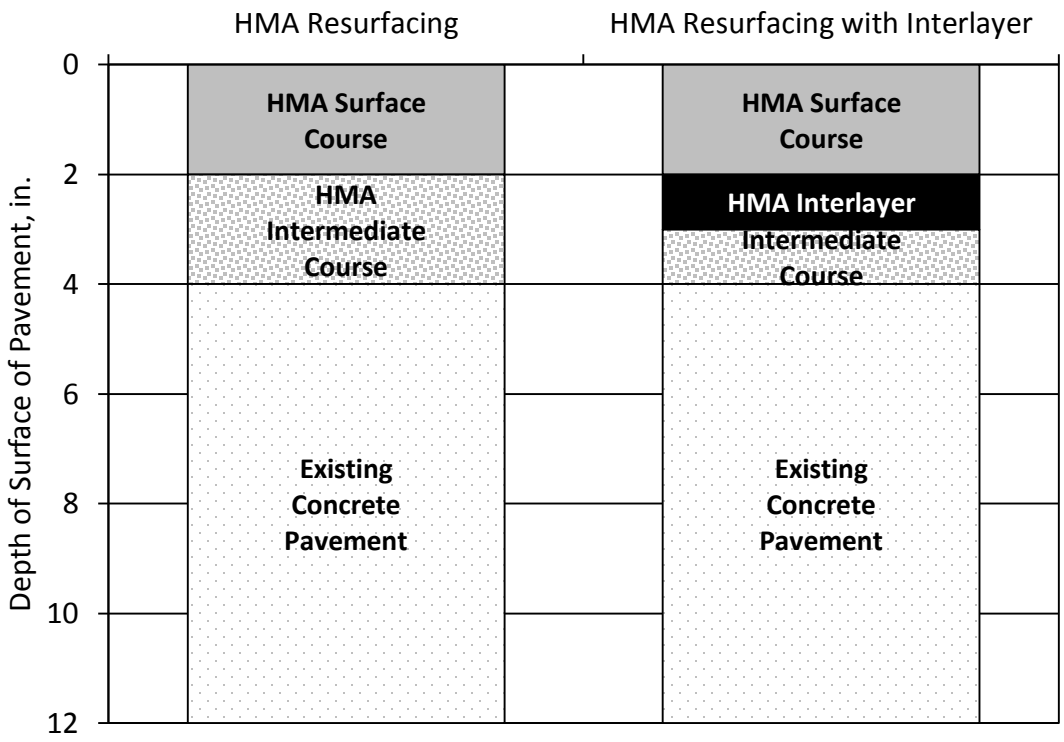

Figure 21. Cross sections of US 169 HMA resurfacing

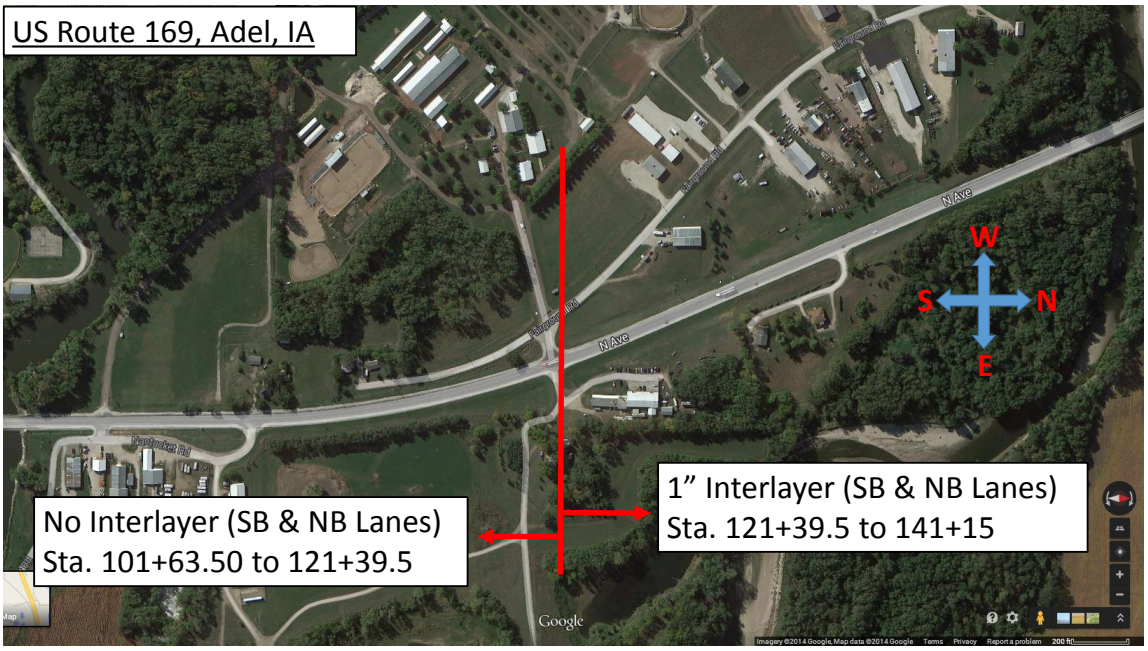

Figure 22. Satellite view of US 169 project limits

A sample of the field produced mix was obtained by the contractor and split between the Iowa DOT and Iowa State. As shown in Table 18, quality assurance testing conducted by the Iowa DOT revealed the laboratory air voids of the field mix sample was 4.8 percent, which was much higher than the 1.0 percent production tolerance. The reason for the high air voids is evident from the low asphalt content as measured by the reading from the asphalt flow meter at the HMA production plant. The asphalt content was 6.25 percent which was outside the production tolerance of 0.3 percent. Iowa State's laboratory verified the low asphalt content by testing the split sample in the ignition furnace. A 6.12 percent asphalt content was measured after calibrating the furnace with a dry aggregate batch of the mix design.

Table 18. Quality Assurance Testing Results

Mix Design Target Values	Quality Assurance Test Results
1.5% air voids	4.8% air voids
7.38% asphalt content	6.25% (plant flow meter) 6.12% (laboratory ignition furnace)

Producing the interlayer with high air voids and a low asphalt content resulted in the interlayer mix failing the four-point bending beam 100,000 load cycle requirement. The average load cycles at 50 percent initial stiffness was only 63,985 for the interlayer mix (Table 19). A reduction in asphalt content resulted in a material with a higher air void content and a higher flexural stiffness. In a strain-controlled test environment, an increase in these two variables will reduce the fatigue life of the pavement (Cooper and Pell 1974). Had the volumetrics been closer to the intended design, the performance of the interlayer in the four-point bending beam would have improved.

Table 19. Four-point bending beam results on field produced interlayer

	Beam-1	Beam-2	Average
Air Voids	2.3	2.4	2.4
µStrain	2000	2000	
Initial Stiffness (@ 200 Load Cycles) (Mpa)	1510	1593	
Flexural Stiffness at end of test (Mpa)	684	710	
Load Cycles at 50% of Initial Stiffness	66,120	61,850	63,985

Post-Construction Assessment

Pavement Condition Survey

Before and after pictures of the asphalt intermediate (base) course paving were captured by Google Street View. Figure 23 shows a screen capture of the PCC pavement on US 169 in the future non-interlayer section, dated August 2011, two years before the overlay project. Transverse and longitudinal joint deterioration can be seen in the screen capture. Joint deterioration of this magnitude is the primary cause of reflective cracking in HMA overlays, thereby, making this overlay project a perfect candidate to evaluate the effectiveness of a crack-relief interlayer.

Figure 24 shows a screen captures of the same location in August 2013, at least three to four weeks after the intermediate course was paved for the overlay project. In the non-interlayer pavement section, the intermediate course overlay is two inches thick. The screen capture shows the intermediate HMA course to be in good condition.

Figure 23. Pre-construction view of non-interlayer section on US 169

Figure 24. Post-construction view of intermediate course in non-interlayer section on US 169

Similar screen captures were obtained from Google Street View images for the interlayer overlay section as well (Figures 25 and 26). In Figure 25, a high level of joint deterioration can be seen in the future interlayer section. And unlike the non-interlayer section, the intermediate course is already cracking in the same construction season (Figure 26). The difference between the two different overlay sections is the thickness of the intermediate course. The intermediate course in the interlayer section was only one inch thick, not two inches thick, to provide room for the interlayer. This demonstrates just how quickly reflective cracks form in thin overlays (one inches) and is precisely the reason why overlays for distressed PCC pavements are designed to have a certain minimum thickness. In the case of this project, the overlay thickness design was four inches. However, by waiting several weeks between construction of the intermediate course and the surface course, the one inch course was thin enough to crack prior to paving the second lift.

Figure 25. Pre-construction view of interlayer overlay section on US 169

Figure 26. Post-construction view of intermediate course in interlayer section on US 169

A pavement condition survey was conducted in April 2014, one winter season after the overlay project was completed, to assess the amount of cracking in the interlayer and non-interlayer overlays. Transverse cracking distresses are evident in the pavement as shown Figure 27. The cracks are mostly like reflective cracks since the distance (20 feet) between the cracks exactly matches the joint spacing of the underlying PCC pavement.

Figure 27. Photo of reflective cracks in non-interlayer overlay on US 169 in April 2014

Results of the survey are summarized in Figures 28 and 29. Transverse cracks were measured in both the interlayer section and non-interlayer section. The below average temperatures Iowa experienced in 2013-2014 winter season may have accelerated the severity of the cracking distresses between the end of construction in August 2013 and the pavement survey in April 2014. Survey results are presented in Figures 28 and 29. After one winter season, more cracking occurred in the pavement with the traditional overlay than in the pavement with the crack-relief interlayer. 474 linear feet of transverse cracking was measured in the traffic lanes of the interlayer section compared to 336 transverse cracking in the non-interlayer test section. These results are particularly positive for the interlayer test section since the quality assurance and performance testing results of the field produced mix (Table 18 above) revealed the interlayer was low on asphalt content and high on air voids with an air void level similar to a traditional HMA mix design. The four-point bending beam

tests also revealed the interlayer did not meet the performance testing requirement. Nevertheless, the interlayer test section still contained 29 percent less reflective cracking than the non-interlayer test section. Even less cracking would exist in the interlayer overlay had the volumetrics of the interlayer been closer to the intended mix design targets.

Not only do the results of the survey demonstrate that more cracking occur in the non-interlayer section, but also the severity level of the cracking was greater in the non-interlayer section. In the non-interlayer section, 41 percent of the total transverse crack lengths measured contained moderate severity cracks. In the interlayer section, 4 percent of the total crack lengths measured contained moderate severity cracks. Moderate severity cracks have a width between 0.25 and 0.75 inches while low severity cracks have a width less than 0.25 inches.

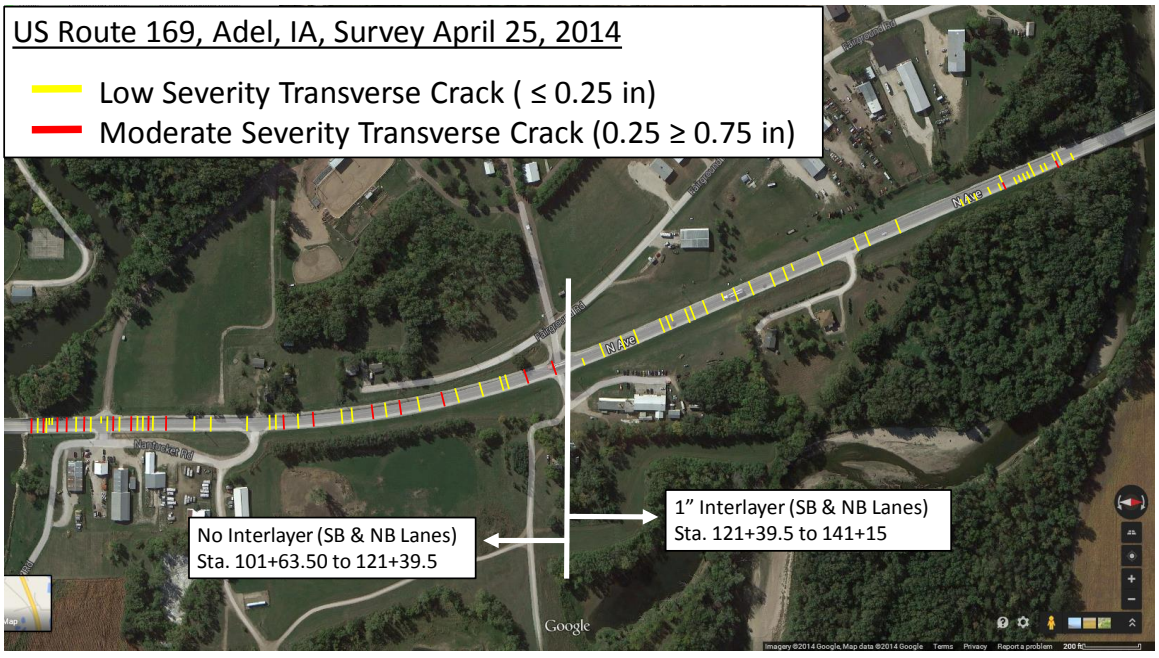

Figure 28. Satellite view of transverse cracking on US 169

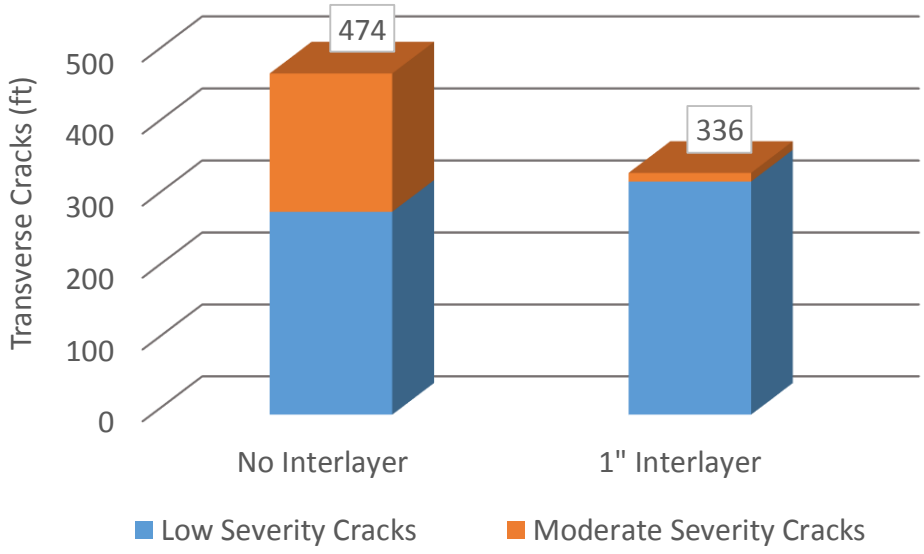

Figure 29. Total transverse cracking in traffic lanes

Pavement Core Samples

Subsequent to the pavement condition surveys, cores were obtained at four transverse crack locations: two in the interlayer section and two in the non-interlayer section. Broken concrete and joint sealant material at the bottom of each HMA core confirmed the cracks were above PCC joints and are indeed reflective. A full depth crack was found in the first core obtained from the interlayer section as shown in Figure 30a. This indicates the interlayer was susceptible to cracking; however, this was not true for all transverse cracked areas. The photograph of the second core obtained from the interlayer section (Figure 30b) shows no crack in the interlayer mix. While the pavement did crack over the PCC joint, the interlayer was effective in preventing the crack from becoming a full depth crack. No cracks were visible in the intermediate course, but it is possible a microcrack does exist in the

intermediate course and will grow with time. Upon recovering this core from the drill bit, the core separated at the surface course and interlayer interface raising the question of possible delamination. Delamination can occur due to insufficient bond strength in the tack coat or moisture infiltration. Based on a literature review of field investigations for overlay systems using an interlayer, delamination of overlays containing crack-relief interlayers has not been reported to have occurred at a higher frequency compared to typical overlays. Since this was the only core that showed signs of delamination, it may be an isolated incident or may have been caused by the force of the core drill.

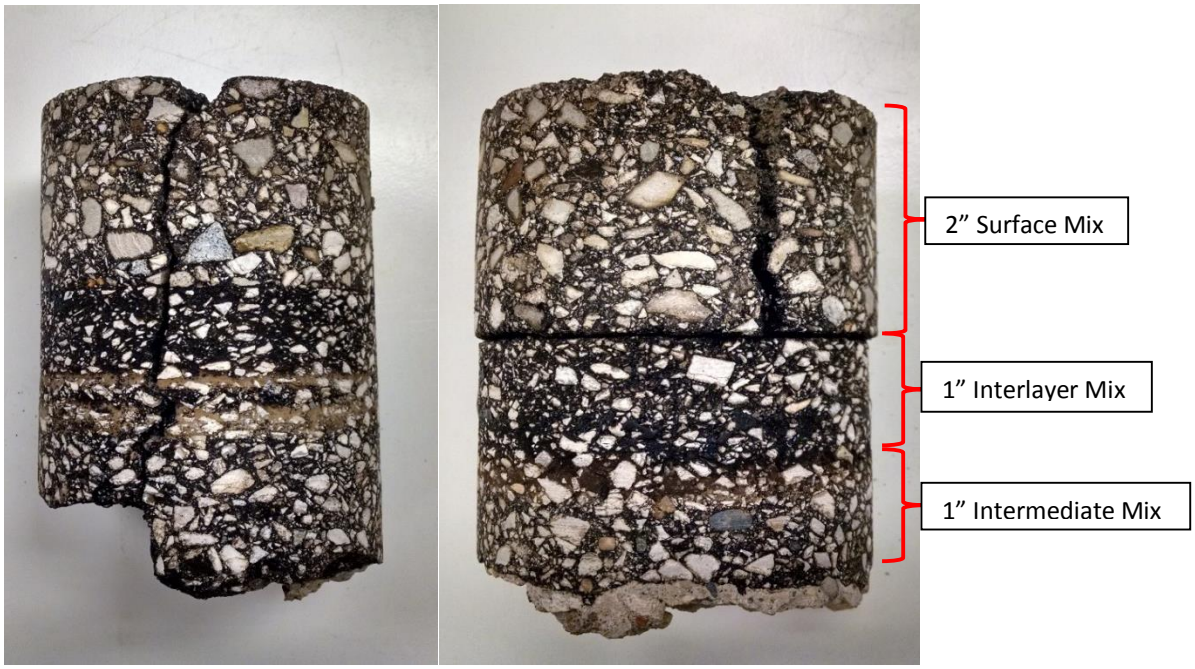

(a) (b)

Figure 30. Cores obtained from pavement section with interlayer in SB lane (a) Sta. 140+12 (b) Sta. 137+85

The cores shown in Figure 31 were obtained in the non-interlayer section over PCC joints. Full depth cracks in both cores indicate the traditional HMA overlay strategy resulted in reflective cracking in the overlay.

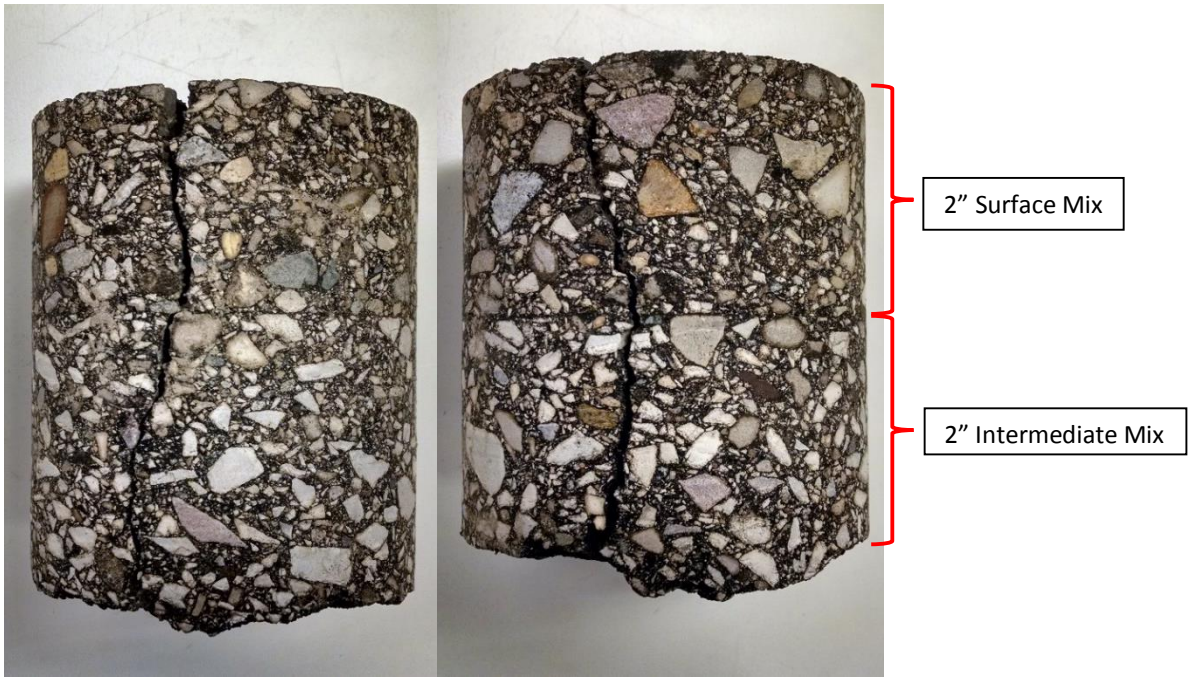

(a) (b)

Figure 31. Cores obtained from pavement section with no interlayer in SB lane (a) Sta. 111+86 (b) Sta. 113+98

Economic assessment

Interlayer mixes will typically cost more than a conventional HMA mixes since highly polymer modified asphalt is used in the design. To determine the additional cost of using an interlayer, the published bid quantities from Des Moines Asphalt were used to analyze the cost differences between the pavement section with and without the interlayer. Since the length of the interlayer pavement section was 1975.5 feet and the length of the non-

interlayer section was 1976 feet, the bid quantities were appropriately divided for assessing the cost of the two pavement sections.

The total cost for constructing the HMA overlay without the interlayer was $157,759.03 and the total cost for constructing the HMA overlay with the interlayer was $174,479.61 (Table 20). This equates to a 10.6 percent increase in materials and paving costs for constructing an HMA overlay with an interlayer. The benefit of the additional costs was realized from the 29 percent reduction in transverse cracking after the first year of paving with a decrease in the severity of the transverse cracks (41 percent moderate severity vs. 4 percent moderate severity). Furthermore, the reduction in cracking would more than likely have been greater if the field produced interlayer met the volumetric and laboratory performance testing requirements (see Table 18).

Table 20. Interlayer cost comparison from contractor bid tab

Item Description	Quantity (Ton)	Unit Price	Amount
Overlay with no Interlayer			
HMA 1/2" Surface Course	817.35	$ 55.00	$ 44,954.25
HMA 1/2" Intermediate Course	826.00	$ 55.00	$ 45,430.00
Asphalt Binder PG 58-28	126.17	$ 534.00	$ 67,374.78
Total			**$ 157,759.03**
Overlay with Interlayer			
HMA 1/2" Surface Course	817.35	$ 55.00	$ 44,954.25
HMA 3/8" Interlayer Course	412.00	$ 74.00	$ 30,488.00
HMA 3/8" Intermediate Course	413.80	$ 74.00	$ 30,621.20
Asphalt Binder PG 58-28	94.53	$ 534.00	$ 50,479.02
Asphalt Binder PG 64-34	24.70	$ 726.20	$ 17,937.14
Total			**$ 174,479.61**

Conclusions and recommendations

The Iowa Department of Transportation's (Iowa DOT) crack-relief interlayer specification was structured to create an HMA mix design with a high volume of asphalt and low percentage of air voids. This was accomplished, in part, by specifying a low level of design gyrations (50 gyrations) for laboratory compaction, a minimum VMA of 16 percent, and an air void content less than two percent. Performance testing the interlayer using the four-point bending beam ensured the final design is a highly flexible fatigue-resistant asphalt mixture.

For the US 169 HMA overlay project, the initial interlayer mix design failed the minimum 100,000 load cycle criteria in the four-point bending beam but eventually passed the criteria after the polymer modified binder used for the mix design was re-engineered. Rather than using the minimum amount of SBS polymer to formulate a PG 64-34 binder, a highly polymer modified binder was designed for the interlayer mix. The polymer used was an SBS polymer design by Kraton, Inc. (D0432) which can be added to asphalt at higher polymer concentrations without reducing workability. Seven and a half percent of the D0432 was selected to be blended in a base PG 52-34 binder. Once the new highly polymer modified binder was used for the mix design, the average number of load cycles achieved in the bending beam apparatus increased from 18,235 to 201,390, thereby passing the 100,000 load cycle criteria.

For the US 169 project, the performance of the overlay with the interlayer exceeded the performance of the conventional overlay that did not have the interlayer. After one winter season, 29 percent less reflective cracking was measured in the pavement section with the interlayer than the pavement section without the interlayer. The level of cracking severity

was also reduced by using the interlayer in the overlay. In the non-interlayer section, 41 percent of the total transverse crack lengths measured contained moderate severity cracks. In the interlayer section, 4 percent of the total crack lengths measured contained moderate severity cracks. Thus, the crack-relief interlayer successfully delayed reflective cracking in the HMA overlay.

Pavement performance improved by using the interlayer in spite of the interlayer not meeting the volumetric and laboratory performance testing requirements – the result of a low asphalt content during production. Had the volumetrics of the interlayer been closer to the mix design targets, the overlay would most likely have exhibited even less cracking. Since the cost of using an interlayer only increased the overlay construction costs by 10.6 percent, this project demonstrates the economic benefit of using an interlayer for HMA overlays. Based on the substantial reduction in reflective cracking and only marginal cost increases from using the interlayer on US 169, it is recommended that future HMA overlay projects in Iowa consider incorporating the crack-relief interlayer to delay reflective cracking. The provisional crack-relief interlayer specification drafted by the Iowa Department of Transportation proved to be effective in reducing reflective cracking in the HMA overlay. Therefore no change in the specification is recommended at this time. However, since the field produced interlayer did not meet the four-point bending beam performance criteria, this project demonstrates the importance of verifying the laboratory fatigue performance of the field produced interlayer.

For future interlayer mixes that do not initially meet the minimum 100,000 load cycle criteria in the four-point bending beam, the number of load cycles the mix design can achieve in the performance test can be increased by improving the elastic and fatigue resistant

properties of the binder. Based on the laboratory test results for this project, a highly modified 7.5 percent SBS asphalt binder formulation can be used to create an interlayer mix design that meets four-point bending beam performance criteria.

Acknowledgements

The authors would like to thank the Iowa Highway Research Board for sponsoring this research. The authors also would like to thank Bhooshan Karnik and Scott Schram of the Iowa Department of Transportation and District 4 of the Iowa Department of Transportation for their cooperation with the project. Additionally, the authors would like to also thank the Asphalt Pavement Association of Iowa (APAI) for hosting the field demonstration project.

References

Baek, J., I.L. Al-Qadi. 2011. Sand mix interlayer to control reflective cracking in Hot-Mix-Asphalt overlay. *Transportation Research Record. Journal of the Transportation Research Board.* No. 2227. 53-60

Blankenship, P., J. Drbohlav, and N. Iker. 2005. Interlayer and design considerations to retard reflective cracking. *Transportation Research Record. Journal of the Transportation Research Board.* No. 1896. 177-186

Blomberg, J.M. 2000. *Superpave overlay of sand anti-fracture layer over PCCP.* Research Investigation RI97-045. Missouri Department of Transportation, Research, Development, and Technology

Buttlar, B. 2007. Reflective crack relief interlayers. *OMG Brown Bag Seminar Series.* University of Illinois at Urbana-Champaign, Urbana

Button, J.W. and R.L. Lytton. 2007. Guidelines for using geosynthetics with Hot-Mix-Asphalt overlays to reduce reflective cracking. *Transportation Research Record*. Journal of the Transportation Research Board. 111-119

Chen, C., R.C. Williams, M.G. Marasinghe, J.S. Omundson, and S.A. Schram. 2014. Survival analysis for composite pavement performance in Iowa. *Transportation Research Board 93rd Annual Meeting*. Paper #14-4688

Cooper, K.E., P.S. Pell. 1974. *The effect of mix variables on the fatigue strength of bituminous materials.* Laboratory Report 633. Transport and Road Research Laboratory

Hajj. E.Y., P.E. Seboly, and L. Loria. 2008. *Reflective cracking of flexible pavements Phase 1 and II recommendations.* Research Report No. 13JF-1. Reno, Nevada. Nevada Department of Transportation

Huang, Y.H. 2004. *Pavement Analysis and Design.* Second Edition. Upper Saddle River, NJ: Pearson Prentice Hall

Makowski, L., D.L. Bischoff, P. Blankenship, D. Sobczak, and F. Haulter. 2005. Wisconsin experiences with reflective crack relief projects. *Transportation Research Record. Journal of the Transportation Research Board.* No. 1905. 44-55

Mukhtar, M.T., and B.J. Dempsey. 1996. Interlayer Stress Absorbing Composite for Mitigating Reflective Cracking in Asphalt Concrete Overlays. *Transportation Engineering Series, No. 94*. University of Illinois, Urbana-Champaign, Urbana.

Owusu-Antwi, E.B., L. Khazanovich, and L. Titus-Glover. 1998. Mechanistic-based model for predicting reflective cracking in asphalt concrete-overlaid pavements. *Transportation Research Record.* No. 1629. 234-241

CHAPTER 4. INVESTIGATION OF BITUMEN MODIFIED WITH BIOPOLYMERS DERIVED FROM SOYBEAN OIL

A paper published in the conference proceedings of the 5th European Asphalt Technology Association Conference, Braunschweig, Germany, June 3-5, 2012

Andrew A Cascione[1] [2], Nacú Hernández[3], Eric W. Cochran[4], and R. Christopher Williams[5]

Abstract

Here we report advances in polymerization technology enabling the synthesis of thermoplastic block copolymers (BCPs) comprised of styrene and soybean oil-derived triglycerides. These new breeds of biopolymers have elastomeric properties comparable to well-established butadiene-based styrenic BCPs (SBS) commonly used for bitumen modification. We evaluated the potential of these biopolymers as bitumen modifiers by

[1] Ph.D. candidate, Department of Civil, Construction, and Environmental Engineering, Iowa State University, Ames, IA 50011. E-mail: aacascio@iastate.edu

[2] Primary researcher and author

[3] Associate Scientist, Department of Chemical and Biological Engineering, Iowa State University, Ames, IA 50011. E-mail: nacu23@iastate.edu

[4] Associate Professor, Department of Chemical and Biological Engineering, Iowa State University, Ames, IA 50011. E-mail: ecochran@iastate.edu

[5] Professor of Civil Engineering, Department of Civil, Construction, and Environmental Engineering, Iowa State University, Ames, IA 50011. E-mail: rwilliam@iastate.edu

comparing two commonly used commercial SBS polymers. Rheology of the bitumen-polymer blends shows the biopolymers improves the complex shear modulus of the bitumen to a similar and even greater extent as the SBS polymer. However, the current biopolymer formulation and blending technique produces bitumen with a slightly lower elastic response than blends prepared with SBS. Our results show excellent potential for the future of these biopolymers as economically and environmentally favorable alternatives to their petrochemically-derived analogs.

Introduction

Bitumen is commonly modified with poly(styrene-*block*-butadiene-*block*-styrene) (SBS), a thermoplastic elastomer (TPE). Polymer modification is known to substantially improve the physical and mechanical properties of bitumen in asphalt paving mixtures. Polymer modification increases bitumen elasticity at high temperatures, as a result of an increased storage modulus and a decreased phase angle, which improves rutting resistance. It also increases the complex modulus, but lowers creep stiffness at low temperatures, improving cracking resistance (Isacsson and Lu, 1999). SBS type polymers are typically added to asphalt mixtures when additional performance is desired or when optimizing life cycle costs is warranted. SBS allows for the production of many specialty mixes including cold mixes, emulsion chip seals, and micro-surface mixes.

SBS TPEs are block copolymers (BCPs) comprised of styrene-butadiene-styrene polymer chains that create an ordered morphology of cylindrical glassy polystyrene block domains within a rubbery polybutadiene matrix (Bulatovic *et al*., 2012). SBS polymers are *thermoplastic*, meaning that they can be easily processed at high temperatures due to the linear nature of its chains. Upon cooling, the rigid polystyrene end-blocks vitrify and act as

anchors for the liquid rubbery domains by providing a restoring force when stretched (Fried, 2008). SBS is incorporated into bitumen through mixing and shearing at high temperatures to uniformly disperse the polymer. When blended with bitumen, the polymer swells within the bitumen maltene phase to form a continuous tridimensional polymer network (Lesuer, 2009). At high temperatures, the polymer network becomes fluid yet still provides a stiffening effect that increases the modulus of the mixture. At low temperatures, a crosslinked network within the bitumen redevelops without adversely affecting the low temperature cracking performance due to the elastic properties of the polybutadiene (Airey, 2004). The resulting performance properties widen the working temperature range of the bitumen-polymer system.

The butadiene monomer used in SBS is derived from petrochemical feedstocks, a byproduct of ethylene production. It has been rapidly increasing in price, not only due to increases in the price of crude oil, but also global market shifts in supply and demand. As shale gas supplies become more abundant, crackers are more commonly using lighter petrochemical feeds such as ethane to produce ethylene and its co-products. However, using lighter feeds lowers butadiene production, thus tightening the supply (Foster, 2011). Many commercially relevant elastomers require polybutadiene for its soft and rubbery properties. As a result, there is growing interest in sustainable biopolymers synthesized from plant-based feedstocks to replace the need for their petrochemical counterparts, specifically the identification of alternative feedstocks that can be made to mimic the properties of polybutadiene.

Linseed, rapeseed, flaxseed, and soybean, are just some of the agriculturally available biodegradable and renewable resources composed of triglycerides that can be synthesized

into the rubbery component in BCPs. Soybean oil, as an example, is comprised of 86% of mono- and poly-unsaturated fatty acids - molecules containing the required double bonds for standard polymerization chemistry to produce macromolecules. Nonetheless, the multifunctional nature of soybean oil gives it the potential to crosslink with other polytriglycerides leading to the formation of a thermoset, an irreversibly and highly crosslinked polymer. Larock et al. have shown that a variety of plant oils may be successfully polymerized via cationic polymerization into thermosets with a broad spectrum of physical properties and aesthetic appearances (Bhuyan *et al.*, 2010).

In this paper we present the use of polymerized triglycerides to create a polybutadiene replacement and its incorporation with styrene to form *thermoplastic* elastomeric triblock copolymers. The objective of this research is to develop a family of biopolymers with similar performance properties as SBS that can be used to modify bitumen.

Biopolymer Synthesis

Triglyceride oils are composed of three fatty acid chains joined by a glycerol center. We make use of triglycerides derived from soybean oil for the synthesis of the BCPs using atom transfer radical polymerization (ATRP), a procedure developed by Wang and Matyjesewski (1995) at the University of Carnegie Melon. ATRP, a controlled radical polymerization technique, allows for the construction of macromolecules with precisely defined degrees of polymerization and the ability to form complex molecular architectures such as block copolymers (Heimenz and Lodge, 2007). For the synthesis of the polymers, soybean oil (Renewable Energy Group, Ames, IA) was purified over basic alumina, followed by the epoxidation of the double bonds and subsequent acrylation to yield acrylated epoxidized soybean oil (AESO). AESO and styrene were used as the monomers, copper (I)

chloride (CuCl) as the catalyst, benzyl chloride as the initiator, copper (II) chloride as the counter catalyst, *N,N,N',N'',N''-pentamethyldiethylenetriamine (PMDETA)* as the ligand, and toluene as the solvent during all polymerizations. ATRP polymerization resulted in the creation of a hyper-branched, halogen-terminated thermoplastic poly(styrene-*block*-AESO-*block*-styrene) triblock copolymers (S-AESO-S); the halogen termination provides functional sites for further chemistry. Even though a highly branched polymer does not disperse as finely into bitumen and can be more difficult to incorporate in the blend, it is more effective in binder elasticity improvement compared to a linear polymer (Lu and Isacsson, 1997).

Several polymer parameters determine how a polymer will be effective in bitumen modification; these include chain architecture, composition, and the molecular weight distribution. SBS copolymers should also meet several requirements to be compatible with bitumen: They should be rich in butadiene (generally 60-70%) and the molecular weight of the styrene fraction must exceed 10,000 to obtain polystyrene (PS) rich domains (Lewandowski, 1994). The (S-AESO-S) biopolymers produced for this study contained 72% poly(AESO). Figure 32 shows the increase in molecular weight (number average) and polydispersity of the a) styrene homopolymer and b) poly(styrene-*block*-AESO) diblock as a function of time. After approximately 700 minutes, the molecular weight of the polystyrene increases well beyond 10,000 daltons and the diblock to 150,000 daltons.

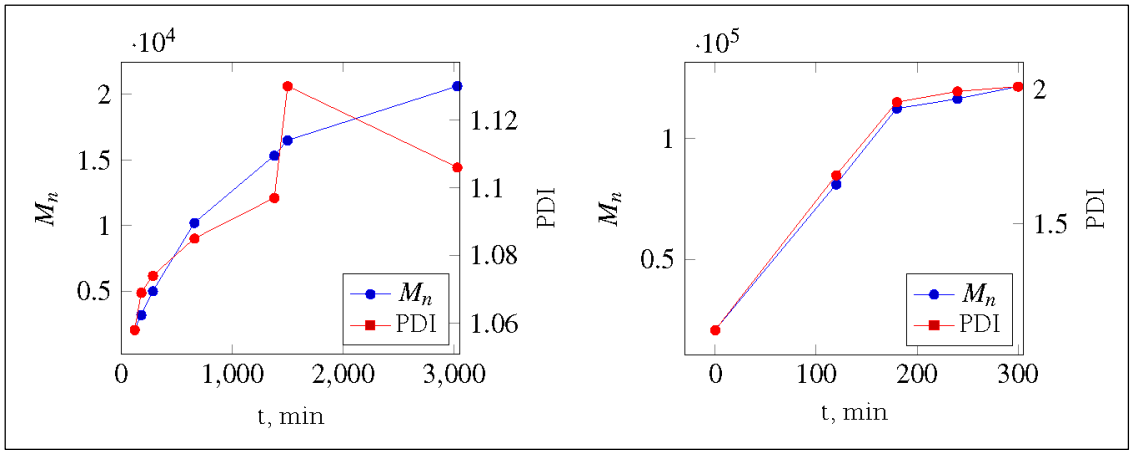

a **b**

Figure 32. Molecular weight and polydispersity homopolymer as a function of time for a) PS and b) P(S-b-AESO).

Experimental Plan

To study the effectiveness of the developed S-AESO-S biopolymer as a bitumen modifier, blends of bitumen modified with the biopolymer were compared to blends of bitumen modified with two commercially available Kraton® SBS polymers, D1101 and D1118. Both of these polymers are linear SBS triblock polymers. D1101 has a styrene content of 31% by weight of polymer and D1118 has a styrene content of 33% by weight of polymer.

A soft bitumen from a local refinery utilizing a Canadian crude source was used as the base bitumen. All bitumen-polymer blends were prepared in the laboratory with a Silverson L4RT shear mixer at 3000 rpm. The bitumen was heated to 150°C, and approximately 500 grams of bitumen were poured into eight different 0.95 Liter aluminum cans for eight 500 gram batches. Polymers were added to the batches at 3% by total weight of the bitumen-polymer blend.

Since the optimal blending temperature for the biopolymer was not known, a blending temperature study was incorporated into the experimental plan. Two batches were prepared with each polymer, with one batch blended for 3 hours at 180°C and the other batch blended for 3 hours at 200°C. The remaining two batches were prepared as the control treatments with no polymer added. One control treatment batch was immediately tested after being poured into the aluminum can, while the other control treatment batch was first placed in the shear mixer for 3 hours at 200°C before being tested. No cross-linking agent such as sulfur was used during the blending process. The softer base binder should contain a relatively low fraction of asphaltenes which will result in improved blend compatibility and stability in an SBS polymer system (Alonso *et al.*, 2010).

After the bitumen-polymer blends were prepared, the complex modulus (G*) and phase angle of the blends were measured at high and low temperatures using the dynamic shear rheometer (DSR) and bending beam rheometer (BBR). Next, the Multiple Stress Creep Recovery (MSCR) test was conducted on rolling thin film oven (RTFO) aged materials by following AASHTO TP 70-11. The test was conducted at 46°C due to the high temperature grade of the virgin bitumen. The original (no aging) material of each blend was also tested in a DSR at multiple temperatures and frequencies so master curves could be constructed that characterize the rheological properties of the bitumen-polymer blends over a wide range of temperatures.

Results and Discussion

The high temperature stiffness of the bitumen-polymer blends before and after aging in the RTFO, 1.0kPa and 2.2kPa respectively, is presented in Figure 33. The virgin bitumen Performance Grade (PG) according to AASHTO M320 "Standard Specification for Performance Graded Asphalt Binder" is a 46-34 since the original bitumen has a governing G*/Sin(δ) value of 51.3°C. After 3 hours of mixing in the shear mill at 200°C, the PG of the virgin bitumen only slightly increased to a G*/Sin(δ) value of 52.6°C. This essentially shows the blending procedure used in this study does not significantly age harden the bitumen and increase the high temperature performance grade. Any increase in complex modulus or decrease in phase angle is mostly caused by the polymer influencing the rheological properties of the bitumen.

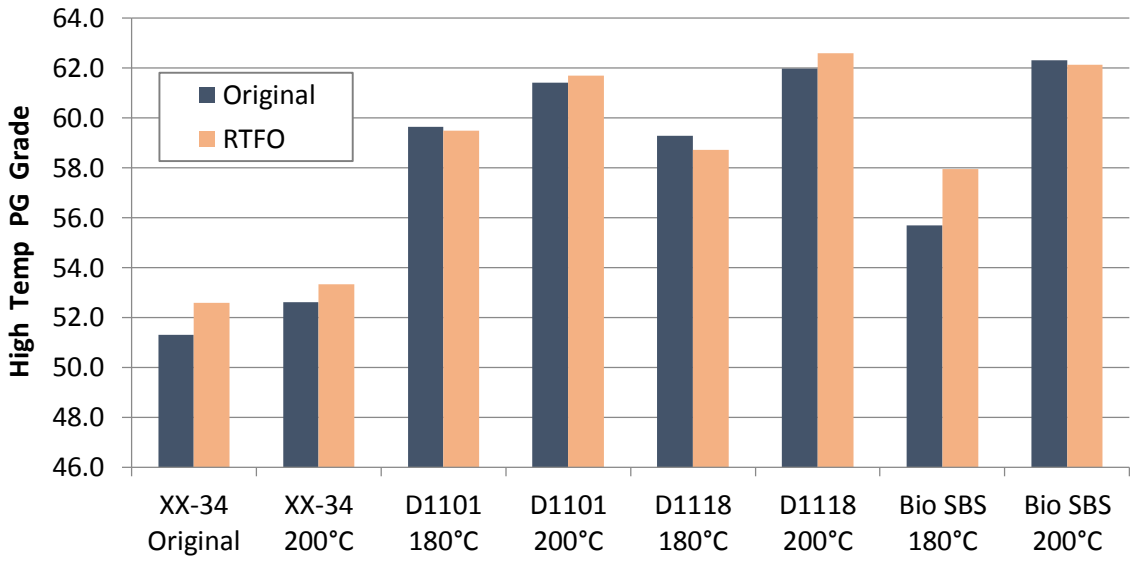

Figure 33. High temperature performance grade of bitumen-polymer blends

Figure 33 also shows that raising the blending temperature from 180°C to 200°C increases the high temperature PG of the bitumen-polymer blends. The two commercial SBS blends performed similarly with D1118 having a slightly higher original G*/Sin(δ) value of 62.0°C when blended at 200°C. The increase in blending temperature had the greatest affect on the biopolymer blend. At 180°C the biopolymer blend original G*/Sin(δ) value was 55.7°C compared to a value of 62.3°C at 200°C. A comparison of all the original G*/Sin(δ) values show the biopolymer blended at 200°C has the highest PG temperature.

Figure 34 presents the critical low temperatures with a limiting creep stiffness (300MPa) and limiting m-value (0.3) determined at a loading time of 60 seconds in the BBR. The critical low temperature of the virgin bitumen is -36.3°C and increases one degree to -35.3°C after blending for 3 hours in the shear mixer. The critical low temperature also increases for each polymer blend when the blending temperature increased from 180°C to 200°C indicating the increased performance benefits on the high temperature side were compromised on the low temperature side.

With the exception of the biopolymer blends, each bitumen-polymer blend passed the -34°C criteria to be graded as a 46-34 bitumen. However, the continuous grade range in presented in Table 21 shows the grade range of the biopolymer blended at 200°C is only 0.3°C less than the D1101 SBS and 1.4°C less than the D1118 SBS. The continuous PG range indicates the temperature susceptibly of the biopolymers and their physical performance benefit over a working range of temperatures is very close to the commercially available SBS polymers. These are results before any study has been conducted to optimize the formulation of the S-AESO-S biopolymer as a bitumen modifier.

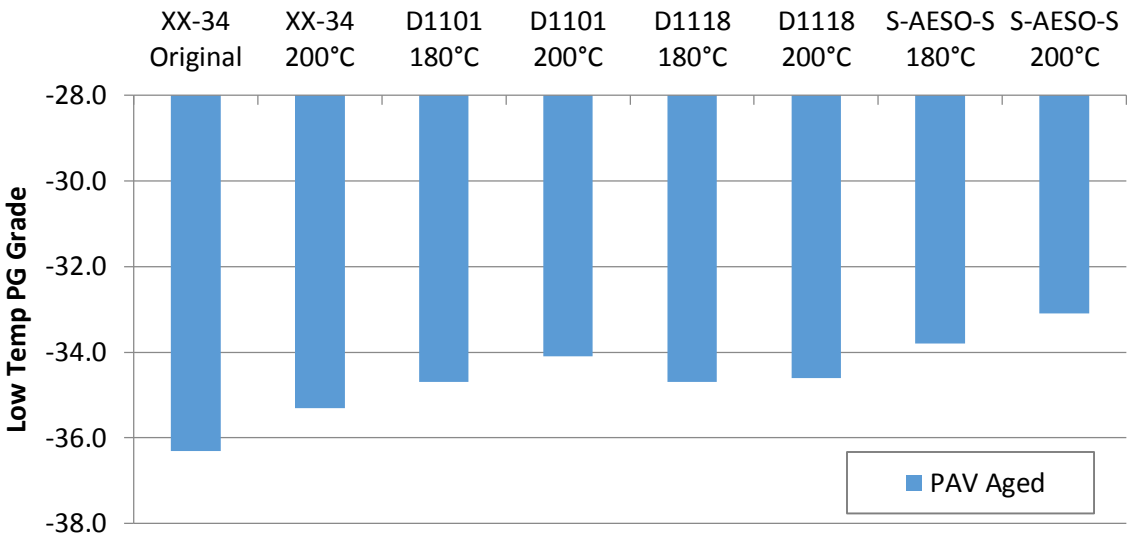

Figure 34. Low temperature performance grade of bitumen-polymer blends

Table 21. Continuous PG range of bitumen-polymer blends

Bitumen-Polymer Blend	Continuous Grade Range, (°C)
46-34 Original	87.6
46-34 blended at 200°C	87.9
D1101 blended at 180°C	94.2
D1118 blended at 200°C	95.5
D1101 blended at 180°C	94.0
D1118 blended at 200°C	96.6
S-AESO-S Biopolymer blended at 180°C	89.5
S-AESO-S Biopolymer blended at 200°C	95.2

Although many transportation state agencies in the United States use a form of AASTHO M-320 as a bitumen acceptance specification, the high temperature test parameter G*/Sin(δ) has been shown to not apply a high enough strain level that sufficiently tests polymer modified binders for their rutting resistance. More recently, the Multiple Stress Creep Recovery (MSCR) test was developed in the United States which uses the DSR to

apply higher levels of strain to capture the stiffening effects and delayed elastic response of the polymer in a polymer modified bitumen (D'Angelo *et al*., 2007).

The procedure AASHTO TP70-11 "Multiple Stress Creep Recovery (MSCR) Test of Asphalt Binder Using a Dynamic Shear Rheometer" was followed for the MSCR test. The MSCR procedure measures the creep compliance and elastic response of bitumen by using the DSR to test rolling thin-film oven residue at two stress levels at a specified temperature. The specified temperature is the high temperature performance grade of the bitumen. Since the base bitumen was graded as a PG 46-34, the base bitumen and bitumen-polymer blends were tested at 46°C. A 25-mm parallel plate geometry with 1-mm gap setting was used in the DSR. The MSCR test consists of 20 cyclic stress and recovery periods. For the first 10 periods, the bitumen samples are tested in shear creep at a stress level of 0.1 kPa for one second, followed by nine seconds of recovery. The one-second creep and nine-second recovery count as one period. For the next 10 periods, each period consists of a one-second 3.2 kPa shear creep load, again followed by nine seconds of recovery.

The non-recoverable creep compliance (J_{nr}) calculated from the MSCR test is presented in Figure 35. The commercial bitumen-polymer blends and biopolymer blend at 200°C have the lowest Jnr values. Lower Jnr values indicate good resistance to rutting. The biopolymer blends along with the commercial blends at 200°C meet the highest traffic level criteria of "Extremely Heavy Traffic" since their J_{nr} values fall below 0.5kPa.

In addition to the J_{nr} values, the MSCR test also measures the "recovery" value which indicates the percent strain the bitumen recovered during the test. Higher percentages of strain recovery indicate the presence of an elastomeric polymer in the bitumen and a quality blend between the bitumen and polymer. In Figure 36, the higher blending temperature

appears to improve the polymer network established in the binder. Similar results were found by D'Angelo and Dongre (2009) in an SBS blending study using the MSCR test. The results of this test also show the contrast in elastic recovery between the commercial polymer blends (47.8% for D1101 and 48.6% for D1118) and the biopolymer blend (21.1%) at the higher blending temperature.

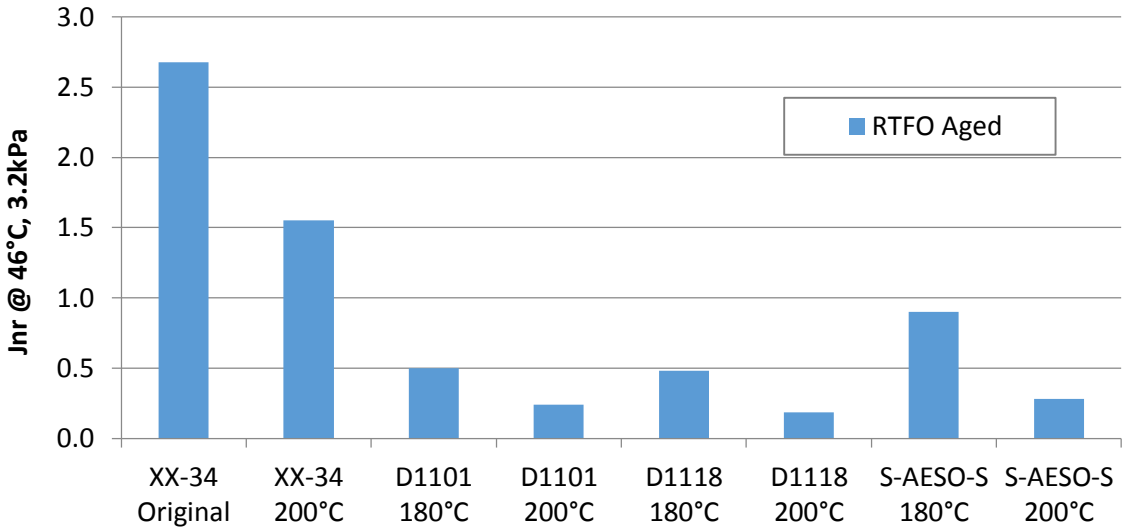

Figure 35. Non-recoverable creep compliance (J_{nr}) values

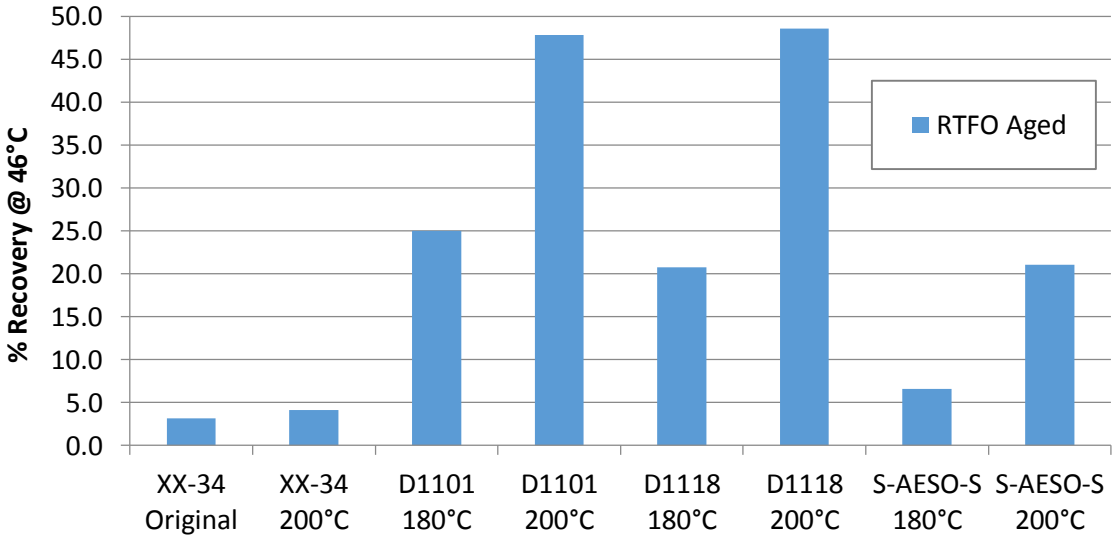

Figure 36. Percent recovery of bitumen-polymer blends

Figure 37 plots the MSCR recovery as a function of Jnr. The curve in the plot represents the recommended minimum percent recovery values a polymer modified bitumen should have for sufficient delayed elastic response. Values that plot above the line indicate the presence of an elastomeric polymer and a quality bitumen-polymer blend. The biopolymer percent recovery does not plot above the curve which means the blending procedure and/or biopolymer formulation can be improved upon with further research. The commerical polymers are linear and therefore should be more compatible with a bitumen than a radial polymer when a crosslinking agent is not used. In contrast, the biopolymer has a highly branched network due to the polytriglycerides. A crosslinking agent may improve the ability of the biopolymer to form an evenly dispersed and slightly crosslinked network in the bitumen.

Master curves used to analyze the rheological properties of the bitumen-polymer blends were constructed from data using the DSR. Frequency sweeps were conducted on 25 mm plate samples in the materials linear viscoelastic range from 0.1 Hz to 50 Hz at 6°C intervals from 16°C to 70°C. The master curve for the complex shear modulus (G*) data was constructed using Excel Solver. G* isochrones were shifted to fit the Williams-Landel-Ferry (WLF) model with 40°C as the reference temperature. The shift factors were then used to shift the phase angle data to build the phase angle master curve. Equation 1 presents the WLF equation:

$$Log\ a_T = \frac{-C_1(T-T_r)}{C_2+T-T_r} \quad [1]$$

where; a_T= shift factor, C_1 and C_2= constants, T_r= reference temperature, and T= temperature of the material.

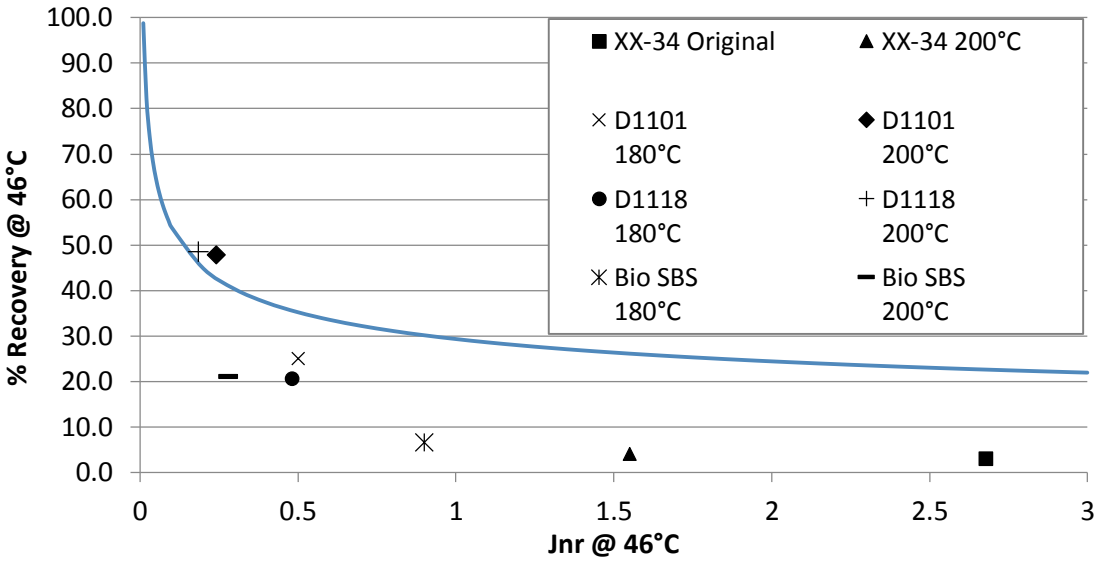

Figure 37. Percent recovery versus non-recoverable creep compliance

The shear modulus master curves in Figure 38 shows the biopolymer increases the stiffness of the bitumen across a wide frequency range. In Figure 39, the biopolymer also reduces the phase angle of the bitumen, but not to levels as low as the two SBS polymers. In Figure 8, the bitumen modifed with the two SBS polymers have a dip in the phase angle showing evidence of the polymer rubbery plateau. There does not appear to be any evidence of the rubbery plateau in the biopolymer modified bitumen. Similar to the MSCR recovery values, this data indicates the biopolymer may not be providing the bitumen with a sufficient elastic response. The lowered phase angle may be the result of the stiffening effect from the glassy polystyrene phase. To improve the elasticity of the biopolymer-bitumen blends, future studies will be conducted on the blending procedure and formulation of the biopolymer.

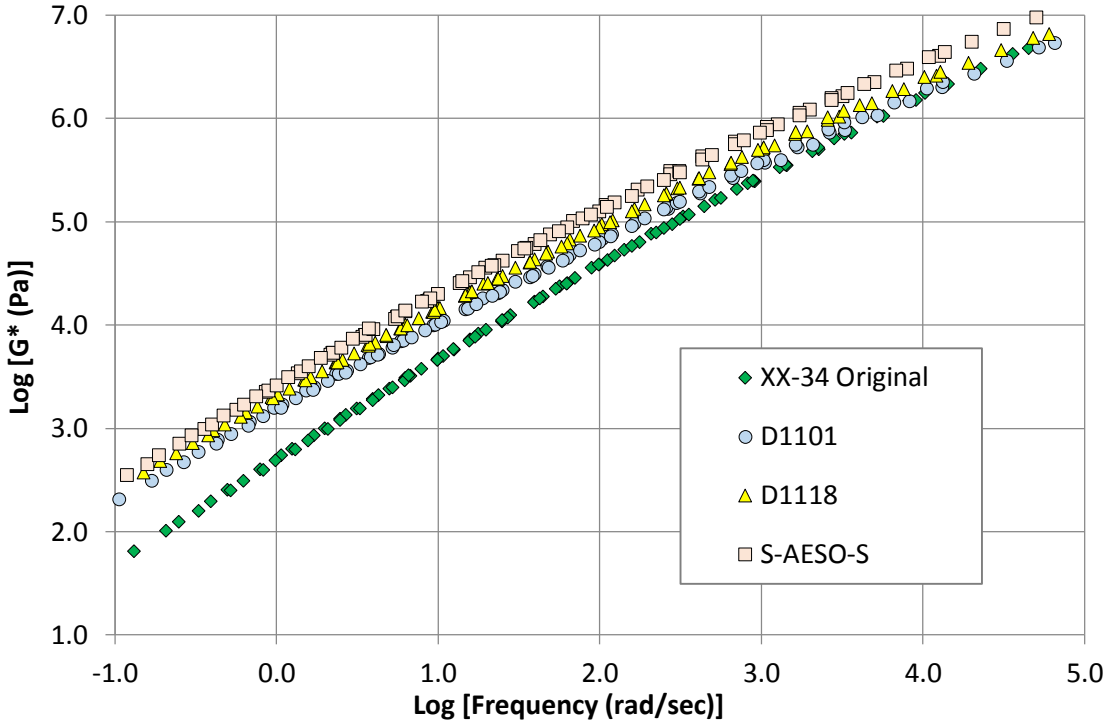

Figure 38. Log complex shear modulus (G*) versus log reduced frequency, rad/sec

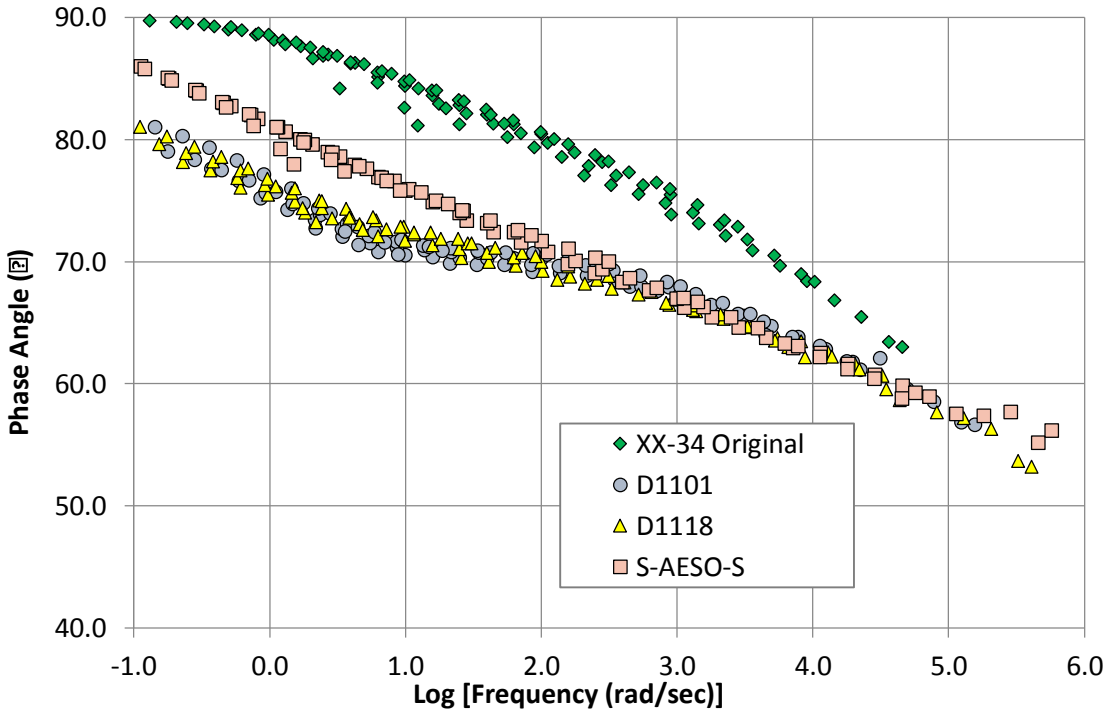

Figure 39. Phase angle versus log reduced frequency, rad/sec

Conclusions

Recent advances in polymerization technology have led to the development of thermoplastic elastomeric block copolymers produced with polystyrene and polymerized soy-derived triglycerides. In contrast, the past two decades of plant-oil based polymer research has yielded only thermosets. Using the polymerized triglycerides, SBS-like triblock copolymers were produced where the "B" block was replaced with polymerized soybean oil. ATRP polymerization technique was used to synthesize the biopolymers as it allows for the construction of macromolecules with precisely defined degrees of polymerization and the ability to form complex molecular architectures such as block copolymers.

A laboratory investigation was conducted to evaluate the effectiveness of the newly derived S-AESO-S biopolymer as a bitumen modifier. Bitumen modified with the biopolymer was compared to bitumen modified with two commercially available Kraton® linear SBS polymers. All bitumen-polymer blends were prepared with bitumen modified with 3 percent polymer. Rheology test results showed the biopolymer has the ability to widen the grade range of bitumen almost identically as the commercially available SBS polymers. However, the S-AESO-S biopolymer increased the bitumen low critical temperature 1.4°C higher than the D1118 SBS polymer.

In the phase angle master curves, the commercially available SBS polymers increased the elasticity of the bitumen by lowering its phase angle and altering the shape of the curve so that it exhibited evidence of a rubbery plateau. While the biopolymers also lowered the phase angle of the bitumen, the bitumen-biopolymer blend master curves did not show evidence of a rubbery plateau.

The MSCR test results showed the biopolymer lowered the J_{nr} value of the bitumen as low as the two commercially available SBS polymers can, indicating the biopolymer has the ability to improve rutting resistance of the bitumen as well as the commercially available polymers. With respect the elastic response as measured by the MSCR test, the bitumen-biopolymer blend only contained a 21.1 percent recovery while the bitumen modified with D1118 SBS polymer contained a 48.6 recovery. However, the commercially available SBS polymers used in this study were linear while the biopolymer was highly branched. A crosslinking agent such as sulfur was not used during blending. The future use of a crosslinking agent may improve the blend compatibility of the biopolymer more so than the commercial polymers because of the branched network in the biopolymer. Furthermore, the formulation of the biopolymer has not yet been optimized for bitumen blending. Future research can improve upon its molecular architecture, styrene content, and molecular weight distribution to ultimately produce an SBS biopolymer that modifies bitumen similarly to petrochemical based SBS polymers.

References

Alonso S., Luis M-T., Zitzumbo R., Avalos F., "Rheology of asphalt styrene-butadiene blends", *Journal of Materials Science*, Vol. 45, 2010, pp. 2591-2597

Airey G. D., "Styrene butadiene styrene polymer modification of road bitumens", *Journal of Materials Science*, Vol. 39, 2004, p. 951-959.

Bhuyan S., Sundararajan S., Andjelkovic D., Larock R., "Micro- and nano-tribological behavior of soybean oil-based polymers of different crosslinking densities", *Tribology International*, Vol. 43, 2010, p. 2231-2239.

Bulatovic V.O., Rek V., Markovic K.J., "Polymer modified bitumen", *Materials Research Innovations*, Vol. 16, No. 1, 2012, p. 1-6.

D'Angelo J., Dongre R., "Practical use of multiple stress creep and recovery test", Transportation Research Record 2126, Transportation Research Board, National Research Council, Washington, D.C., 2009, p. 73-82.

D'Angelo J., Kluttz R., Dongre R., Stephens K., Zanzotto L., "Revision of the Superpave High Temperature Binder Specification: The Multiple Stress Creep Recovery Test", *Journal of the Association of Asphalt Paving Technologists*, Vol. 76, 2007, p. 123-162.

Foster J., "Lighter feeds in US steam crackers brings new attitude toward on-purpose butadiene, propylene prospects", Platts Special Report: Petrochemicals, 2011, p. 1-6.

Fried J.R., *Polymer Science and Technology*, Second edition, Prentice Hall, Upper Saddle River, NJ, 2008.

Hiemenz P.C., Lodge T.P., *Polymer Chemistry*, Second edition, CRC Press, Boca Raton, FL, 2007.

Isacsson U., Lu X., "Characterization of bitumens modified with SEBS, EVA and EBA polymer", *Journal of Materials Science*, Vol. 34, 1999, p. 3737-3745.
Lu X., Isacsson U., "Compatibility and storage stability of styrene-butadiene-styrene copolymer modified bitumens", *Materials and Structures*, Vol. 30, 1997, p. 618-626.

Lesueur D., "The colloidal structure of bitumen: consequences on the rheology and on the mechanisms of bitumen modification", *Advances in Colloid and Interface Science*, Vol. 145, 2009, p. 42-82.

Lewandowski L.H., "Polymer modification of paving asphalt binders", *Rubber Chemistry and Technology*, Vol. 76, No. 3, 1994, p. 447.

Wang J., Matyjaszewski K., "Controlled/"Living" radical polymerization. Atom transfer radical polymerization in the presence of transition-metal complexes", *Journal of the American Chemical Society*, Vol. 117, 1995, p. 5614-5615.

Wen G., Zhang Y., Zhang Y., "Improved properties of SBS-modified asphalt with dynamic vulcanization", *Polymer Engineering and Science*, Vol. 42, No. 5, 2002, p. 1070-1082.

CHAPTER 5. DEVELOPMENT OF BIO-BASED POLYMERS FOR USE IN ASPHALT

A paper to be submitted to *Road Materials and Pavement Design*, published by Taylor and Francis

Andrew A Cascione[1] [2], R. Christopher Williams[3], Eric W. Cochran[4], and Nacú Hernández[5]

Abstract

Asphalt binder is typically modified with poly(styrene-butadiene-styrene) (SBS) type polymers to improve its rheological properties and performance grade. The elastic and principal component of SBS polymers is butadiene. For the last decade, butadiene prices have fluctuated and significantly increased, leading state highway agencies to search for economically viable alternatives to butadiene based materials. This paper reports the recent

[1] Ph.D. candidate, Department of Civil, Construction, and Environmental Engineering, Iowa State University, Ames, IA 50011. E-mail: aacascio@iastate.edu

[2] Primary researcher for formulating and characterizing blends of bio-polymer modified asphalt binder

[3] Professor of Civil Engineering, Department of Civil, Construction, and Environmental Engineering, Iowa State University, Ames, IA 50011. E-mail: rwilliam@iastate.edu

[4] Associate Professor, Department of Chemical and Biological Engineering, Iowa State University, Ames, IA 50011. E-mail: ecochran@iastate.edu

[5] Associate Scientist, Department of Chemical and Biological Engineering, Iowa State University, Ames, IA 50011. E-mail: nacu23@iastate.edu

advances in polymerization techniques that have enabled the synthesis of elastomeric, thermoplastic, block-copolymers (BCPs) comprised of styrene and soybean oil, where the "B" block in SBS polymers is replaced with polymerized triglycerides derived from soybean oil. These new breeds of biopolymers have elastomeric properties comparable to well-established butadiene-based styrenic BCPs.

Two types of biopolymer formulations are evaluated for their ability to modify asphalt binder. Laboratory blends of asphalt modified with the biopolymers are tested for their rheological properties and performance grade. Blends of asphalt modified with the biopolymers are compared to blends of asphalt modified with two commonly used commercial polymers. The viscoelastic properties of the blends show that biopolymers improve the performance grade of the asphalt to a similar and even greater extent as the commercial SBS polymers. Results indicate there is an excellent potential for the future of these biopolymers as economically and environmentally favorable alternatives to their petrochemically-derived analogs.

Introduction

The performance of asphalt pavements at in-service temperatures depends on the grade of asphalt binder used in the paving mixture. In many cases, the characteristics of asphalt binder need to be altered to improve its rheological properties. Asphalt binder needs sufficient properties to resist cracking at low temperatures and rutting caused by shear forces from sustained loads at high temperatures. The physical properties of asphalt binder are typically modified with elastomeric polymers to produce an improved performance grade. The most common elastomeric polymers used for asphalt modification are styrenic block copolymers (SBC). SBCs are composed of blocks of polybudiene and polystyrene to produce

styrene-butadiene (SB) diblock polymers and styrene-butadiene-styrene (SBS) triblock polymers.

In 2008, there was a shortage of SB and SBS polymers for use in the asphalt industry. The shortage was due to a lack of global butadiene supply, the principal component of SBC grades for asphalt modification. Butadiene is a by-product of the production of ethylene, which is produced from the steam cracking process of petroleum based feedstocks. Steam cracker facilities can use either liquid petroleum products or gaseous products such as ethane, butane, or propane as the raw material to produce ethylene. The by-products that result from the steam cracking reaction depend on the composition of the raw material. Butadiene is only a by-product when liquid feeds, not gaseous feeds, are used as the raw materials.

As shale gas supplies become more abundant, crackers are more commonly using lighter petrochemical feeds such as ethane to produce ethylene and its by-products. However, using lighter feeds lowers butadiene production and tightens the supply (Foster 2011). This in-part led to the 2008 butadiene shortage as well as short term closure of some facilities. Although the butadiene supply has rebounded since then, it remains volatile and has been susceptible to rapid price increases. The butadiene market in the United States is particularly sensitive to global supply since butadiene is not substantially produced domestically but primarily imported from Asian and European countries.

As the asphalt industry continues to grow, it will increasingly need SBCs to modify asphalt binder. The global asphalt market is projected to reach 118.4 million metric tons by 2015, according to a January 2011 report by Global Industry Analysts, Inc. With increasing growth in the developing markets of China, India, and Eastern Europe, asphalt will be needed to construct their roadway infrastructure well into the next decade and beyond. The demand

for asphalt, along with the need for improved asphalt pavement performance, will put pressure on butadiene supplies that have already experienced shortages. As a result, there is a growing need in finding sustainable and renewable SBC alternatives.

The successful synthesis of elastomeric SBCs requires a polymer like polybutadiene for its soft and rubbery properties. With the advent of new polymerization technologies that can produce polymers from biorenewable sources rather than petroleum, it may be possible to synthesize a biopolymer from plant-based feedstocks that mimics the properties of polybutadiene. A bio-based alternative that could replace the petrochemically based polybutadiene in SBCs would help solve the economic and environmental concerns of using them.

Indeed, many advances have been made in this area, most notably in the production of vegetable-oil-based thermosets via both traditional cationic and free radical polymerization routes. Lu and Larock (2009) have shown that a variety of plant oils may be successfully polymerized via cationic polymerization into thermosets with a broad spectrum of physical properties and aesthetic appearances. While these thermoset materials may supplant a number of petrochemically-derived thermosets, the vast majority of commodity polymers, including SB and SBS, are thermoplastic materials that can be reheated and processed at high temperatures.

In laboratory studies, the authors have identified soybean oil as a viable renewable and biodegradable feedstock that can be polymerized into a material with similar properties as polybutadiene. By replacing butadiene with the polymerized soybean oil in the SB and SBS block copolymer structure, a new class of renewable elastomeric SBCs is available to be used for the asphalt industry as well as many others.

Objectives

This paper documents the development of a polymer modified asphalt using innovative thermoplastic-elastomeric SBCs based largely on soybean oil, a renewable and biodegradable feedstock. The new class of SBCs contains a biopolymer derived from triglycerides in soybean oil that replaces the "B" block polymer (polybutadiene) in the block copolymer structure of SB and SBS. The efficacy these soy-based block copolymers as an alternative to the traditional polymer modifiers used in the asphalt industry are evaluated through laboratory rheology experiments.

Literature Review

Asphalt binder is commonly modified with polymers to improve its rheological properties in a paving mixture and to lower its temperature susceptibility over a range of in-service temperatures. Figure 40 compares the stiffness of a conventional asphalt binder to an ideal modified asphalt binder at different in-service temperatures. At high temperatures, polymer modification increases binder stiffness and elasticity, as a result of an increased storage modulus and a decreased phase angle. Both increasing the storage modulus and decreasing the phase angle improves rutting resistance of the pavement (Bahia and Anderson 1995). At low temperatures, polymer modification lowers creep stiffness of the asphalt which improves resistance to thermal cracking (Isacsson and Lu 1999).

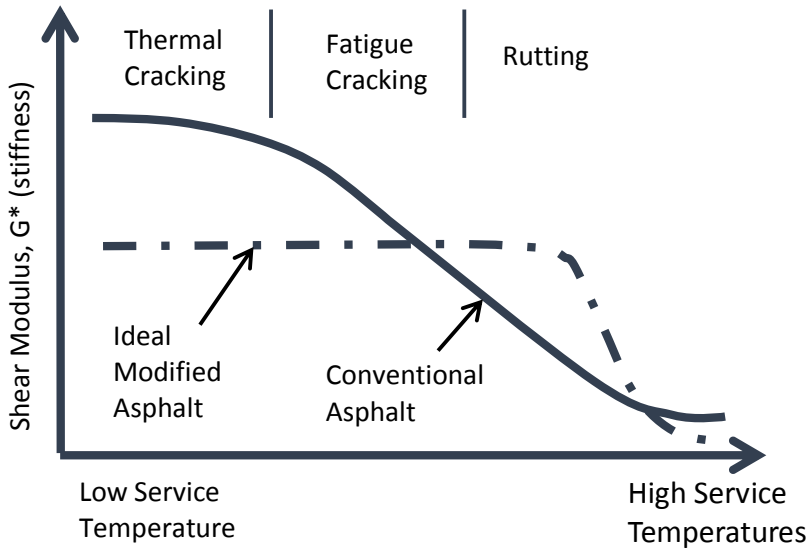

Figure 40. Effects of polymer modification in asphalt binder (after Epps, J.A.)

Polymers are very large molecules formed by linking together multiple small molecules called monomers. When a polymer consists of more than one repeating monomer unit, either in a random or block arrangement, it is termed a copolymer. The length of the polymer chain, monomer sequence, and chemical structure determine the physical properties of the resulting polymer. Polymers with blocks of repeating homopolymer chains are termed block copolymers (Odian 1991).

Thermoplastic Elastomers

The most important block copolymer used in commercial practice is the ABA triblock (Hiemenz 2007). The A block is usually polystyrene, and the B block is an elastomer such as isoprene or butadiene. Such polymers are known as thermoplastic elastomers. SBS is the most widely used thermoplastic elastomer for asphalt modification. It is comprised of polystyrene-polybutadiene-polystyrene chains that create an ordered morphology of cylindrical glassy polystyrene block domains within a rubbery polybutadiene matrix (Bulatovic et al. 2012). The polystyrene end-blocks provide strength to the polymer, while

the polybutadiene mid-block gives the material its elasticity (Figure 41). SBS polymers are thermoplastic, meaning that they can be easily processed at high temperatures due to the linear nature of their chains. When heated above the polystyrene glass transition temperature (100°C), the crosslinked structure breaks down allowing the polymer to flow. Upon cooling, the rigid polystyrene end-blocks vitrify and act as anchors for the liquid rubbery domains by providing a restoring force when stretched (Fried 2008).

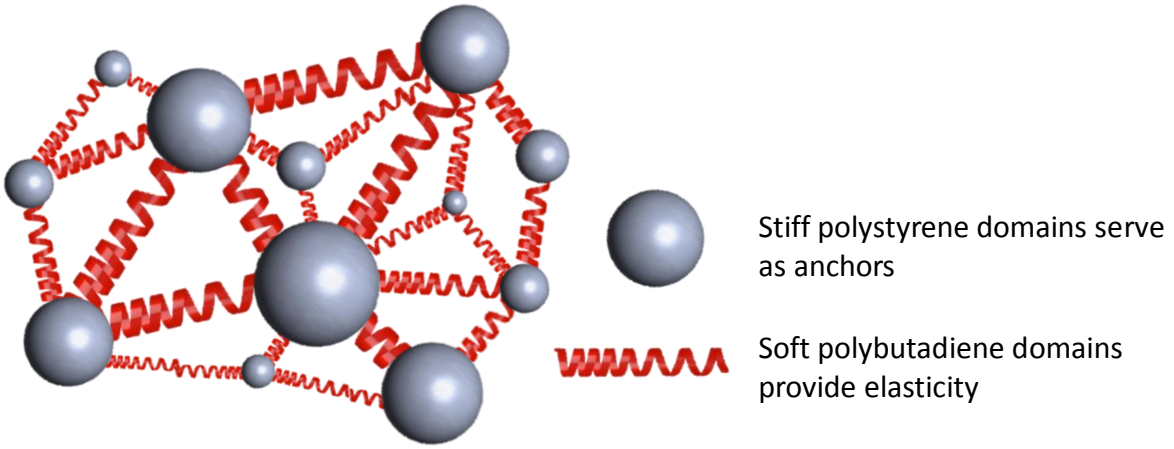

Figure 41. SBS polymer structure

The mechanism that allows SBS to possess the dual properties of thermoplasticity and elasticity in styrenic block copolymer arises from polymer thermodynamics and the chain architecture of the polymer. Flory-Huggins theory illustrates that nearly all polymers are mutually immiscible, due to the drastic loss of mixing entropy. The chemically dissimilar monomer sequences found in the block copolymers may be thought of conceptually as immiscible homopolymers bound covalently end-to-end. Due to this constraint, when a block copolymer phase separates, incompatible polymer types form meso-domains with a well-

defined geometry dictated by the block composition and with a size governed by the overall molecular weight (Bates et al. 1999).

In a typical SBS elastomer, the styrene composition is about 10-30 wt% such that spherical or cylindrical styrene domains form in a matrix of butadiene. When the temperature is below the glass transition temperature of polystyrene (Tg =100°C), the polybutadiene matrix is liquid (Tg < -90 °C) but is bound between the vitreous polystyrene spheres, which serve as physical crosslinks. When the temperature is above the glass transition temperature of polystyrene, the entire elastomer system is molten and may be processed easily. Crosslinked poly(soybean oil) has been reported to have Tg values as low as -56 °C (Yang et al. 2010). Comparatively, polybutadiene has a Tg of -90°C. Thus, the poly(soybean oil) is an excellent candidate to serve as the liquid component in thermoplastic elastomers based on styrenic block copolymers.

SBS is incorporated into asphalt binder, normally between 2 and 5 percent by weight of the total binder, through mixing and shearing at high temperatures to uniformly disperse the polymer. When blended with asphalt, the polymer swells within the asphalt maltene phase to form a continuous tridimensional polymer network (Lesuer 2009). At high temperatures, the polymer network becomes fluid yet still provides a stiffening effect that increases the modulus of the mixture. At low temperatures, a linked network within the asphalt redevelops without adversely affecting the low temperature cracking performance due to the elastic properties of the polybutadiene (Airey 2004). The resulting performance properties widen the working temperature range of the asphalt/polymer system.

SBS and Asphalt Compatibility

The differences in properties such as molecular weight, density, viscosity, and solubility coefficients between SBS and asphalt result in two distinct phases when using mechanical mixing to obtain SBS-modified asphalt (Sun et al., 2006). This can lead to thermodynamically unstable blends that have a tendency to segregate during hot storage (160°C). For polymers to impart desirable properties to asphalt binder, the binder and the polymer must be compatible. Incompatible asphalt-polymer blends lack a homogenous network of polymer chains throughout the blend, thereby reducing the polymer's effectiveness, and from a practical perspective, face handling issues.

Masson et al. (2003) showed that asphalt binder and polymer composition affect the stability of the blends. Asphalt binder consists of a complex system of hydrocarbon molecules that can be fractionated into asphaltene and maltene components (Hoiberg 1979). Asphaltenes are the heaviest components of the asphalt binder matrix and contribute to the stiffness of the asphalt, whereas maltenes are the lightest components and consist of compounds known as saturates, aromatics, and resins. The asphaltenes are dispersed throughout the maltene components in the asphalt matrix. Since the molecular weights of the polymeric chains are higher than or similar to those of the asphaltenes, they compete for the solvency of the maltene fraction and a phase separation may occur if there is an imbalance between the components (Fernandes et al. 2008). Therefore, it is recognized that asphalts with a lower asphaltene content and higher aromatics content are more compatible with SBS polymers (Alonso et al. 2010).

Several polymer parameters determine how a polymer will be effective in asphalt modification; these include chain architecture, composition, and the molecular weight

distribution. Lu and Isacsson (1997) compared branched SBS polymer to linear SBS polymer modified asphalt. They concluded that linear SBS polymers displayed a finer dispersion in modified asphalt which results in a lower phase separation during hot storage. Masson et al. (2003) concluded that the lower stability of branched SBS in asphalt was not necessarily due to its branched structure but its high molecular weight. SBS modified asphalt studies have reported linear SBS polymers to have molecular weights between 130,000 to 170,000 daltons and radial SBS polymers to have molecular weights between 210,000 to 350,000 daltons.

SBS copolymers should also meet several requirements to be compatible with asphalt: they should be rich in butadiene (generally 60-70%) and the molecular weight of the styrene fraction must exceed 10,000 daltons to obtain polystyrene rich domains (Lewandowski 1994).

The interaction between asphalt and SB is different from that with SBS (Martinez-Estrada et al. 2010). Maltenes have a more favorable interaction with the polybutadiene block compared with the PS block due to maltenes swelling the polybutadiene block and not the polystyrene block. In contrast, asphaltenes are incompatible with both polybutadiene and polystyrene. Therefore, interactions between asphalt and SB are more favorable than interactions between asphalt and SBS since SB only has one polystyrene block compared to the multiple end blocks of SBS. However, SBS is more commonly used for asphalt modification due to its ability to form an elastic network through physical entanglements in the polymer rich phase.

Commercially Available SBS and SB Polymers

Commercially available SBS and SB copolymers used for modifying asphalt binders in the United States are supplied by Kraton Performance Polymers, Inc. (Kraton®). D1101 and D1118 are commonly used grades of Kraton® for asphalt modification. D1101 is a clear, linear triblock copolymer (SBS), and D1118 is a clear, diblock copolymer (SB). Other SB and SBS polymers are produced by LG Chem, Korea Kumho Petrochemical Co., Taiwan Synthetic Rubber Corporation (TSRC), and others.

Polymers Synthesized from Vegetable Oils

Vegetable oils have been considered as monomeric feedstocks for the plastics industry for over 20 years. Polymers from vegetable oils have obtained increasing attention as public policy makers and corporations alike have been interested in replacing traditional petrochemical feedstocks due to their environmental and economic impact.

To date, moderate success has been achieved through the application of traditional cationic and free radical polymerization routes to vegetable oils to yield thermoset plastics (i.e., plastics which, once synthesized, permanently retain their shape and are not subject to further processing). For example, a variety of polymers, ranging from soft rubbers to hard, tough plastics were made by using cationic copolymerization of vegetable oils, mainly soybean oil (SBO), using boron triflouridediethyletherate (BFE) as initiator (Andjelkovic et al. 2006, Pfister & Larock 2010). Soybean oil-based waterborne polyurethane films were synthesized with different properties ranging from elastomeric polymers to rigid plastics by changing the polyol functionality and hard segment content of the polymers (Lu et al. 2005, Lu et al. 2011). Moreover, soybean oil was used to synthesize different bio-based products such as sheet molding composites, elastomers, coatings, foams, etc. (Zhu et al. 2006). Bunker

et al. synthesized pressure sensitive adhesives using mini-emulsion polymerization of acrylatedmethyloleate, a monoglyceride derived from soybean oil (Bunker et al. 2002, Bunker et al. 2003). The polymers produced were comparable to their petroleum counterparts. Zhu et al. generated an elastic network based on acrylated oleic methyl ester through bulk polymerization using ethylene glycol as the crosslinker, obtaining a high molecular weight linear polymer using mini-emulsion polymerization (Zhu et al. 2006). Lu et al. created thermosetting resins synthesized from soybean oil that can be used in sheet molding compound applications by introducing acid functionality onto the soybean and reacting the acid groups with divalent metallic oxides or hydroxides, forming the sheet (Lu et al. 2005). Bonnaillie et al. created a thermosetting foam system using a pressurized carbon dioxide foaming process of acrylated epoxidized soybean oil (AESO) (Bonnaillie et al. 2007).

Uncontrolled chain branching and crosslinking is inevitable by using these conventional polymerization routes due to the multifunctional nature of triglycerides, multiple initiation sites along the chain backbone, and chain transfer/termination reactions. While these thermoset materials may indeed supplant a number of petrochemically-derived thermosets, the vast majority of commodity polymers are highly processable thermoplastic materials. There is thus a need to develop highly processable thermoplastic and elastomeric polymers from vegetable oils with a wide range of applications and physical properties.

Synthesis of thermoplastic block copolymers

Soybean oil is particularly suitable for polymerization, because it possesses multiple carbon-carbon double bonds that allow for modifications such as conjugation, epoxidation of the double bonds, etc. Soybean oils are mixtures of triglycerides containing a number of

double bonds that may serve as candidates for polymerization. For the synthesis of the polymers, soybean oil was purified over basic alumina, followed by the epoxidation of the double bonds and subsequent acrylation to yield acrylated epoxidized soybean oil (AESO). The radically polymerizable triglyceride monomer (AESO) was polymerized with polystyrene via reversible addition-fragmentation chain-transfer (RAFT) polymerization, in the presence of a free radical initiator and a chain transfer agent, to form a thermoplastic block copolymer. The polymerizing step was carried out under conditions effective to achieve a number average degree of polymerization (Nn) for the thermoplastic block copolymer of up to 100,000 repeat units per molecule without gelation.

Using this process, two types of soy-based, thermoplastic, elastomeric, block copolymers were developed: P(styrene-b-AESO-b-styrene) and P(styrene-b-AESO). Images of the final soy-based biopolymers are presented in Figures 42 and 43. The PS-PAESO diblock is shown in Figure 42, and the PS-PAESO-PS triblock is shown in Figure 43.

Figure 42. PS-PAESO diblock

Figure 43. PS-PAESO-PS triblock

Table 22 shows the molecular weights and polydispersidy index of the biopolymers which are comparative to commercially produced SBCs used for asphalt modification. The

results show 33 percent styrene in the PS-PAESO diblock and 49 percent styrene in the PS-PAESO-PS triblock with molecular weights above 10,000 daltons.

Table 22. Biopolymer molecular weights and styrene contents

	M.W.[a]	PDI[b]	%Styrene[c]	1st [d]	2nd [e]
PAESO	29,500	1.39	0	-	-
PS-PAESO	40,980	1.34	33	13,900	-
PS-PAESO-PS	53,300	1.84	49	13,900	12,200

[a]Total molecular weight of block copolymer
[b]Total molecular weight of block copolymer
[c] Percent styrene in block copolymer
[d] Molecular weight of styrene in first block
[e] Molecular weight of styrene in second block

Experimental Plan

The PS-PAESO-PS and PS-PAESO biopolymers were blended with asphalt binder to evaluate the rheological properties of the biopolymer-asphalt blend and to determine the if the biopolymers are suitable for developing a formulation that increases the performance grade of the base asphalt binder. Two commercially available Kraton® polymers were also blended with the same asphalt binder to compare the biopolymer modified asphalt to commercially used polymer asphalt modified. The two Kraton® polymers selected for the study were D1101 (SBS triblock) and D1118 (SB diblock).

A soft asphalt from Flint Hills Resources' Pine Bend Refinery in Rosemount, Minnesota graded as a PG XX-34 was used as the base asphalt. All asphalt-polymer blends were prepared in the laboratory with a Silverson L4RT shear mixer at 3000 rpm and 180°C. For each polymer-asphalt batch, 500 grams of asphalt was poured into a 1 quart aluminum can. Polymer was added to each can at two percent by total weight of the asphalt-polymer blend. The high shear mixing process was carried out for 1.5 hours.

A control batch of asphalt binder was also prepared to compare the properties of the base asphalt to the polymer-asphalt blends. It was processed following the same procedure as the polymer-asphalt batches where a 1 quart can of the base asphalt was mixed in the shear mixer at 180°C for 1.5 hours. In total, five polymer-asphalt batches were prepared; they are as follows:

XX-34 base asphalt processed in shear mill,

XX-34 + SBS Kraton® D1101,

XX-34 + SB Kraton® D1118,

XX-34 + PS-PAESO-PS, and

XX-34 + PS-PAESO

The subsequent rheological testing of the blends is outlined below in Figure 44 and follows the American Association of State Highway and Transportation Officials (AASHTO) M 320 testing for determining the performance grade of the modified asphalt binders. The polymer-asphalt blends were tested a dynamic shear rheometer (DSR) at high and intermediate temperatures and tested in a bending beam rheometer at low temperatures (BBR). A rolling thin film oven (RTFO) and pressure aging vessel (PAV) were used to conduct simulated aging of the blends representative of the aging of binders that occurs during production of asphalt mixtures and the in-situ aging, respectively.

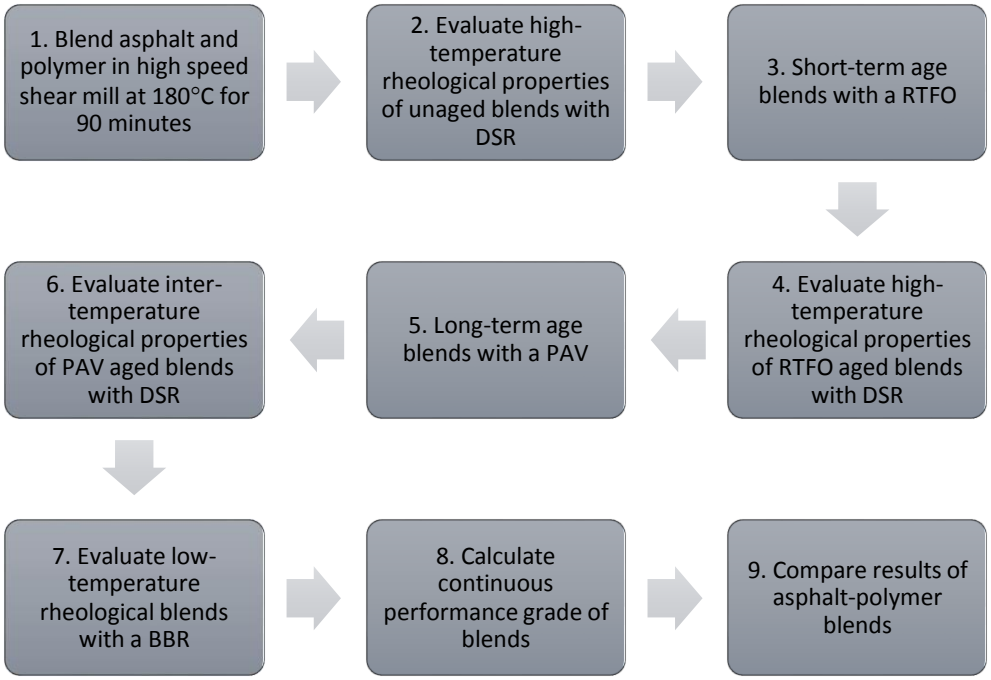

Figure 44. Rheological testing of asphalt-polymer blends

Results and Discussion

Evaluation of Asphalt Modified with the Commercial Polymers

Prior to evaluating blends of asphalt with the soy-based block copolymer, the XX-34 base asphalt was blended with Kraton® D1101 SBS triblock and Kraton® D1101 SB diblock at different percentages of polymer. The high PG failing temperature for each blend was evaluated using the DSR. The high performance grade (PG) temperature of an asphalt represents the temperature in degrees Celsius where the phase angle (δ) divided by the complex shear modulus (G*) is equal to 1kPa for unaged binders and 2.2kPa for rolling thin film oven aged binders. Lower phase angles increase the elastic component of an asphalt binder, and higher complex shear modulus values increase the stiffness of the material. Thus, the higher the PG failure temperature of an asphalt binder, the greater its ability will be to resist pavement rutting from vehicular loading.

In Table 23, the DSR results show the unaged XX-34 base asphalt contained a continuous high PG of 51.09. Kraton® D1101 SBS polymer was then added to the base asphalt at levels of 1, 2, 3, 4, and 5 percent, to evaluate how the percentage of D1101 would change the PG of the binder. As expected, the continuous high PG increased as the polymer content increased. Similar results were obtained for the RTFO aged D1101 polymer-asphalt blends (Table 24).

Table 23. DSR results for unaged asphalt modified with Kraton® D1101

Temp	Measurement	Base Asphalt	w/ 1% Kraton® D1101	w/ 2% Kraton® D1101	w/ 3% Kraton® D1101	w/ 4% Kraton® D1101	w/ 5% Kraton® D1101
46°C	|G*| (Pa)	2023	2816	4500	5152		
	δ (degrees)	86.36	84.05	79.40	76.44		
	G*/sin(δ) (kPa)	2.03	2.83	4.58	5.30		
52°C	|G*| (Pa)	879	1205	1962	2361	3560	4790
	δ (degrees)	87.75	85.85	81.85	79.38	64.64	60.63
	G*/sin(Δ) (kPa)	0.88	1.21	1.98	2.40	3.94	5.50
58°C	|G*| (Pa)		569	928	1141	1946	2703
	δ (degrees)		87.01	83.48	81.44	68.8	64.77
	G*/sin(δ) (kPa)		0.57	0.93	1.15	2.09	2.99
64°C	|G*| (Pa)				588	1076	1532
	δ (degrees)				82.36	71.78	68.65
	G*/sin(δ) (kPa)				0.59	1.13	1.65
70°C	|G*| (Pa)					614	902
	δ (degrees)					75.8	70.50
	G*/sin(δ) (kPa)					0.64	0.96
PG Failing Temp (°C)		**51.09**	**53.67**	**57.42**	**59.45**	**65.59**	**69.7**

Table 24. DSR results for RTFO aged asphalt modified with Kraton® D1101

Temp	Measurement	Base Asphalt	w/ 1% Kraton® D1101	w/ 2% Kraton® D1101	w/ 3% Kraton® D1101	w/ 4% Kraton® D1101	w/ 5% Kraton® D1101
46°C	|G*| (Pa)	5449	7038	9619	11395		
	δ (degrees)	81.66	78.49	73.95	70.27		
	G*/sin(δ) (kPa)	5.51	7.18	10.01	12.11		
52°C	|G*| (Pa)	2250	2998	4276	5230	6944	8541
	δ (degrees)	84.13	81.33	77.59	74.14	67.80	62.57
	G*/sin(δ) (kPa)	2.26	3.03	4.38	5.44	7.50	9.62
58°C	|G*| (Pa)	994	1349	1973	2475	3359	4516
	δ (degrees)	86.09	83.87	81.03	78.36	73.11	65.74
	G*/sin(δ) (kPa)	1.00	1.36	2.00	2.53	3.510	4.95
64°C	|G*| (Pa)				1198	1653	2442
	δ (degrees)				82.06	77.11	70.00
	G*/sin(δ) (kPa)				1.21	1.70	2.60
70°C	|G*| (Pa)						1331
	δ (degrees)						73.61
	G*/sin(δ) (kPa)						1.39
PG Failing Temp (°C)		**52.38**	**54.45**	**57.22**	**59.20**	**61.89**	**65.60**

Tables 25 and 26 show the DSR results of the unaged and RTFO aged XX-34 base asphalt modified with Kraton® D1118 SB polymer, respectively, at polymer contents of 1, 2, 3, 4, and 5 percent. The D1118 polymer did not increase the grade of the base asphalt as much as the D1101 polymer. For example, when 5 percent D1118 polymer was blended with the base asphalt, the continuous grade of the base asphalt increased to 62.2°C; whereas when 5 percent D1101 polymer was blended with the base asphalt, the continuous grade of the base asphalt increased to 65.6°C. The high PG temperatures for the D1101 modified asphalt was expected since SBS is known to have a greater ability than SB to from an elastic network of physical chain entanglements in the polymer rich phase of an asphalt-polymer blend.

Table 25. DSR results for unaged asphalt modified with Kraton® D1118

Temp	Measurement	Base Asphalt	w/ 1% Kraton® D1118	w/ 2% Kraton® D1118	w/ 3% Kraton® D1118	w/ 4% Kraton® D1118	w/ 5% Kraton® D1118
46°C	|G*| (Pa)	2023	2674	3170	4745		
	δ (degrees)	86.36	83.89	81.14	75.27		
	G*/sin(δ) (kPa)	2.03	2.69	3.21	4.91		
52°C	|G*| (Pa)	879	1162	1438	2242	2229	2870
	δ (degrees)	87.75	85.73	83.54	77.96	75.86	72.95
	G*/sin(δ) (kPa)	0.88	1.17	1.45	2.29	2.299	3.00
58°C	|G*| (Pa)		546	689	1102	1126	1488
	δ (degrees)		87.14	85.49	80.80	77.34	74.26
	G*/sin(δ) (kPa)		0.55	0.69	1.12	1.15	1.55
64°C	|G*| (Pa)				565	601	812
	δ (degrees)				82.42	78.04	74.57
	G*/sin(δ) (kPa)				0.57	0.61	0.84
Failing Temp (°C)		**51.09**	**53.37**	**55.03**	**59.12**	**59.51**	**62.30**

Table 26. DSR results for RTFO aged asphalt modified with Kraton® D1118

Temp	Measurement	Base Asphalt	w/ 1% Kraton® D1118	w/ 2% Kraton® D1118	w/ 3% Kraton® D1118	w/ 4% Kraton® D1118	w/ 5% Kraton® D1118
46°C	|G*| (Pa)	5449	7233	8100	10065		
	δ (degrees)	81.66	78.39	75.76	72.06		
	G*/sin(δ) (kPa)	5.51	7.38	8.36	10.58		
52°C	|G*| (Pa)	2250	3091	3575	4666	5079	6319
	δ (degrees)	84.13	80.74	77.60	73.72	72.2	68.68
	G*/sin(δ) (kPa)	2.26	2.13	3.66	4.86	5.34	6.78
58°C	|G*| (Pa)	994	1418	1695	2271	2540	3231
	δ (degrees)	86.09	83.05	79.90	76.07	73.96	70.22
	G*/sin(δ) (kPa)	1.00	1.43	1.72	2.34	2.64	3.43
64°C	|G*| (Pa)				1142	1311	1731
	δ (degrees)				78.84	76.43	72.41
	G*/sin(δ) (kPa)				1.16	1.35	1.82
Failing Temp (°C)		**52.38**	**54.74**	**56.02**	**58.65**	**59.67**	**62.20**

The low temperature creep stiffness and the m-value of the base asphalt and Kraton® polymer-asphalt blends were evaluated using a bending beam rheometer (BBR) (Table 27).

Three percent Kraton® D1101 and D1118 each increased the continuous low temperature PG only by about three degrees which kept the low PG at -34°C.

Table 27. BBR results for PAV aged asphalt modified with Kraton® D1101 and D1118

		Base Asphalt		w/ 3% Kraton® D1101		w/ 3% Kraton® D1118	
Temp	Measurement	PAV Aged		PAV Aged		PAV Aged	
-24°C	Stiffness (MPa)	182	-	245	244	245	237
	m-value	0.346	-	0.310	0.306	0.311	0.307
-30°C	Stiffness (MPa)	479	-	520	489	492	495
	m-value	0.271	-	0.239	0.241	0.244	0.235
Continuous Low Grade (°C)		**-37.68**		**-34.71**		**-34.78**	

Evaluation of Asphalt Modified with the Biopolymers

PS-PAESO and PS-PAESO-PS were blended with the base asphalt to determine how the biopolymers affected the base asphalt's PG. Each biopolymer was added to the base asphalt at a polymer content of 2 percent. (The biopolymers were not evaluated in the asphalt at multiple contents similarly to the Kraton® polymers, due to limited laboratory production capabilities. Since the completion of this study, a larger reactor has been purchased which allows for larger biopolymer production capacity.) The blends were compared to the base asphalt as well as the base asphalt processed in the shear mill without polymer. The results in Table 28 highlight the high heat levels that occur during shear mill processing which cause the asphalt to age, resulting in a 2.5 to 3 degree increase of the high PG temperature. Although a continuous high PG of 51.09°C was measured in the base asphalt with the DSR, 53.64°C should be used as the base asphalt PG for a proper comparison to respective polymer modified asphalt blends since all polymer-asphalt blends were processed in a shear mill.

When two percent PS-PAESO diblock was added to the base asphalt, the base asphalt's continuous high PG increased from 53.64°C to 69.08°C. The PS-PASEO-PS triblock at 2 percent increased the continuous high PG to 70.4°C. Both PG values are higher than the asphalt modified with 2 percent D1101 and D1118, which were 57.22°C and 55.03°C respectively. The higher PG values in the biopolymer modified asphalt are a result of a lower phase angle and higher shear modulus value than the Kraton® polymer modified asphalt.

Table 28. DSR results for asphalt modified with biopolymers

		Base Asphalt		Base Asphalt processed in shear mill w/o polymer		Base Asphalt w/ 2%PS-PAESO		Base Asphalt w/ 2%PS-PAESO-PS	
Temp	Measurement	Unaged	RTFO Aged	Unaged	RTFO Aged	Unaged	RTFO Aged	Unaged	RTFO Aged
46°C	|G*| (Pa)	2023	5449	2843	8219				
	δ (degrees)	86.36	81.66	84.37	79.35				
	G*/sin(δ) (kPa)	2.027	5.51	2.857	8.362				
52°C	|G*| (Pa)	879	2250	1214	3383	9599	18900	11250	21275
	δ (degrees)	87.75	84.13	86.03	82.24	73.92	67.98	73.12	67.56
	G*/sin(δ) (kPa)	0.88	2.26	1.216	3.414	9.988	20.39	11.76	23.02
58°C	|G*| (Pa)		994	557.2	1494	4323	8646	5100	9893
	δ (degrees)		86.09	87.26	84.55	77.01	71.39	76.34	70.85
	G*/sin(δ) (kPa)		1.00	0.5579	1.501	4.436	9.124	5.248	10.48
64°C	|G*| (Pa)					2012	4043	2384	4680
	δ (degrees)					79.85	74.90	79.40	74.34
	G*/sin(δ) (kPa)					2.04	4.19	2.43	4.86
70°C	|G*| (Pa)					983	1941	1157	2233
	δ (degrees)					82.24	78.23	82.11	77.72
	G*/sin(δ) (kPa)					0.99	1.98	1.17	2.29
76°C	|G*| (Pa)							583	1094
	δ (degrees)							84.44	80.76
	G*/sin(δ) (kPa)							0.59	1.11
PG Failing Temp (°C)		**51.09**	**52.38**	**53.64**	**55.26**	**69.82**	**69.08**	**71.42**	**70.42**

The asphalt properties from DSR testing at intermediate pavement temperatures on PAV aged blends are presented in Table 29. The intermediate PG temperature is calculated as the temperature in degrees Celsius where the complex shear modulus multiplied by the phase angle equals 5000 kPa. Lower intermediate PG temperatures indicate an asphalt binder has a greater ability to deform without building up large stresses. A more compliant material will help reduce structural fatigue cracking in pavements. The biopolymers increased the intermediate PG temperatures four to six degrees Celsius. The PS-PAESO-PS modified asphalt contained a lower continuous PG intermediate temperature (12.96°C) than the PS-PAESO modified asphalt (15.11°C). The main factor contributing to this difference was the larger G* value component in the PS-PAESO modified asphalt. Although both PS-PAESO and PS-PAESO-PS asphalt blends possess similar elastic properties at intermediate temperatures as evident from the phase angles, the presence of the second polystyrene block in the PS-PAESO-PS may be contributing the polymers ability to form a network of physical entanglements throughout the asphalt binder to create a more compliant material at intermediate temperatures.

Table 29. DSR results for PAV aged asphalt modified with biopolymers

		Base Asphalt	Base Asphalt processed in shear mill w/o polymer	Base Asphalt w/ 2%PS-PAESO	Base Asphalt w/ 2%PS-PAESO-PS
Temp	Measurement	PAV Aged	PAV Aged	PAV Aged	PAV Aged
22°C	|G*| (Pa)	8.22E+05		3.24E+06	2.49E+06
	δ (degrees)	57.71		43.42	43.77
	G*/sin(δ) (kPa)	694.5		2228	1725
19°C	|G*| (Pa)	1.35E+06		4.80E+06	3.72E+06
	δ (degrees)	55.17		41.42	41.77
	G*/sin(δ) (kPa)	1110		3177	2476
16°C	|G*| (Pa)	2.20E+06	2.47E+06	7.08E+06	5.49E+06
	δ (degrees)	52.51	50.26	39.37	39.77
	G*/sin(δ) (kPa)	1748	1894	4490	3510
13°C	|G*| (Pa)	3.61E+06	3.93E+06	1.03E+07	8.07E+06
	δ (degrees)	49.61	47.49	37.39	37.76
	G*/sin(δ) (kPa)	2746	2900	6248	4937
10°C	|G*| (Pa)	5.80E+06	6.21E+06		1.18E+07
	δ (degrees)	46.7	44.68		35.75
	G*/sin(δ) (kPa)	4216	4366		6884
6°C	|G*| (Pa)	9.13E+06	9.76E+06		
	δ (degrees)	43.73	41.78		
	G*/sin(δ) (kPa)	6310	6495		
PG Failing Temp (°C)		**8.78**	**9.02**	**15.11**	**12.96**

After intermediate temperature testing, the long-term aged biopolymer-asphalt blends from the PAV were evaluated for their low temperature properties (Table 30). When the base asphalt was processed in the shear mill without polymer, the creep stiffness increased and the m-value decreased at low temperatures which resulted in a higher critical cracking temperature. The critical cracking temperature is the temperature at which an asphalt binder's creep stiffness is greater than 300 MPa or m-value is less than 0.300. Both the creep stiffness and m-value are determined from BBR testing after 60 seconds of loading. Adding two percent biopolymers to the base asphalt resulted in the critical cracking temperature

increasing from -36.3°C to -32.8°C for the PS-PAESO modified asphalt and -33.0°C for the PS-PAESO-PS modified asphalt.

Table 30. BBR results for PAV aged asphalt modified with biopolymers

		Base Asphalt		Base Asphalt processed in shear mill w/o polymer		Base Asphalt w/ 2%PS-PAESO		Base Asphalt w/ 2%PS-PAESO-PS	
Temp	Measurement	PAV Aged		PAV Aged		PAV Aged		PAV Aged	
-18°C	Stiffness (MPa)	-	-	-	-	117	-	128	-
	m-value	-	-	-	-	0.360	-	0.336	-
-24°C	Stiffness (MPa)	182	-	190	223	267	279	271	274
	m-value	0.346	-	0.319	0.327	0.291	0.280	0.296	0.290
-30°C	Stiffness (MPa)	479	-	444	479	471	-	-	-
	m-value	0.271	-	0.261	0.267	0.214	-	-	-
Continuous Low Grade (°C)		**-37.68**		**-36.34**		**-32.83**		**-33.02**	

A PG temperature grade comparison of the base asphalt, asphalt modified with Kraton® polymers, and asphalt modified with the biopolymers, is shown in Figures 45 and 46. The charts highlight the differences among base asphalt modified with different polymers at two percent. The D1101 and D1118 polymers increased the high PG temperature approximately one grade, from 51.1°C to 57.2°C and 55.0°C, respectively. For the biopolymers, when two percent PS-PAESO was added to the base asphalt, the high PG temperature increased from 51.1°C to 69.1°C; and when two percent PS-PAESO-PS was added to the base asphalt, the high PG temperature increased to 70.4°C. These increases equate to approximately three grade bumps and demonstrate the effectiveness of the biopolymers. By adding two percent of either biopolymer to the base asphalt, the increase in high temperature PG will enhance the rutting resistance of an asphalt pavement.

While the biopolymers were more effective than the Kraton® polymers at increasing the high temperature performance grade, the biopolymers increased the low temperature PG of the base asphalt one grade while the Kraton® polymers did not (Figure 45). This increase in the low temperature PG caused the asphalt binder to be more susceptible to low temperature cracking at -34°C. The benefit of adding two percent Kraton® polymers was increasing the high PG temperature one grade without changing the low PG. Thus the Kraton® polymers were effective in reducing the temperature susceptibility of the base asphalt. (The Kraton® modified asphalt samples that were tested for low temperature properties contained three percent polymer, not two percent polymer. Since additional polymer will increase the low temperature PG, the extra 1% polymer in these samples should not affect the analysis.)

Therefore, the biopolymers were more effective than the Kraton® polymers in increasing the high temperature, but not as effective in retaining the low stiffness modulus of the base asphalt. Adding two percent of either biopolymer to the base asphalt, increased the low temperature PG one grade (from -34 to -28). Even so, adding two percent PS-PAESO-PS increased the grade range (the high PG minus the low PG) from 88.8 to 103.4 which substantially increases the performance temperature range of the base asphalt.

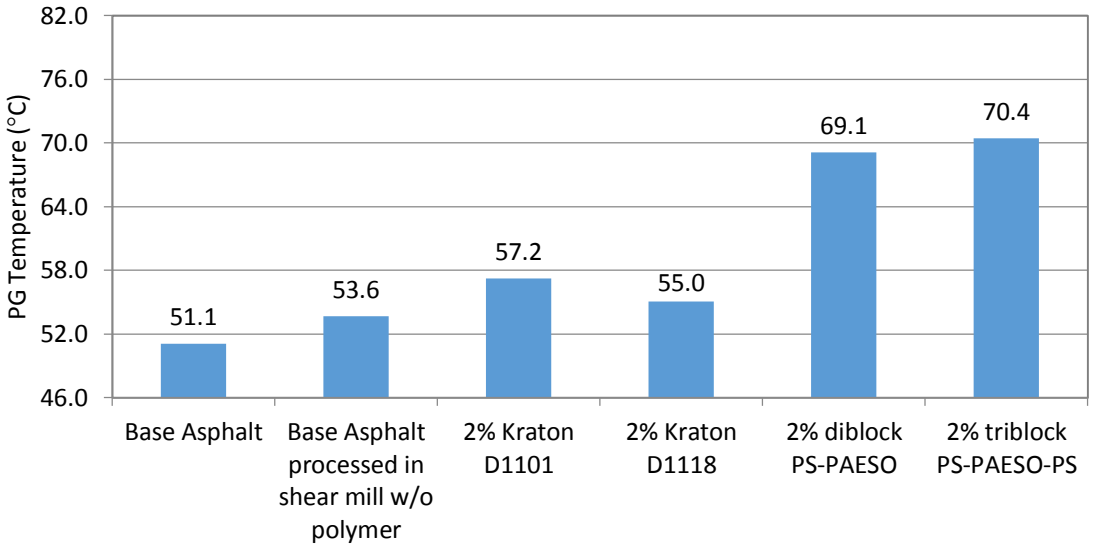

Figure 45. Comparison of high temperature continuous performance grades

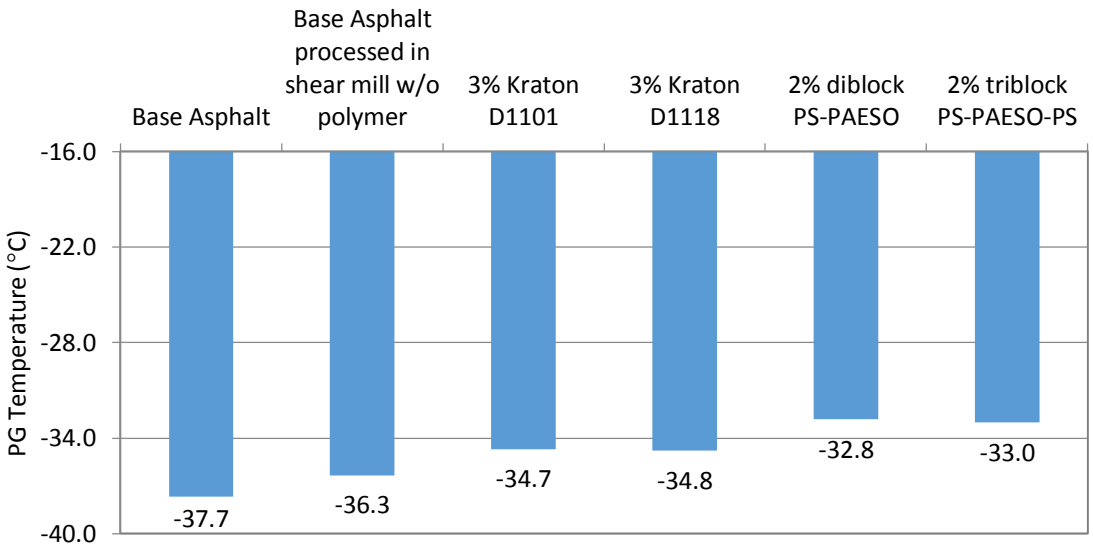

Figure 46. Comparison of low temperature continuous performance grades

Reproducibility of the Test Results

To verify the reproducibility of the dynamic shear rheometer test results when testing the biopolymer modified asphalt, split samples of the base asphalt modified with 2% PS-

PAESO-PS were tested on two different DSRs. The results are reported in Table 32. The DSR used to obtain the results for column A is the DSR used to obtain all the previously mentioned test results in this paper. The DSR used to obtain the results for column B is a DSR from a different manufacturer and located in a different laboratory. DSR A measured the G*/sin(δ) parameter of the split sample as 4.86 kPa at 64°C, and DSR B measured the G*/sin(δ) parameter of the split sample as 5.00 kPa at 64°C. The range of the two test results as a percent of their mean is (d2s%) is 2.84%. This values meet the precision requirement in ASTM D7175 "Standard Test Method for Determining the Rheological Properties of Asphalt Binder Using a Dynamic Shear Rheometer" for multilaboratory precision which is prescribes a maximum d2s% of 22.2% as the greatest difference between two test results that would be considered acceptable.

Table 31. Rheology test results from two different DSRs

RTFO Aged Base Asphalt w/2% PS-PAESO-PS			
Temp	Measurement	DSR A	DSR B
52°C	|G*| (Pa)	21275	23502
	δ (degrees)	67.56	66.4
	G*/sin(δ) (kPa)	23.02	25.6
58°C	|G*| (Pa)	9893	10375
	δ (degrees)	70.85	69.9
	G*/sin(δ) (kPa)	10.48	11.0
64°C	|G*| (Pa)	4680	4779.5
	δ (degrees)	74.34	72.9
	G*/sin(δ) (kPa)	4.86	5.00
70°C	|G*| (Pa)	2233	2231.7
	δ (degrees)	77.72	75.3
	G*/sin(δ) (kPa)	2.29	2.30
76°C	|G*| (Pa)	1094	1046.7
	δ (degrees)	80.76	76.8
	G*/sin(δ) (kPa)	1.11	1.075
PG Failing Temp (°C)		**70.42**	**70.35**

Economic Analysis

The most significant cost in manufacturing SBS polymers is the price of butadiene. For the last decade butadiene has been subject to large price fluctuations from crude oil price increases and global market shifts in supply and demand. Butadiene supply has been tightening due to the abundance of shale gas supplies. Since shale gas has become more available, lighter petrochemical feeds such as ethane have been more commonly used as a feedstock at cracking facilities to produce ethylene and its co-products that include butadiene. However, butadiene is only a co-product when heavier liquid feeds, not lighter feeds, are used. The effects this has had on the price of butadiene over the last several years are shown in Figure 47.

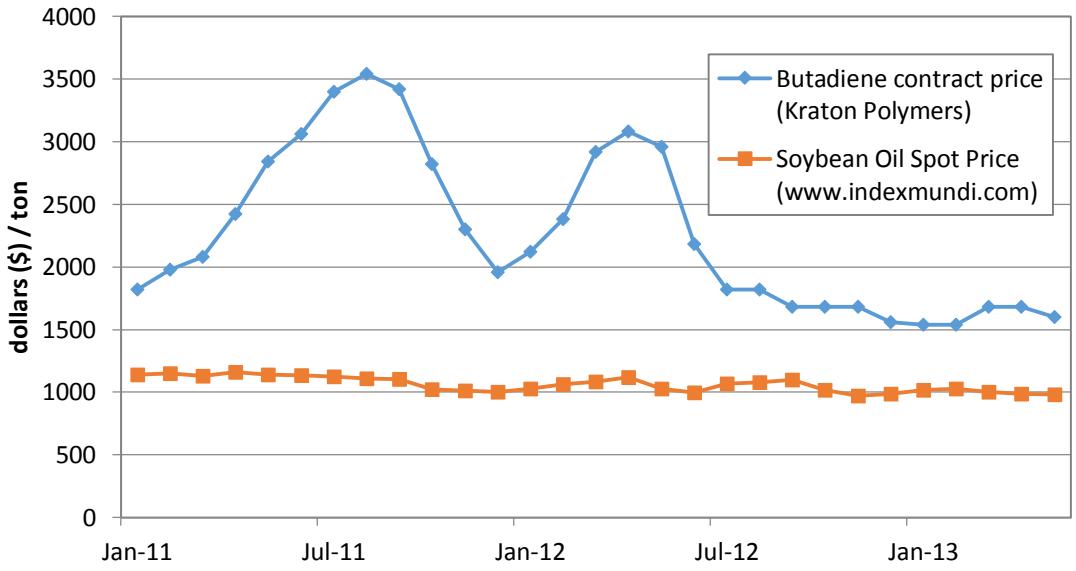

Figure 47. Commodity costs comparison

In contrast, polymerized triglycerides, such as those found in soybean oil, are intrinsically renewable, are environmental friendly, and may also be shown to exhibit biodegradability. The research presented in this report indicates the elastomeric properties of

soybean oil polymer appear to be competitive with modern commodities such as polybutadiene (synthetic rubber). Further, the cost of the soybean oil monomer has become highly competitive in recent years. As shown in Figure 47, soybean oil as a biomonomer is more economical than butadiene monomer feedstocks (e.g., a ton of soybean oil costs less than $1,000, whereas a ton of butadiene has cost up to $3,500). The lower raw materials costs of soybean oil translate into lower costs of polymer modified asphalt. The handling of vegetable oils in producing the bioelastomers and subsequent linking with styrene is also much safer and has less impact on the environment. Thus, the novel soy-based, thermoplastic, elastomeric, block copolymers provide a cost-effective, environment-friendly, viable alternative for the conventional petrochemically-derived polymeric SBS and SB. With future implementation of the developed biopolymers, soybean oil source materials can be utilized to produce polymers for commercial use. Preliminary simulations estimate PAESO will cost about $2000 per ton as compared with $3200 per ton for polybutadiene. This estimate is conservative as it does not consider the reduced amount of storage and handling needed for PAESO compared to polybutadiene. Overall, the estimated lower cost of PAESO compared to polybutadiene can create improved economic conditions for producing soybeans resulting in greater economic opportunities for soy-based biomaterials in the future.

Conclusions and recommendations

Recent advances in polymerization technology have led to the development of elastomeric block copolymers produced with polystyrene and polymerized soy-derived triglycerides. While the past two decades of plant-oil based polymer research has yielded only thermosets, the produced polymers are highly processable thermoplastics. They were produced by first polymerizing acrylated, epoxidized triglyceride molecules in soybean oil to

yield PAESO. SBS-like triblock copolymers were then synthesized by replacing the "B" block (typically polybutadiene) in the ABA triblock structure with PAESO to create polystyrene-*b*-polyAESO-*b*-polystrene (PS-PAESO-PS). Styrene and AESO monomer were polymerized using reversible addition-fragmentation chain-transfer polymerization (RAFT), in the presence of a free radical imitator and a chain transfer agent, to form the block copolymers. The polymerizing step was carried out under conditions effective to achieve a number average degree of polymerization (N_n) for the thermoplastic block copolymer of up to 100,000 without gelation. Following the same process, SB diblock copolymers were also produced using polystyrene and polyAESO.

A laboratory investigation was conducted to characterize the PS-PAESO-PS and PS-PASEO biopolymers and to evaluate their effectiveness as a liquid asphalt modifier. Asphalt modified with the biopolymers was compared to asphalt modified with two commercially available Kraton® polymers, D1101 (SBS) and SB D1118 (SB). Rheology test results showed the biopolymer has the ability to widen the grade range of asphalt and reduce its temperature susceptibility. The base asphalt tested as a continuous PG 51.1-37.7 for a grade range of 88.8°C. Adding two percent D1101 to the base asphalt increased its continuous high PG to a 57.2°C without changing its -34°C grade qualification on the low temperature side. Adding two percent PS-PAESO-PS to the base asphalt changed its continuous PG to a 70.4-33.0 for a 103.4°C grade range. With the addition of two percent PS-PAESO, the base asphalt changed to a continuous PG of 69.1-32.8 for a 101.9°C grade range. Thus, biopolymers significantly enhanced the performance properties of the base asphalt. By adding two percent of either biopolymer to an asphalt binder, the rutting resistance and temperature performance range of an asphalt pavement will improve.

Currently, at a polymer content of two percent, a base asphalt's low temperature PG may increase one grade, which may warrant the use a softer base asphalt to compensate for that effect. As more data from asphalt-modification experiments become available, additional or improved polymer formulation designs may be developed. Future research can improve upon the biopolymers molecular architecture, styrene content, and molecular weight distribution.

Acknowledgements

The authors would like to thank the Iowa Highway Research Board for sponsoring this research as well as the Iowa Department of Transportation, the Asphalt Pavement Association of Iowa (APAI), and the members of the APAI for their participation as technical advisory committee members.

References

Airey, G. D. 2004. Styrene butadiene styrene polymer modification of road bitumens. *Journal of Materials Science* 39:951-959.

Alonso, S., M-T. Luis, R. Zitzumbo, and F. Avalos. 2010. Rheology of asphalt styrene-butadiene blends. *Journal of Materials Science* 45:2591-2597.

Andjelkovic, D. D., L. Fengkui, and R. C. Larock. 2006. Novel Polymeric Materials from Soybean Oils: Synthesis, Properties, and Potential Applications. *ACS Symposium Series* 921:67–81.

Bahia, H.U. and D.A. Anderson. 1995. The SHRP binder rheological parameters: why are they required and how do they compare to conventional properties. *Transportation Research Board.* Record No. 1488: 32-39. Washington D.C.

Bates, F. S., and G. H. Fredrickson. 1999. Block copolymers-designer soft materials. *Physics Today* 52(2):32-38.

Bonnaillie, L. M., and R. P. Wool. 2007. Thermosetting Foam With a High Bio-Based Content From Acrylated Epoxidized Soybean Oil and Carbon Dioxide. *Journal of Applied Polymer Science* 105(3):1042–52.

Bunker, S., C. Staller, N. Willenbacher, and R. Wool. 2003. Miniemulsion Polymerization of Acrylated Methyl Oleate for Pressure Sensitive Adhesives. *International Journal of Adhesion and Adhesives* 23(1):29–38.

Bulatovic, V. O., V. Rek, and K. J. Markovic. 2012. Polymer modified bitumen. *Materials Research Innovations* 1:1-6.

Bunker, S., and R. P. Wool. 2002. Synthesis and Characterization of Monomers and Polymers for Adhesives from Methyl Oleate. *Journal of Polymer Science Part A: Polymer Chemistry* 40(4):451–58.

Epps, J.A. 1986. Asphalt Pavement Modifiers. *Civil Engineering Magazine* April.

Fernandes, M. R. S., M. M. C. Forte, and L. F. M. Leite. 2008. Rheological Evaluation of Polymer-Modified Asphalt Binders. *Materials Research* 11(3):381-386.

Foster, J. 2011. Lighter feeds in US steam crackers brings new attitude toward on-purpose butadiene, propylene prospects. *Platts Special Report: Petrochemicals* 1-6.

Fried, J. R. 2008. *Polymer Science and Technology*. Second edition. Upper Saddle River, NJ: Prentice Hall.

Hiemenz, P. C., and T. P. Lodge. 2007. *Polymer Chemistry*. Second edition. Raton, FL: CRC Press.

Isacsson, U., and X. Lu. 1999. Characterization of bitumens modified with SEBS, EVA and EBA polymer. *Journal of Materials Science* 34:3737-3745.

Larock, R. C., X. Dong, S. Chung, K. Reddy, and L. E. Ehlers. 2001. Preparation of Conjugated Soybean Oil and Other Natural Oils and Fatty Acids by Homogeneous Transition Metal Catalysis. *Journal of the American Oil Chemists' Society* 78:447-453.

Lesueur, D. 2009. The colloidal structure of bitumen: consequences on the rheology and on the mechanisms of bitumen modification. *Advances in Colloid and Interface Science* 145:42-82.

Lewandowski, L. H. 1994. Polymer modification of paving asphalt binders. *Rubber Chemistry and Technology* 76(3)447.

Lu, J., K. Shrikant, and R. P. Wool. 2005. New Sheet Molding Compound Resins From Soybean Oil. I. Synthesis and Characterization. *Polymer* 46(1):71–80.

Lu, X., and U. Isacsson. 1997. Compatibility and storage stability of styrene-butadiene-styrene copolymer modified bitumens. *Materials and Structures* 30:618-626.

Lu, Y, and R. C. Larock. 2009. Novel Polymeric Materials from Vegetable Oils and Vinyl Monomers: Preparation, Properties and Applications. *ChemSusChem* 2:136-147.

Lu, Y., Y. Xia., and R. C. Larock. 2011. Surfactant-Free Core-Shell Hybrid Latexes From Soybean Oil-Based Waterborne Polyurethanes and Poly(Styrene-Butyl Acrylate). *Progress in Organic Coatings* 71(4):336–42.

Martinez-Estrada A., A. E. Chavez-Castellanos, M. Herrera-Alonso, and R. Herrera-Najera. 2010. Comparative Study of the Effect of Sulfur on the Morphology and Rheological Properties of SB and SBS modified asphalt. *Journal of Applied Polymer Science* 115:3409-3422.

Masson, J.-F., P. Collins, G. Robertson, J. R. Woods, and J. Margeson. 2003. Thermodynamics, Phase Diagrams, and Stability of Bitumen-Polymer Blends. *Energy & Fuels* 17:714-724.

Odian, G. 1991. *Principles of Polymerization*. Third edition. New York: John Wiley and Sons, Inc.

Pfister, D. P., and R. C. Larock. 2010. Thermophysical properties of conjugated soybean oil/corn 30 stover biocomposites. *Bioresource Technology* 101(15):6200–06.

Robertson, M. L., K. Chang, W. M. Gramlich, and M. A. Hillmyer. 2010. Toughening of Polylactide with Polymerized Soybean Oil. *Macromolecules* 43:1807-1814.

Yang, L., C. Dai, L. Ma, and S. Lin. 2010. Conjugation of soybean oil and its free-radical copolymerization with acrylonitrile. *Journal of Polymers and the Environment* 19:189-195

Zhu, L., and R. P. Wool. 2006. Nanoclay Reinforced Bio-Based Elastomers: Synthesis and Characterization. *Polymer* 47(24):8106–15.

CHAPTER 6. GENERAL CONCLUSIONS

Evaluation of Recycled Asphalt Shingles in Hot Mix Asphalt

To comprehensively answer the design, performance, and environmental questions about using RAS in HMA, Transportation Pooled Fund (TPF)-5(213) was created as collaboration of seven state transportation agencies in the United States to research the effects of RAS on the performance of asphalt applications. As part of TPF-5(213), each state highway agency proposed a unique field demonstration project that investigated different aspects of asphalt mixes containing RAS specific to their state needs. The demonstration projects of Transportation Pooled Fund TPF-5(213) showed that pavements using RAS alone or in combination with other cost saving technologies (e.g., WMA, RAP, GTR, SMA) can be successfully produced and meet state agency quality assurance requirements for mix asphalt content, gradation, and volumetrics. These mixes have very promising prospects since laboratory test results indicate good rutting resistance based on the flow number and dynamic modulus tests. The mixes also demonstrated good fatigue cracking resistance in the four-point bending beam apparatus, with the SMA mixes from Illinois (which used 5% RAS and no added fibers) exhibiting the most desirable fatigue characteristics. Fracture properties of the mixes at low temperatures determined by the SCB fracture energy test showed no statistical change in mixes with RAS compared to the mixes without RAS for the Missouri, Minnesota, Indiana, Wisconsin, and Colorado projects. Based on the SCB results, the addition of RAS materials to HMA is not detrimental to its fracture resistance.

The test results of the extracted binder from these mixes showed that when RAS is used in HMA, the performance grade of the base binder increases on the high and low side.

The average results of all the mixes in the study showed that for every 1 percent increase in RAS, the low temperature grade of the base binder increased 1.9°C; and for every 1 percent increase in RAP, the low temperature grade of the base binder increased 0.3°C.

Based on these results, it is recommended that state highway agencies understand the material quality and binder characteristics of RAS materials that are being processed in their respective state before implanting a RAS specification. Depending on the RAS source and the area of the country post-consumer shingles have originated from, the RAS binder properties can widely vary. The binder properties of the RAS will help state highway agencies determine the amount of RAS that can be added before a softer virgin base binder will be needed to ensure the total binder matrix of the hot mix asphalt meets the intended performance grade design criteria. As a starting point for state highway agencies that have not conducted initial RAS research, a level of three percent RAS or 14 percent binder replacement is the maximum recommended amount of RAS binder used in HMA without requiring a six degree grade bump in the base binder.

Delaying Reflective Cracking using Crack-Relief Interlayers

The laboratory performance of a crack-relief interlayer mix design was assessed for resistance to cracking from repeated strains by using the four-point bending beam apparatus. The initial interlayer mix design failed the minimum 100,000 load cycle criteria in the four-point bending beam but eventually passed the criteria after the polymer modified binder was re-engineered using SBS polymer Kraton D0432. Afterwards, the average number of load cycles achieved in the bending beam apparatus increased from 18,235 to 201,390, thereby passing the 100,000 load cycle criteria.

Using the interlayer as part of an overlay pavement system on US 169 in Adel, IA only increased the overlay construction costs by 10.6 percent while decreasing reflective cracking by 29 percent after one winter season. Had the interlayer been produced closer to the mix design targets, the overlay would most likely have exhibited even less cracking. Based on the substantial reduction in reflective cracking and only marginal cost increases from using the interlayer on US 169, it is recommended that future HMA overlay projects in Iowa incorporate the crack-relief interlayer to delay reflective cracking.

The pavement test sections on US 169 should be monitored for cracking at least once per year for the next five years to determine the long-term performance of the interlayer and non-interlayer overlay test sections. Additionally, more trial projects using the interlayer should be conducted to obtain a more complete understanding of how effective the interlayer is at delaying reflective cracking.

For future interlayer mixes that do not initially meet the minimum 100,000 load cycle criteria in the four-point bending beam, the number of load cycles the mix design can achieve in the performance test can be increased by improving the elastic and fatigue resistant properties of the binder. Based on the laboratory test results for this project, this can be accomplished by using a high percentage of Kraton D0243 SBS to create a highly polymer modified binder.

Development of Bio-Based Thermoplastic-Elastomeric Block-Copolymers

The third and fourth paper of this dissertation reports the recent advances in polymerization techniques that have enabled the synthesis of elastomeric, thermoplastic, block-copolymers comprised of styrene and soybean oil, where the “B” block in SBS polymers is replaced with polymerized triglycerides derived from soybean oil. These new

breeds of biopolymers have elastomeric properties comparable to well-established butadiene-based styrenic block-copolymers.

Thermoplastic-elastomeric block-copolymers were produced using controlled radical polymerization techniques of atom transfer radical polymerization (ATRP) and reversible addition-fragmentation chain-transfer (RAFT) polymerization to create block copolymers. Triblock copolymers were synthesized by polymerizing acrylated epoxidized soybean oil (AESO) and styrene monomer to create polystyrene-*b*-polyAESO-*b*-polystrene (PS-PAESO-PS) and its diblock conjugations. Laboratory investigations were conducted to evaluate the effectiveness of the newly derived PS-PAESO-PS and PS-PAESO polymers as asphalt modifiers.

The laboratory results from the third paper demonstrated that adding three percent PS-PAESO-PS polymer to asphalt binder increased the low critical temperature of the base asphalt binder 3.0°C while increasing its high critical temperature 10.8°C. This change in grade range was similar to SBS's effect on the asphalt binder. In contrast, the laboratory results from the fourth paper demonstrated that adding two percent PS-PAESO-PS to asphalt binder increased the low critical temperature of the base asphalt binder 3.3°C while increasing its high critical temperature 15.2°C. The differences between the reported results in these two papers is attributed to the differences in materials (both polymer and asphalt batches) and asphalt-binder blending processes used between the two studies. Nevertheless, the biopolymers significantly enhanced the rheological properties of the base asphalt and improved its resistance to shear deformation. Since the critical low temperature of the base asphalt increased approximately 3°C in both studies from the addition of the PS-PAESO-PS modifier, the use of a softer base asphalt binder may be warranted to ensure the base asphalt

binder's low temperature PG does not increase when formulating a polymer modified asphalt using the biopolymer.

Implementation Readiness and Benefits

Most vegetable oils (*e.g.* rapeseed, linseed, soybeans) can be used as a triglyceride source for polymer synthesis in this process. Soybean oil is used since it is the most abundant vegetable oil on earth, and it is readily available in the United States. It currently costs 40 percent less than butadiene. These lower costs will translate into lower costs of polymer-modified asphalt. Polymerized triglycerides are also intrinsically renewable, environmentally friendly, and safer to handle than butadiene.

Future Work

As additional data from asphalt-modification experiments become available, additional or improved polymer formulation designs may be developed. Future research can improve upon the biopolymers molecular architecture, styrene content, and molecular weight distribution.

A larger reactor has been purchased that is capable of making two kilogram samples, which is substantially larger than the approximately 100 gram samples produced for these studies. In addition, a pilot plant is currently being constructed that will be able to produce even larger quantities of the biopolymers for future research.

Further work evaluating asphalt mixtures for rutting, low temperature cracking, and moisture susceptibility should also be conducted. Based upon the evaluation of the mixture, an additional phase of research should include a field demonstration project that tests the performance of asphalt pavement containing terminally blended asphalt binder modified with the soy-based block copolymers.

APPENDIX A. DYNAMIC MODULUS STATISTICAL OUTPUT

Oneway Analysis of Missouri Dynamic Modulus (MPa) 37°C, 5 Hz By Mix Type

Oneway Anova
Summary of Fit

Rsquare	0.16291
Adj Rsquare	0.023395
Root Mean Square Error	390.3071
Mean of Response	3288.467
Observations (or Sum Wgts)	15

Analysis of Variance

Source	DF	Sum of Squares	Mean Square	F Ratio	Prob > F
Missouri Mix Type	2	355770.5	177885	1.1677	0.3441
Error	12	1828075.2	152340		
C. Total	14	2183845.7			

Means for Oneway Anova

Level	Number	Mean	Std Error	Lower 95%	Upper 95%
15 RAP	5	3243.20	174.55	2862.9	3623.5
5 CRAS/10 RAP	5	3126.60	174.55	2746.3	3506.9
5 FRAS/10 RAP	5	3495.60	174.55	3115.3	3875.9

Std Error uses a pooled estimate of error variance

Means Comparisons
Comparisons for all pairs using Tukey-Kramer HSD
Confidence Quantile

q*	Alpha
2.66776	0.05

Connecting Letters Report

Level		Mean
5 FRAS/10 RAP	A	3495.6000
15 RAP	A	3243.2000
5 CRAS/10 RAP	A	3126.6000

Levels not connected by same letter are significantly different.

Oneway Analysis of Iowa Dynamic Modulus (MPa) 37°C, 5 Hz By Iowa Mix Type

Oneway Anova
Summary of Fit

Rsquare	0.04869
Adj Rsquare	-0.12968
Root Mean Square Error	409.3114
Mean of Response	1299.105
Observations (or Sum Wgts)	20

Analysis of Variance

Source	DF	Sum of Squares	Mean Square	F Ratio	Prob > F
Iowa Mix Type	3	137196.7	45732	0.2730	0.8440
Error	16	2680573.4	167536		
C. Total	19	2817770.0			

Means for Oneway Anova

Level	Number	Mean	Std Error	Lower 95%	Upper 95%
0 RAS	5	1376.64	183.05	988.59	1764.7
4 RAS	5	1160.06	183.05	772.01	1548.1
5 RAS	5	1339.92	183.05	951.87	1728.0
6 RAS	5	1319.80	183.05	931.75	1707.8

Std Error uses a pooled estimate of error variance

Means Comparisons
Comparisons for all pairs using Tukey-Kramer HSD
Confidence Quantile

q*	Alpha
2.86102	0.05

Connecting Letters Report

Level		Mean
0 RAS	A	1376.6400
5 RAS	A	1339.9200
6 RAS	A	1319.8000
4 RAS	A	1160.0600

Levels not connected by same letter are significantly different.

Oneway Analysis of Minnesota Dynamic Modulus (MPa) 37°C, 5 Hz By Mix Type

Oneway Anova
Summary of Fit

Rsquare	0.303094
Adj Rsquare	0.186943
Root Mean Square Error	362.3303
Mean of Response	1235.627
Observations (or Sum Wgts)	15

Analysis of Variance

Source	DF	Sum of Squares	Mean Square	F Ratio	Prob > F
Minnesota Mix Type	2	685163.0	342581	2.6095	0.1146
Error	12	1575399.3	131283		
C. Total	14	2260562.3			

Means for Oneway Anova

Level	Number	Mean	Std Error	Lower 95%	Upper 95%
30 RAP	5	933.88	162.04	580.8	1286.9
5 PC RAS	5	1371.40	162.04	1018.3	1724.5
5 PM RAS	5	1401.60	162.04	1048.5	1754.7

Std Error uses a pooled estimate of error variance

Means Comparisons
Comparisons for all pairs using Tukey-Kramer HSD
Confidence Quantile

q*	Alpha
2.66776	0.05

Connecting Letters Report

Level		Mean
5 PM RAS	A	1401.6000
5 PC RAS	A	1371.4000
30 RAP	A	933.8800

Levels not connected by same letter are significantly different.

Oneway Analysis of Indiana Dynamic Modulus (MPa) 37°C, 5 Hz By Mix Type

Oneway Anova
Summary of Fit

Rsquare	0.369499
Adj Rsquare	0.243398
Root Mean Square Error	439.5345
Mean of Response	2590.846
Observations (or Sum Wgts)	13

Analysis of Variance

Source	DF	Sum of Squares	Mean Square	F Ratio	Prob > F
Indiana Mix Type	2	1132172.2	566086	2.9302	0.0996
Error	10	1931905.5	193191		
C. Total	12	3064077.7			

Means for Oneway Anova

Level	Number	Mean	Std Error	Lower 95%	Upper 95%
15 RAP HMA	3	3112.33	253.77	2546.9	3677.8
3 RAS HMA	5	2349.80	196.57	1911.8	2787.8
3 RAS WMA	5	2519.00	196.57	2081.0	2957.0

Std Error uses a pooled estimate of error variance

Means Comparisons
Comparisons for all pairs using Tukey-Kramer HSD
Confidence Quantile

q*	Alpha
2.74129	0.05

Connecting Letters Report

Level		Mean
15 RAP HMA	A	3112.3333
3 RAS WMA	A	2519.0000
3 RAS HMA	A	2349.8000

Levels not connected by same letter are significantly different.

Oneway Analysis of Wisconsin Dynamic Modulus (MPa) 37°C, 5 Hz By Mix Type

Oneway Anova
Summary of Fit

Rsquare	0.917371
Adj Rsquare	0.896713
Root Mean Square Error	44.41471
Mean of Response	1379.167
Observations (or Sum Wgts)	6

t Test
No Evotherm®-Evotherm® 3G

Difference	241.667	t Ratio	6.664008
Std Err Dif	36.264	DF	4
Upper CL Dif	342.353	Prob > |t|	0.0026*
Lower CL Dif	140.980	Prob > t	0.0013*
Confidence	0.95	Prob < t	0.9987

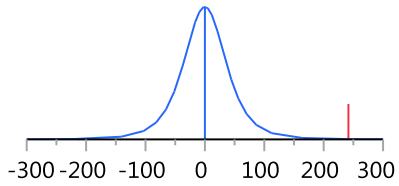

Analysis of Variance

Source	DF	Sum of Squares	Mean Square	F Ratio	Prob > F
Wisconsin Mix Type	1	87604.167	87604.2	44.4090	0.0026*
Error	4	7890.667	1972.7		
C. Total	5	95494.833			

Means for Oneway Anova

Level	Number	Mean	Std Error	Lower 95%	Upper 95%
Evotherm® 3G	3	1258.33	25.643	1187.1	1329.5
No Evotherm®	3	1500.00	25.643	1428.8	1571.2

Std Error uses a pooled estimate of error variance

Means Comparisons
Comparisons for all pairs using Tukey-Kramer HSD
Confidence Quantile

q*	Alpha
2.77645	0.05

Connecting Letters Report

Level		Mean
No Evotherm®	A	1500.0000
Evotherm® 3G	B	1258.3333

Oneway Analysis of Colorado Dynamic Modulus (MPa) 37°C, 5 Hz By Mix Type

Oneway Anova
Summary of Fit

Rsquare	0.825569
Adj Rsquare	0.781961
Root Mean Square Error	83.41263
Mean of Response	1438.833
Observations (or Sum Wgts)	6

t Test
3 RAS/15 RAP-20 RAP

Difference	-296.33	t Ratio	-4.35105
Std Err Dif	68.11	DF	4
Upper CL Dif	-107.24	Prob > |t|	0.0121*
Lower CL Dif	-485.43	Prob > t	0.9939
Confidence	0.95	Prob < t	0.0061*

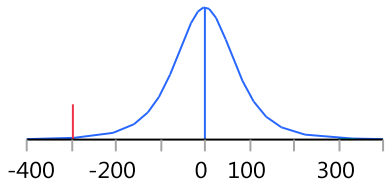

Analysis of Variance

Source	DF	Sum of Squares	Mean Square	F Ratio	Prob > F
Colorado Mix Type	1	131720.17	131720	18.9317	0.0121*
Error	4	27830.67	6958		
C. Total	5	159550.83			

Means for Oneway Anova

Level	Number	Mean	Std Error	Lower 95%	Upper 95%
20 RAP	3	1587.00	48.158	1453.3	1720.7
3 RAS/15 RAP	3	1290.67	48.158	1157.0	1424.4

Std Error uses a pooled estimate of error variance

Means Comparisons
Comparisons for all pairs using Tukey-Kramer HSD
Confidence Quantile

q*	Alpha
2.77645	0.05

Connecting Letters Report

Level		Mean
20 RAP	A	1587.0000
3 RAS/15 RAP	B	1290.6667

Oneway Analysis of Illinois Dynamic Modulus (MPa) 37°C, 5 Hz By Mix Type

Oneway Anova
Summary of Fit

Rsquare	0.362256
Adj Rsquare	0.322397
Root Mean Square Error	368.7949
Mean of Response	1824.944
Observations (or Sum Wgts)	18

t Test
11 RAP-0 RAP

Difference	524.111	t Ratio	3.014704
Std Err Dif	173.852	DF	16
Upper CL Dif	892.660	Prob > |t|	0.0082*
Lower CL Dif	155.562	Prob > t	0.0041*
Confidence	0.95	Prob < t	0.9959

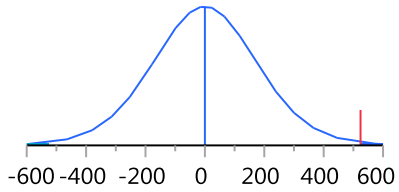

Analysis of Variance

Source	DF	Sum of Squares	Mean Square	F Ratio	Prob > F
Illinois Mix Type	1	1236116.1	1236116	9.0884	0.0082*
Error	16	2176154.9	136010		
C. Total	17	3412270.9			

Means for Oneway Anova

Level	Number	Mean	Std Error	Lower 95%	Upper 95%
0 RAP	9	1562.89	122.93	1302.3	1823.5
11 RAP	9	2087.00	122.93	1826.4	2347.6

Std Error uses a pooled estimate of error variance

Means Comparisons
Comparisons for all pairs using Tukey-Kramer HSD
Confidence Quantile

q*	Alpha
2.11991	0.05

Connecting Letters Report

Level		Mean
11 RAP	A	2087.0000
0 RAP	B	1562.8889

Response Illinois Dynamic Modulus (MPa) 37°C, 5 Hz
Whole Model

Summary of Fit

RSquare	0.711726
RSquare Adj	0.603623
Root Mean Square Error	300.3553
Mean of Response	1830.917
Observations (or Sum Wgts)	12

Analysis of Variance

Source	DF	Sum of Squares	Mean Square	F Ratio
Model	3	1781838.3	593946	6.5838
Error	8	721706.7	90213	**Prob > F**
C. Total	11	2503544.9		0.0149*

Effect Tests

Source	Nparm	DF	Sum of Squares	F Ratio	Prob > F
Sample Type	1	1	741524.08	8.2197	0.0209*
Illinois Mix Type	1	1	848540.08	9.4059	0.0154*
Illinois Mix Type*Sample Type	1	1	191774.08	2.1258	0.1829

Sample Type

Least Squares Means Table

Level	Least Sq Mean	Std Error	Mean
Field	1582.3333	122.61956	1582.33
Lab	2079.5000	122.61956	2079.50

LS Means Plot

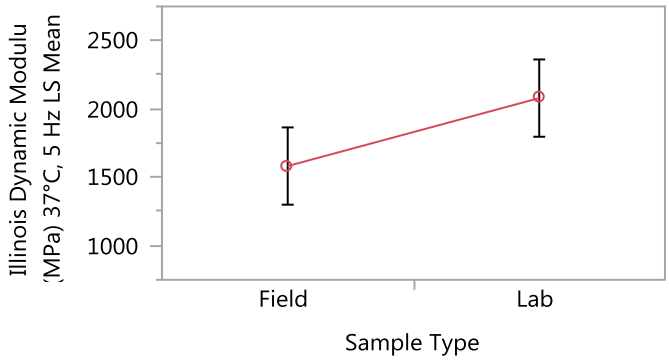

LSMeans Differences Student's t

α=0.050 t=2.306

Level		Least Sq Mean
Lab	A	2079.5000
Field	B	1582.3333

Illinois Mix Type

Least Squares Means Table

Level	Least Sq Mean	Std Error	Mean
0 RAP	1565.0000	122.61956	1565.00
11 RAP	2096.8333	122.61956	2096.83

LS Means Plot

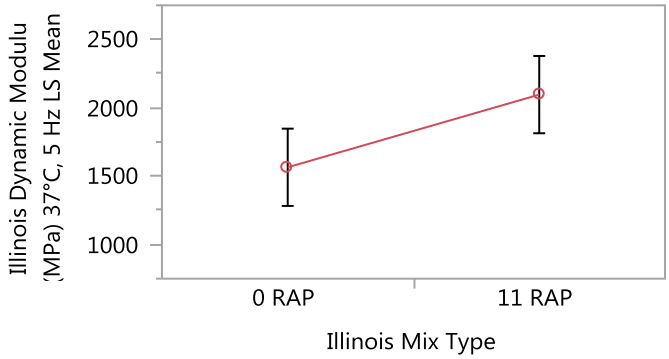

LSMeans Differences Student's t

α=0.050 t=2.306

Level		Least Sq Mean
11 RAP	A	2096.8333
0 RAP	B	1565.0000

Levels not connected by same letter are significantly different.

Illinois Mix Type*Sample Type

LS Means Plot

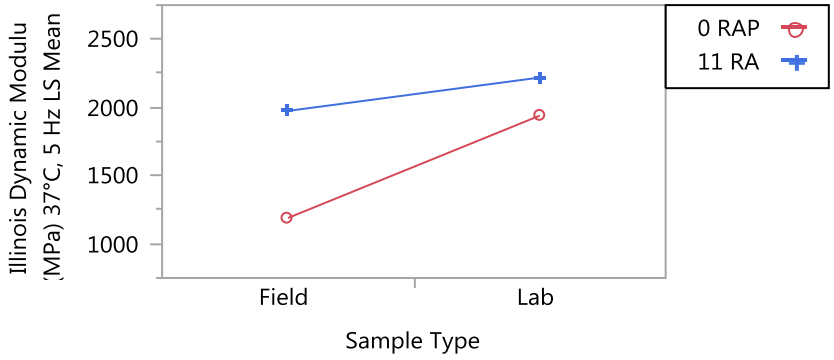

Response Illinois Dynamic Modulus (MPa) 37°C, 5 Hz
Whole Model

Summary of Fit

RSquare	0.470685
RSquare Adj	0.272192
Root Mean Square Error	317.6809
Mean of Response	1946.25
Observations (or Sum Wgts)	12

Analysis of Variance

Source	DF	Sum of Squares	Mean Square	F Ratio
Model	3	717940.9	239314	2.3713
Error	8	807369.3	100921	**Prob > F**
C. Total	11	1525310.3		0.1463

Effect Tests

Source	Nparm	DF	Sum of Squares	F Ratio	Prob > F
Binder Modification	1	1	213066.75	2.1112	0.1843
Illinois Mix Type	1	1	465314.08	4.6107	0.0640
Illinois Mix Type*Binder Modification	1	1	39560.08	0.3920	0.5487

Binder Modification

Least Squares Means Table

Level	Least Sq Mean	Std Error	Mean
GTR	1813.0000	129.69269	1813.00
Polymer	2079.5000	129.69269	2079.50

LS Means Plot

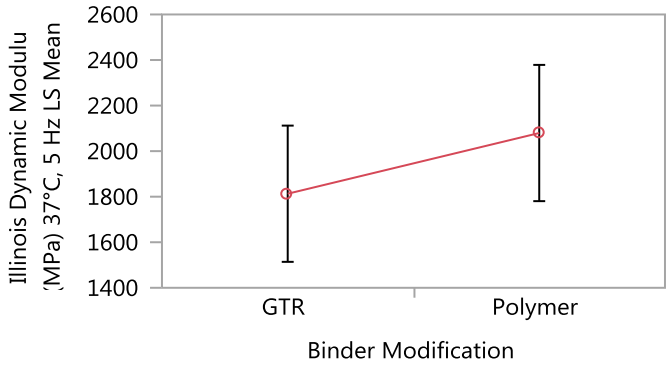

LSMeans Differences Student's t

α=0.050 t=2.306

Level		Least Sq Mean
Polymer	A	2079.5000
GTR	A	1813.0000

Illinois Mix Type

Least Squares Means Table

Level	Least Sq Mean	Std Error	Mean
0 RAP	1749.3333	129.69269	1749.33
11 RAP	2143.1667	129.69269	2143.17

LS Means Plot

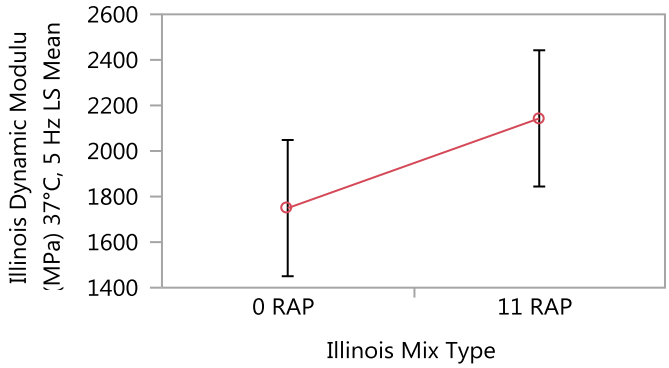

LSMeans Differences Student's t

α=0.050 t=2.306

Level		Least Sq Mean
11 RAP	A	2143.1667
0 RAP	A	1749.3333

Levels not connected by same letter are significantly different.

Illinois Mix Type*Binder Modification

LS Means Plot

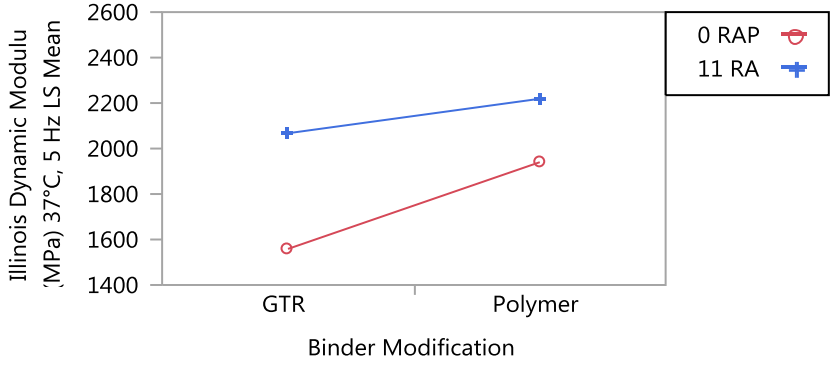

APPENDIX B. FLOW NUMBER STATISTICAL OUTPUT

Oneway Analysis of Flow Number By Iowa Mix Type

Oneway Anova
Summary of Fit

Rsquare	0.745595
Adj Rsquare	0.681994
Root Mean Square Error	1348.672
Mean of Response	3633.75
Observations (or Sum Wgts)	16

Analysis of Variance

Source	DF	Sum of Squares	Mean Square	F Ratio	Prob > F
Iowa Mix Type	3	63969367	21323122	11.7230	0.0007*
Error	12	21826983	1818915.2		
C. Total	15	85796349			

Means for Oneway Anova

Level	Number	Mean	Std Error	Lower 95%	Upper 95%
0 RAS	4	710.75	674.34	-759	2180.0
4 RAS	4	2937.75	674.34	1468	4407.0
5 RAS	4	4987.50	674.34	3518	6456.8
6 RAS	4	5899.00	674.34	4430	7368.3

Std Error uses a pooled estimate of error variance

Means Comparisons
Comparisons for all pairs using Tukey-Kramer HSD
Confidence Quantile

q*	Alpha
2.96880	0.05

Connecting Letters Report

Level			Mean
6 RAS	A		5899.0000
5 RAS	A	B	4987.5000
4 RAS		B	C 2937.7500
0 RAS			C 710.7500

Levels not connected by same letter are significantly different.

Oneway Analysis of Flow Number By Minnesota Mix Type

Oneway Anova
Summary of Fit

Rsquare	0.790821
Adj Rsquare	0.755958
Root Mean Square Error	406.5274
Mean of Response	1654.4
Observations (or Sum Wgts)	15

Analysis of Variance

Source	DF	Sum of Squares	Mean Square	F Ratio	Prob > F
Minnesota Mix Type	2	7497572.8	3748786	22.6835	<.0001*
Error	12	1983174.8	165265		
C. Total	14	9480747.6			

Means for Oneway Anova

Level	Number	Mean	Std Error	Lower 95%	Upper 95%
30 RAP	5	766.80	181.80	370.7	1162.9
5 PC RAS	5	2496.80	181.80	2100.7	2892.9
5 PM RAS	5	1699.60	181.80	1303.5	2095.7

Std Error uses a pooled estimate of error variance

Means Comparisons
Comparisons for all pairs using Tukey-Kramer HSD
Confidence Quantile

q*	Alpha
2.66776	0.05

Connecting Letters Report

Level		Mean
5 PC RAS	A	2496.8000
5 PM RAS	B	1699.6000
30 RAP	C	766.8000

Levels not connected by same letter are significantly different.

Oneway Analysis of Flow Number By Indiana Mix Type

Oneway Anova
Summary of Fit

Rsquare	0.938622
Adj Rsquare	0.926346
Root Mean Square Error	411.457
Mean of Response	9153
Observations (or Sum Wgts)	13

Analysis of Variance

Source	DF	Sum of Squares	Mean Square	F Ratio	Prob > F
Indiana Mix Type	2	25889709	12944855	76.4625	<.0001*
Error	10	1692969	169296.87		
C. Total	12	27582678			

Means for Oneway Anova

Level	Number	Mean	Std Error	Lower 95%	Upper 95%
15 RAP HMA	3	6578.33	237.55	6049.0	7108
3 RAS HMA	5	9864.60	184.01	9454.6	10275
3 RAS WMA	5	9986.20	184.01	9576.2	10396

Std Error uses a pooled estimate of error variance

Means Comparisons
Comparisons for all pairs using Tukey-Kramer HSD
Confidence Quantile

q*	Alpha
2.74129	0.05

Connecting Letters Report

Level		Mean
3 RAS WMA	A	9986.2000
3 RAS HMA	A	9864.6000
15 RAP HMA	B	6578.3333

Levels not connected by same letter are significantly different.

Oneway Analysis of Flow Number By Wisconsin Mix Type

Oneway Anova
Summary of Fit

Rsquare	0.453618
Adj Rsquare	0.317023
Root Mean Square Error	1198.984
Mean of Response	3020.333
Observations (or Sum Wgts)	6

t Test
No Evotherm®-Evotherm® 3G

Difference	1784.0	t Ratio	1.82233
Std Err Dif	979.0	DF	4
Upper CL Dif	4502.0	Prob > |t|	0.1425
Lower CL Dif	-934.0	Prob > t	0.0712
Confidence	0.95	Prob < t	0.9288

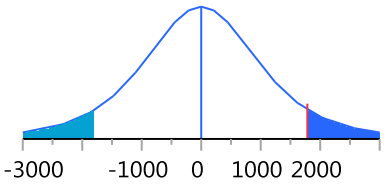

Analysis of Variance

Source	DF	Sum of Squares	Mean Square	F Ratio	Prob > F
Wisconsin Mix Type	1	4773984	4773984	3.3209	0.1425
Error	4	5750253	1437563		
C. Total	5	10524237			

Means for Oneway Anova

Level	Number	Mean	Std Error	Lower 95%	Upper 95%
Evotherm® 3G	3	2128.33	692.23	206.4	4050.3
No Evotherm®	3	3912.33	692.23	1990.4	5834.3

Std Error uses a pooled estimate of error variance

Means Comparisons
Comparisons for all pairs using Tukey-Kramer HSD
Confidence Quantile

q*	Alpha
2.77645	0.05

Connecting Letters Report

Level		Mean
Evotherm® 3G	A	2128.33
No Evotherm®	A	3912.33

Oneway Analysis of Flow Number By Colorado Mix Type

Oneway Anova
Summary of Fit

Rsquare	0.147583
Adj Rsquare	-0.06552
Root Mean Square Error	2189.42
Mean of Response	8276.5
Observations (or Sum Wgts)	6

t Test
3 RAS/15 RAP-20 RAP

Difference	1487.7	t Ratio	0.83219
Std Err Dif	1787.7	DF	4
Upper CL Dif	6451.0	Prob > |t|	0.4521
Lower CL Dif	-3475.7	Prob > t	0.2261
Confidence	0.95	Prob < t	0.7739

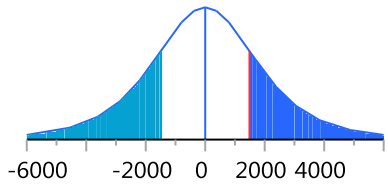

Analysis of Variance

Source	DF	Sum of Squares	Mean Square	F Ratio	Prob > F
Colorado Mix Type	1	3319728	3319728	0.6925	0.4521
Error	4	19174233	4793558		
C. Total	5	22493962			

Means for Oneway Anova

Level	Number	Mean	Std Error	Lower 95%	Upper 95%
20 RAP	3	7532.67	1264.1	4023.1	11042
3 RAS/15 RAP	3	9020.33	1264.1	5510.7	12530

Std Error uses a pooled estimate of error variance

Means Comparisons
Comparisons for all pairs using Tukey-Kramer HSD
Confidence Quantile

q*	Alpha
2.77645	0.05

Connecting Letters Report

Level		Mean
3 RAS/15 RAP	A	9020.3333
20 RAP	A	7532.6667

APPENDIX C. FRACTURE ENERGY STATISTICAL OUTPUT

Response Missouri Fracture Energy (J/m2)
Whole Model

Summary of Fit

RSquare	0.642516
RSquare Adj	0.47867
Root Mean Square Error	57.3209
Mean of Response	410.9829
Observations (or Sum Wgts)	36

Analysis of Variance

Source	DF	Sum of Squares	Mean Square	F Ratio
Model	11	141731.19	12884.7	3.9215
Error	24	78856.45	3285.7	**Prob > F**
C. Total	35	220587.63		0.0025*

Effect Tests

Source	Nparm	DF	Sum of Squares	F Ratio	Prob > F
Missouri Mix Type	2	2	19940.381	3.0344	0.0669
Temperature (°C)	3	3	67943.550	6.8929	0.0017*
Missouri Mix Type*Temperature (°C)	6	6	53847.255	2.7314	0.0363*

Missouri Mix Type

Least Squares Means Table

Level	Least Sq Mean	Std Error	Mean
15 RAP	428.10233	16.547118	428.102
5 CRAS/10 RAP	377.70392	16.547118	377.704
5 FRAS/10 RAP	427.14250	16.547118	427.143

LS Means Plot

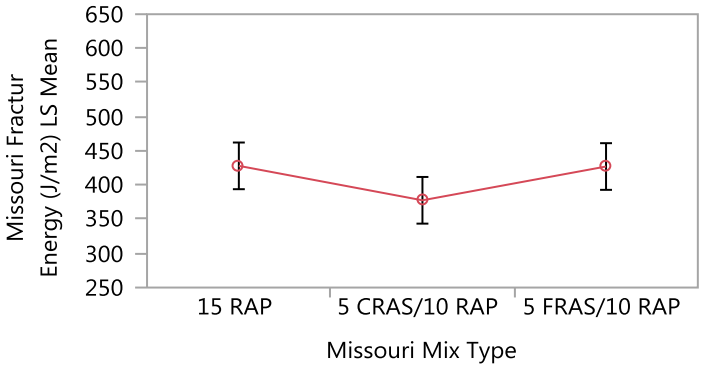

LSMeans Differences Tukey HSD

α=0.050 Q=2.49729

Level		Least Sq Mean
15 RAP	A	428.10233
5 FRAS/10 RAP	A	427.14250
5 CRAS/10 RAP	A	377.70392

Temperature (°C)

Least Squares Means Table

Level	Least Sq Mean	Std Error	Mean
-12	398.61389	19.106966	398.614
-18	361.05478	19.106966	361.055
-22	403.64122	19.106966	403.641
-6	480.62178	19.106966	480.622

LS Means Plot

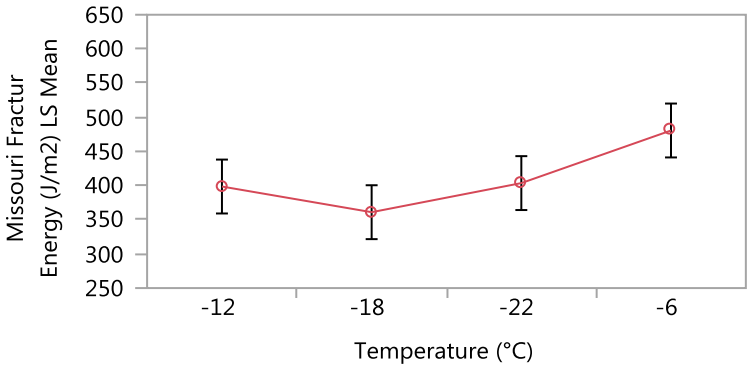

LSMeans Differences Tukey HSD

α=0.050 Q=2.75861

Level		Least Sq Mean
-6	A	480.62178
-22	B	403.64122
-12	B	398.61389
-18	B	361.05478

Missouri Mix Type*Temperature (°C)

LS Means Plot

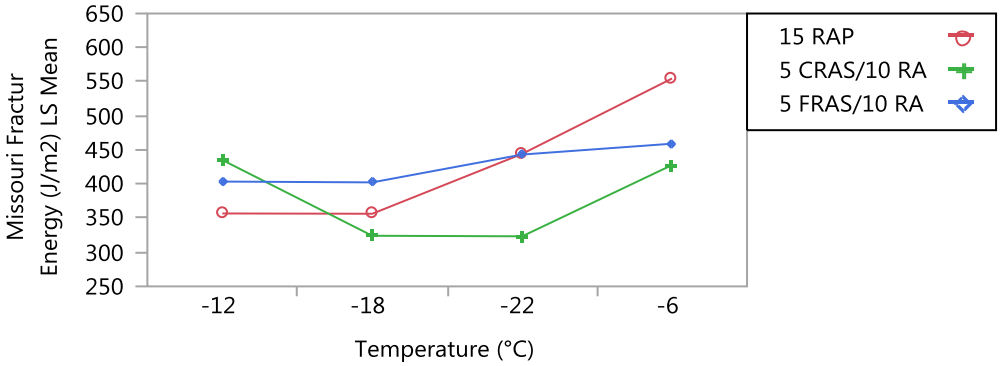

Response Iowa Fracture Energy (J/m2)
Whole Model

Summary of Fit

RSquare	0.57501
RSquare Adj	0.375796
Root Mean Square Error	119.1039
Mean of Response	606.1071
Observations (or Sum Wgts)	48

Analysis of Variance

Source	DF	Sum of Squares	Mean Square	F Ratio
Model	15	614183.7	40945.6	2.8864
Error	32	453943.8	14185.7	**Prob > F**
C. Total	47	1068127.5		0.0058*

Effect Tests

Source	Nparm	DF	Sum of Squares	F Ratio	Prob > F
Iowa Mix Type	3	3	190635.59	4.4795	0.0098*
Temperature (°C)	3	3	399070.61	9.3773	0.0001*
Iowa Mix Type*Temperature (°C)	9	9	24477.53	0.1917	0.9935

Iowa Mix Type

Least Squares Means Table

Level	Least Sq Mean	Std Error	Mean
0 RAS	530.57475	34.382339	530.575
4 RAS	677.14950	34.382339	677.150
5 RAS	557.73567	34.382339	557.736
6 RAS	658.96867	34.382339	658.969

LS Means Plot

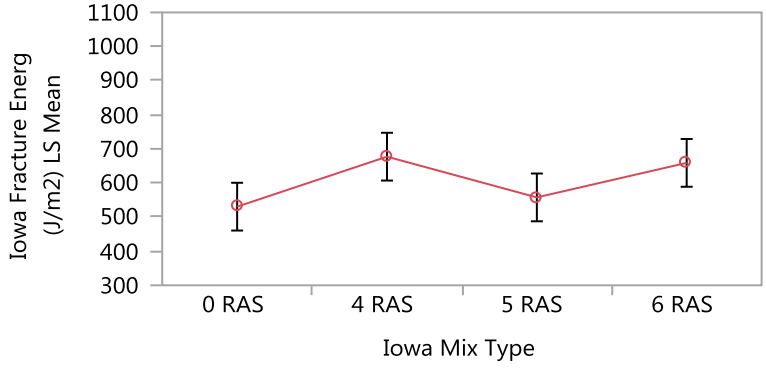

LSMeans Differences Tukey HSD

α=0.050 Q=2.70936

Level			Least Sq Mean
4 RAS	A		677.14950
6 RAS	A	B	658.96867
5 RAS	A	B	557.73567
0 RAS		B	530.57475

Temperature (°C)

Least Squares Means Table

Level	Least Sq Mean	Std Error	Mean
-12	754.67992	34.382339	754.680
-18	591.92675	34.382339	591.927
-22	570.13817	34.382339	570.138
-28	507.68375	34.382339	507.684

LS Means Plot

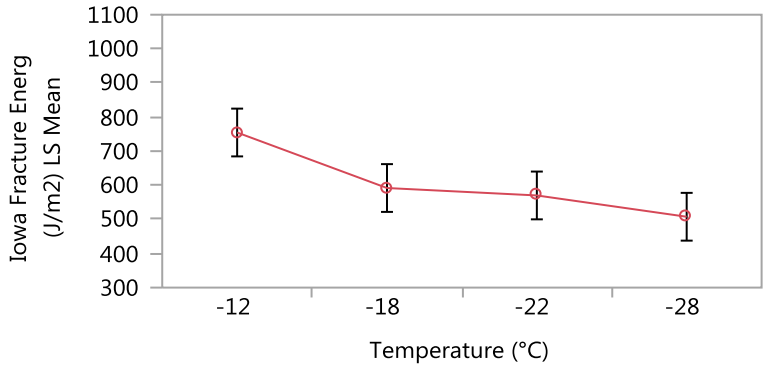

LSMeans Differences Tukey HSD

α=0.050 Q=2.70936

Level			Least Sq Mean
-12	A		754.67992
-18		B	591.92675
-22		B	570.13817
-28		B	507.68375

Iowa Mix Type*Temperature (°C)

LS Means Plot

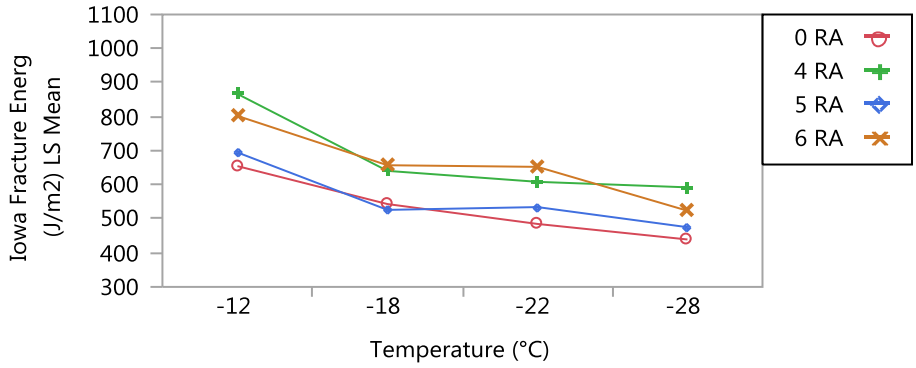

Response Minnesota Fracture Energy (J/m2)
Whole Model

Summary of Fit

RSquare	0.720038
RSquare Adj	0.586144
Root Mean Square Error	135.1554
Mean of Response	761.6012
Observations (or Sum Wgts)	35

Analysis of Variance

Source	DF	Sum of Squares	Mean Square	F Ratio
Model	11	1080567.5	98233.4	5.3776
Error	23	420140.7	18267.0	**Prob > F**
C. Total	34	1500708.2		0.0003*

Effect Tests

Source	Nparm	DF	Sum of Squares	F Ratio	Prob > F
Minesota Mix Type	2	2	9892.63	0.2708	0.7652
Temperature (°C)	3	3	966828.19	17.6425	<.0001*
Minesota Mix Type*Temperature (°C)	6	6	99186.95	0.9050	0.5085

Minesota Mix Type

Least Squares Means Table

Level	Least Sq Mean	Std Error	Mean
30 RAP	741.04342	39.016007	741.043
5 PC RAS	781.92613	41.382725	777.167
5 PM RAS	767.89042	39.016007	767.890

LS Means Plot

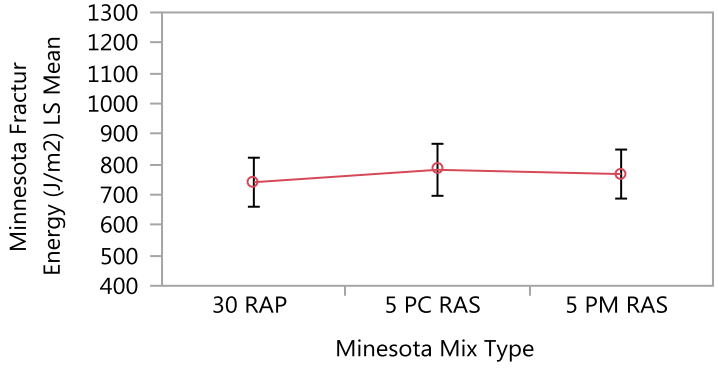

LSMeans Differences Tukey HSD

α=0.050 Q=2.50434

Level		Least Sq Mean
5 PC RAS	A	781.92613
5 PM RAS	A	767.89042
30 RAP	A	741.04342

Temperature (°C)

Least Squares Means Table

Level	Least Sq Mean	Std Error	Mean
-12	1039.5474	45.051804	1039.55
-18	733.6458	48.661510	721.07
-22	628.8634	45.051804	628.86
-28	652.4232	45.051804	652.42

LS Means Plot

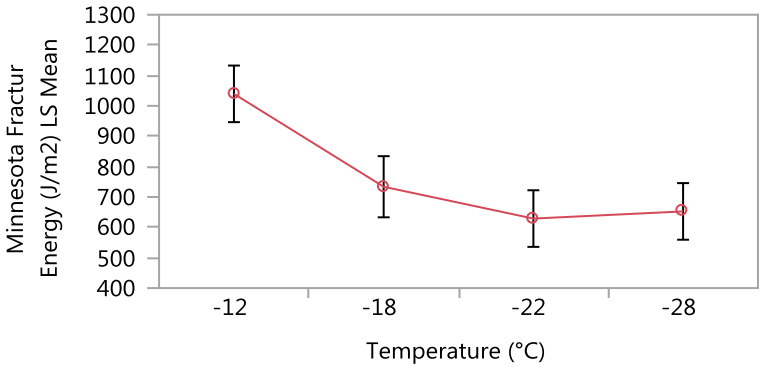

LSMeans Differences Tukey HSD

α=0.050 Q=2.76731

Level		Least Sq Mean
-12	A	1039.5474
-18	B	733.6458
-28	B	652.4232
-22	B	628.8634

Minesota Mix Type*Temperature (°C)

LS Means Plot

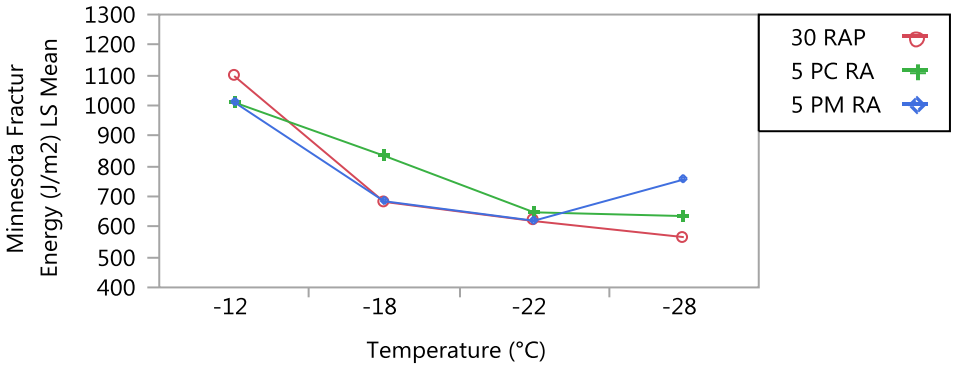

Response Indiana Fracture Energy (J/m2)
Whole Model

Summary of Fit

RSquare	0.819167
RSquare Adj	0.736286
Root Mean Square Error	65.0618
Mean of Response	517.4682
Observations (or Sum Wgts)	36

Analysis of Variance

Source	DF	Sum of Squares	Mean Square	F Ratio
Model	11	460213.15	41837.6	9.8836
Error	24	101592.92	4233.0	**Prob > F**
C. Total	35	561806.06		<.0001*

Effect Tests

Source	Nparm	DF	Sum of Squares	F Ratio	Prob > F
Indiana Mix Type	2	2	20192.81	2.3851	0.1136
Temperature (°C)	3	3	419413.49	33.0270	<.0001*
Indiana Mix Type*Temperature (°C)	6	6	20606.85	0.8113	0.5715

Indiana Mix Type

Least Squares Means Table

Level	Least Sq Mean	Std Error	Mean
15 RAP HMA	499.57025	18.781725	499.570
3 RAS HMA	501.89958	18.781725	501.900
3 RAS WMA	550.93483	18.781725	550.935

LS Means Plot

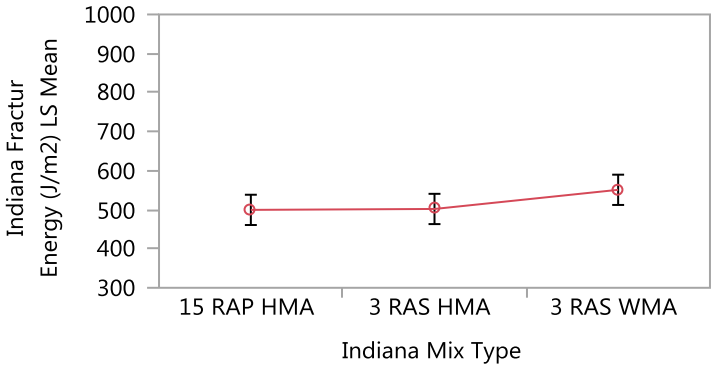

LSMeans Differences Tukey HSD

α=0.050 Q=2.49729

Level		Least Sq Mean
3 RAS WMA	A	550.93483
3 RAS HMA	A	501.89958
15 RAP HMA	A	499.57025

Temperature (°C)

Least Squares Means Table

Level	Least Sq Mean	Std Error	Mean
-12	500.22644	21.687268	500.226
-18	398.16244	21.687268	398.162
-22	479.09367	21.687268	479.094
-6	692.39033	21.687268	692.390

LS Means Plot

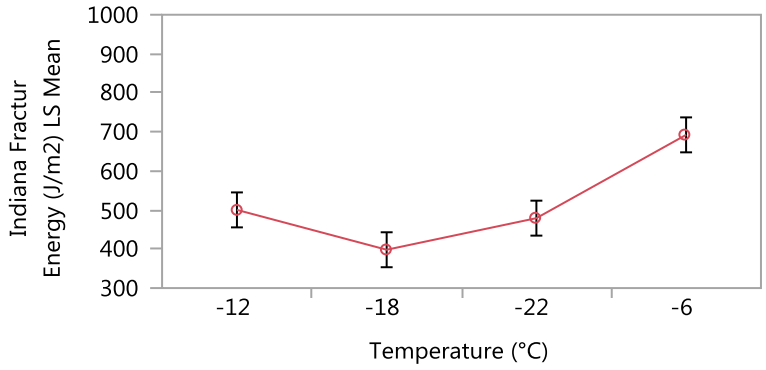

LSMeans Differences Tukey HSD

α=0.050 Q=2.75861

Level			Least Sq Mean
-6	A		692.39033
-12		B	500.22644
-22		B	C 479.09367
-18			C 398.16244

Indiana Mix Type*Temperature (°C)

LS Means Plot

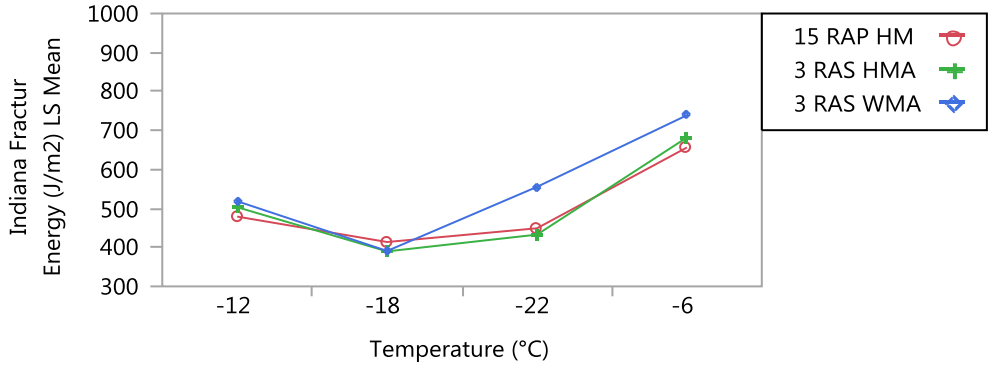

Response Wisconsin Fracture Energy (J/m2)
Whole Model

Summary of Fit

RSquare	0.907451
RSquare Adj	0.82647
Root Mean Square Error	63.30432
Mean of Response	346.9375
Observations (or Sum Wgts)	16

Analysis of Variance

Source	DF	Sum of Squares	Mean Square	F Ratio
Model	7	314345.44	44906.5	11.2058
Error	8	32059.50	4007.4	**Prob > F**
C. Total	15	346404.94		0.0014*

Effect Tests

Source	Nparm	DF	Sum of Squares	F Ratio	Prob > F
Wisconsin Mix Type	1	1	5005.56	1.2491	0.2962
Temperature (°C)	3	3	285450.69	23.7434	0.0002*
Wisconsin Mix Type*Temperature (°C)	3	3	23889.19	1.9871	0.1946

Wisconsin Mix Type

LS Means Plot

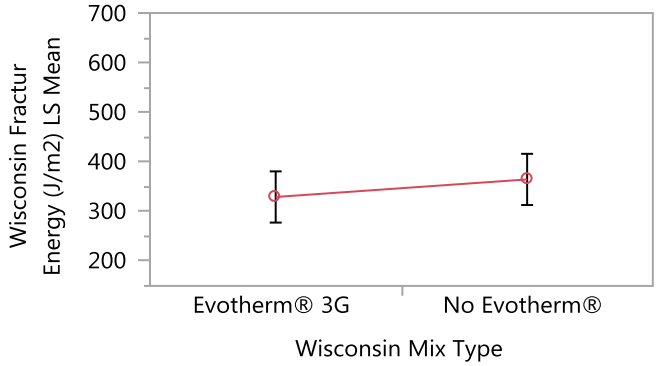

LSMeans Differences Student's t

α=0.050 t=2.306

Level	Least Sq Mean
No Evotherm® A	364.62500
Evotherm® 3G A	329.25000

Levels not connected by same letter are significantly different.

Temperature (°C)

LS Means Plot

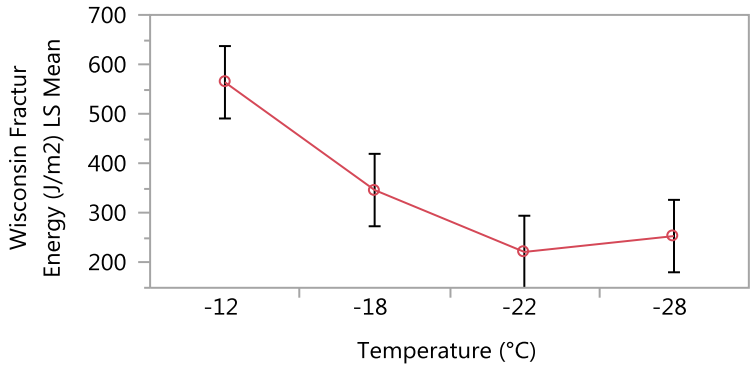

LSMeans Differences Student's t

α=0.050 t=2.306

Level		Least Sq Mean
-12	A	564.25000
-18	B	347.00000
-28	B C	254.25000
-22	C	222.25000

Levels not connected by same letter are significantly different.

Wisconsin Mix Type*Temperature (°C)

LS Means Plot

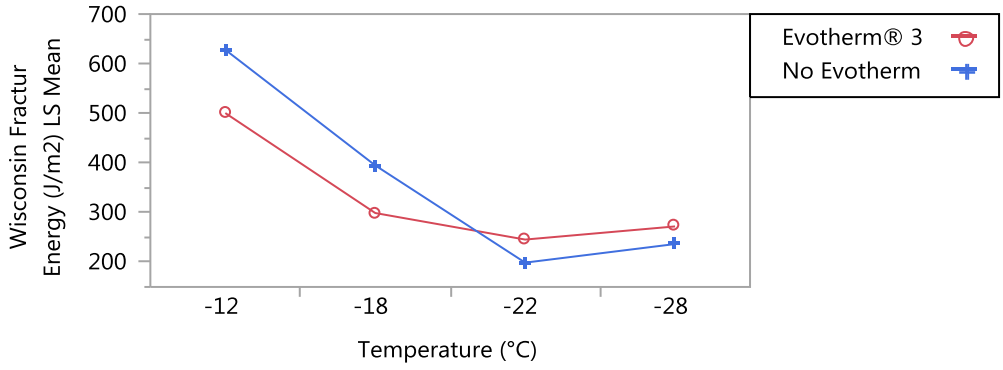

Response Colorado Fracture Energy (J/m2)
Whole Model

Summary of Fit

RSquare	0.802772
RSquare Adj	0.630198
Root Mean Square Error	31.64352
Mean of Response	333.6875
Observations (or Sum Wgts)	16

Analysis of Variance

Source	DF	Sum of Squares	Mean Square	F Ratio
Model	7	32604.938	4657.85	4.6517
Error	8	8010.500	1001.31	**Prob > F**
C. Total	15	40615.438		0.0232*

Effect Tests

Source	Nparm	DF	Sum of Squares	F Ratio	Prob > F
Colorado Mix Type	1	1	4064.063	4.0587	0.0787
Temperature (°C)	3	3	17442.688	5.8066	0.0209*
Colorado Mix Type*Temperature (°C)	3	3	11098.187	3.6945	0.0619

Colorado Mix Type

LS Means Plot

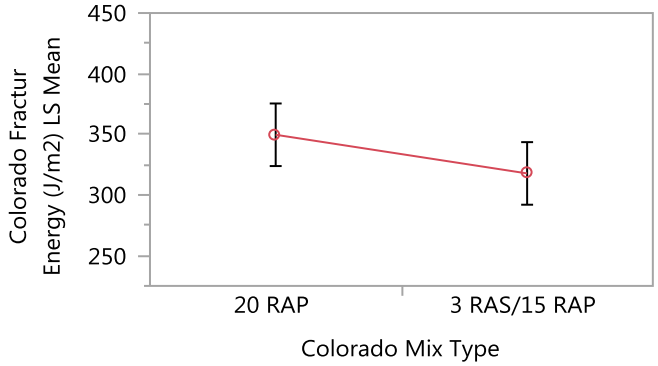

LSMeans Differences Student's t

α=0.050 t=2.306

Level		Least Sq Mean
20 RAP	A	349.62500
3 RAS/15 RAP	A	317.75000

Levels not connected by same letter are significantly different.

Temperature (°C)

LS Means Plot

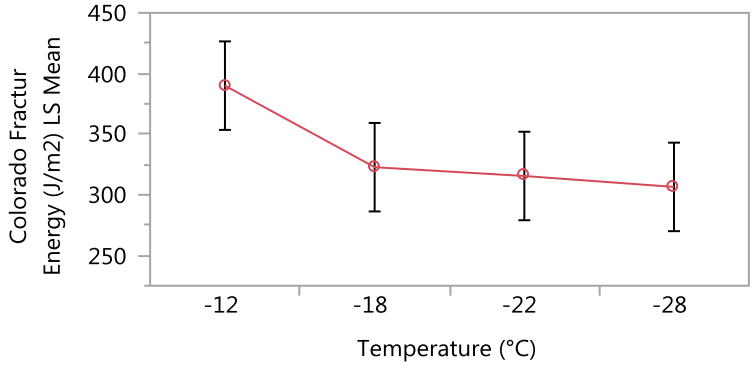

LSMeans Differences Student's t

α=0.050 t=2.306

Level		Least Sq Mean
-12	A	390.00000
-18	B	322.75000
-22	B	315.50000
-28	B	306.50000

Levels not connected by same letter are significantly different.

Colorado Mix Type*Temperature (°C)

LS Means Plot

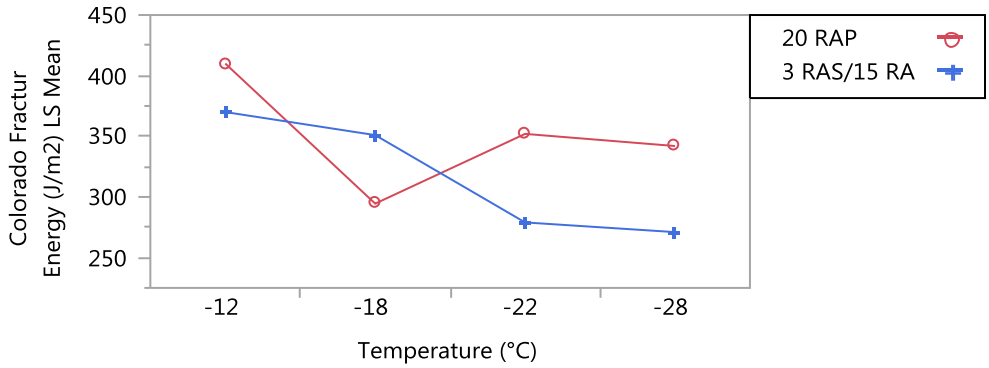

Response Illinois Fracture Energy (J/m2)
Whole Model

Summary of Fit

RSquare	0.396322
RSquare Adj	0.290678
Root Mean Square Error	130.395
Mean of Response	404.375
Observations (or Sum Wgts)	48

Analysis of Variance

Source	DF	Sum of Squares	Mean Square	F Ratio
Model	7	446502.9	63786.1	3.7515
Error	40	680114.3	17002.9	**Prob > F**
C. Total	47	1126617.3		0.0033*

Effect Tests

Source	Nparm	DF	Sum of Squares	F Ratio	Prob > F
Illinois Mix Type	1	1	79870.08	4.6975	0.0362*
Temperature (°C)	3	3	299853.42	5.8785	0.0020*
Illinois Mix Type*Temperature (°C)	3	3	66779.42	1.3092	0.2848

Illinois Mix Type

LS Means Plot

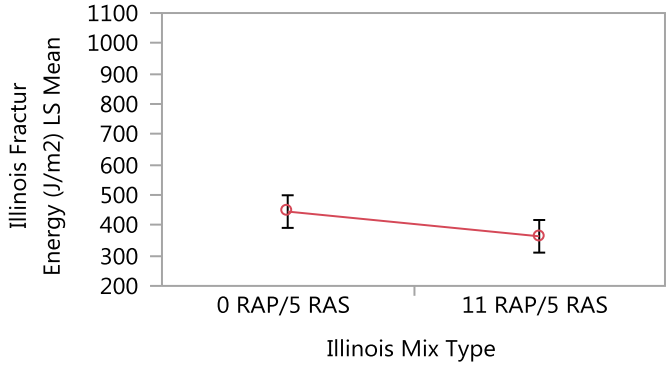

LSMeans Differences Student's t

α=0.050 t=2.02108

Level		Least Sq Mean
0 RAP/5 RAS	A	445.16667
11 RAP/5 RAS	B	363.58333

Levels not connected by same letter are significantly different.

Temperature (°C)

LS Means Plot

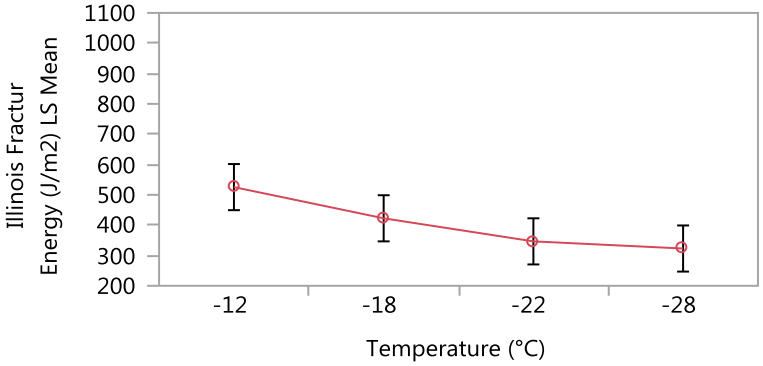

LSMeans Differences Student's t

α=0.050 t=2.02108

Level		Least Sq Mean
-12	A	525.50000
-18	A B	422.58333
-22	B	346.50000
-28	B	322.91667

Levels not connected by same letter are significantly different.

Illinois Mix Type*Temperature (°C)

LS Means Plot

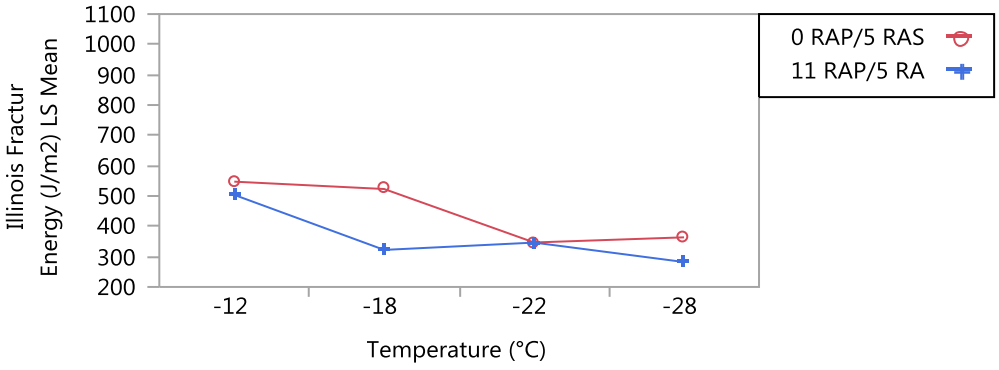

Response Illinois Fracture Energy (J/m2)
Whole Model

Summary of Fit

RSquare	0.619249
RSquare Adj	0.262296
Root Mean Square Error	150.3574
Mean of Response	402.7813
Observations (or Sum Wgts)	32

Analysis of Variance

Source	DF	Sum of Squares	Mean Square	F Ratio
Model	15	588293.97	39219.6	1.7348
Error	16	361717.50	22607.3	**Prob > F**
C. Total	31	950011.47		0.1426

Effect Tests

Source	Nparm	DF	Sum of Squares	F Ratio	Prob > F
Illinois Mix Type	1	1	80100.03	3.5431	0.0781
Temperature (°C)	3	3	216824.09	3.1970	0.0518
Illinois Mix Type*Temperature (°C)	3	3	48214.59	0.7109	0.5596
Sample Type	1	1	1391.28	0.0615	0.8072
Illinois Mix Type*Sample Type	1	1	16698.78	0.7386	0.4028
Temperature (°C)*Sample Type	3	3	157801.84	2.3267	0.1134
Illinois Mix Type*Temperature (°C)*Sample Type	3	3	67263.34	0.9918	0.4217

Response Illinois Fracture Energy (J/m2) – for Whole Model

Summary of Fit

RSquare	0.581187
RSquare Adj	0.18855
Root Mean Square Error	111.036
Mean of Response	401.875
Observations (or Sum Wgts)	32

Analysis of Variance

Source	DF	Sum of Squares	Mean Square	F Ratio
Model	15	273743.50	18249.6	1.4802
Error	16	197264.00	12329.0	**Prob > F**
C. Total	31	471007.50		0.2224

Effect Tests

Source	Nparm	DF	Sum of Squares	F Ratio	Prob > F
Illinois Mix Type	1	1	19602.00	1.5899	0.2254
Temperature (°C)	3	3	118342.50	3.1996	0.0517
Illinois Mix Type*Temperature (°C)	3	3	24003.00	0.6490	0.5950
Binder Modification	1	1	1035.13	0.0840	0.7757
Illinois Mix Type*Binder Modification	1	1	190.13	0.0154	0.9027
Temperature (°C)*Binder Modification	3	3	55171.38	1.4916	0.2547
Illinois Mix Type*Temperature (°C)*Binder Modification	3	3	55399.37	1.4978	0.2531

ACKNOWLEDGEMENTS

I would like to take this opportunity to express my thanks to those who helped me during the completion of this research. First and foremost, I would like to thank Dr. Christopher Williams for his guidance and support not only during this research, but also throughout my undergraduate, graduate studies, and initial stages in my career. I would also like to thank my committee members for their understanding and willingness to work with me: Dr. Vernon Schaefer, Dr. Eric Cochran, Dr. Robert Stephenson, and Dr. Kejin Wang.

Most of all, I would like to thank my wife Jerusha for her hours of love, support, and patience throughout this experience. I would also like to thank Caleb Douglas, Max Prokudin, Sheng Tang, Ashley Buss, Joey Podolsky, Kai Lai Ng, Paul Ledtje, Joana Peralta, Jianhua Yu, Matthew Kirby, Rahman Shaidur, Can Chen, and Mohamed Rashwan for their friendship, support, and sense of humor.